FEASIBILITY STUDY ON DESALTING BRACKISH WATER FROM THE MT. SIMON AQUIFER IN NORTHEASTERN ILLINOIS

Contract No. 14-30-2924
with the Department of the Interior,
Office of Saline Water

Prepared by the Illinois State Water Survey
at the University of Illinois, Urbana, Illinois,
and Hittman Associates, Columbia, Maryland

1973

FEASIBILITY STUDY ON DESALTING BRACKISH WATER FROM THE MT. SIMON AQUIFER IN NORTHEASTERN ILLINOIS

Contract No. 14-30-2924
with the Department of the Interior,
Office of Saline Water

Prepared by the Illinois State Water Survey
at the University of Illinois, Urbana, Illinois,
and Hittman Associates, Columbia, Maryland

1973

ABSTRACT

The feasibility of developing and desalting saline waters stored in a deep artesian aquifer, the Mt. Simon sandstone, in northeastern Illinois was determined as an aid in meeting projected water deficits for the Chicago region. The aquifer is from 1200 to 2800 feet thick. The total dissolved minerals (TDM) increase gradually with depth from less than 500 milligrams per liter (mg/l) to almost 90,000 mg/l at the bottom of the aquifer. Chlorides increase to about 50,000 mg/l at the bottom of the aquifer.

The flow in a water-quality-hydraulic model of the aquifer was simulated by digital computer analysis so that predictions of the mineral quality of water withdrawn from wells (feedwater) could be made to aid in desalting plant design. Analyses made indicated that the mineral concentration of feedwater increases with time of pumping, rapidly at first and then at gradually slower rates, complicating well field and plant design and brine disposal. Important characteristics of the feedwater for desalting plant design are its high hardness and high concentration of iron and TDM. Injection of waste brine through wells open to the lower part of the aquifer was selected as the most practical method of disposal.

The reverse osmosis and freezing processes were considered feasible for 1 million gallons per day (mgd) capacity plants. The distillation process was considered feasible for 5 mgd plants. Costs, including wells, transmission lines, desalting plants, and brine disposal, ranged from 133 cents per thousand gals (¢/1000 gal) for the 1 mgd reverse osmosis plant to 185 eVlOOO gal for the 5 mgd distillation plant. Costs, are much lower (74 I^/IOOO gal in one area) when used in conjunction with available potable groundwater.

It is recommended a pilot plant be constructed to be used as a guideline for future plants. The effects of disposal of waste brine by well injection on the quality of potable groundwater in upper aquifers need to be studied further.

Indexing Terms: Saline-water aquifer, computer model, desalinization processes, water costs, conjunctive use.

CONTENTS

ILLUSTRATIONS

ILLUSTRATIONS (Concluded)

TABLES

ACKNOWLEDGMENTS

This report is the result of a cooperative effort between the Illinois State Water Survey and the Office of Saline Water. The study was funded in part by the Office of Saline Water.

The study was made under the general supervision of William C. Ackermann, Chief of the Water Survey, and Harman F. Smith, Head of the Hydrology Section of the Survey. Hittman Associates of Columbia, Maryland, under subcontract to the Water Survey, carried out the feasibility study of the technical and economic aspects related to desalting the Mt. Simon aquifer water.

Major contributions made by Water Survey personnel are as follows. R. J. Schicht supervised the technical aspects of the study. A. P. Visocky prepared the sections on *Description of the Mt. Simon Aquifer, Water Quality Model,* and *Geohydrologic Model.* He also wrote sections on well design and economics. The statistical analysis of water quality data for the water quality model was made by R. A. Sinclair. T. A. Prickett and Carl Lonnquist developed the digital computer model, carried out the chemical quality predictions, and designed the multiple production well and injection well field schemes. Mrs. J. Loreena Ivens edited the final manuscript. J. W. Brother, Jr., supervised the preparation of illustrations.

INTRODUCTION

The Illinois State Water Survey is engaged in a comprehensive water supply study of the metropolitan Chicago region (northeastern Illinois) (figure 1), an area of about 4000 square miles with a population of about seven million. It is expected that results of this study will determine the state's strategy for meeting the demands for water for the metropolitan Chicago region for this century and beyond. The State Water Survey's study will investigate all alternatives and possibilities from all sources and the economics of each by systems analysis. It is expected that the study will include the conjunctive use of desalted water with conventional groundwater sources, artificial recharge, reuse, diversion of surface water, and other refinements.

Phase I of the study (1), based on the physical analysis of the area, shows that some parts of the region are experiencing water deficits now and that many parts of the region will experience water deficits by the year 1990 unless additional water can be secured from Lake Michigan or developed from new or presently unusable sources.

It may seem strange that Chicago and suburbs do not have unlimited supply of water from Lake Michigan. But the Lake Michigan water supply is limited by the U.S. Supreme Court decree of 1966 to 3200 cubic feet per second (cfs). The Supreme Court decree states: "The State of Illinois may make application for a modification of this decree so as to permit the diversion of additional water from Lake Michigan for domestic use when and if it appears that the reasonable needs of the Northeastern Illinois Metropolitan Region (comprising Cook, DuPage, Kane, Lake, McHenry, and Will Counties) for water for such use cannot be met from the water resources available to the region, including both ground and surface water and the water authorized by act of Congress and permitted by this' decree to be diverted from Lake Michigan", and if it further appears that all feasible means reasonably available to the State of Illinois and its municipalities, political subdivision, agencies and instrumentalities have been employed to improve the water quality of the Sanitary and Ship Canal and to conserve and manage the water resources of the region and the use of water therein in accordance with the best modern scientific knowledge and engineering practice."

The purpose of this study is to determine the feasibility of developing and desalting the brackish waters stored in the Mt. Simon aquifer. It appears that desalting technology has progressed to the point where various desalting processes should be considered as a means of converting the large quantities of brackish water into a water resource to meet future demands in northeastern Illinois.

Hittman Associates, under subcontract to the Water Survey, carried out the feasibility study of the technical and economic aspects related to the desalting of Mt. Simon aquifer water. Close liaison between the staffs of Hittman Associates arid the Survey was maintained during the preparation of this study. Data on water chemistry, feed rate, and cost of water conveyance were provided by the Water Survey.

(1) Numbers refer to bibliography at the end of the appendix.

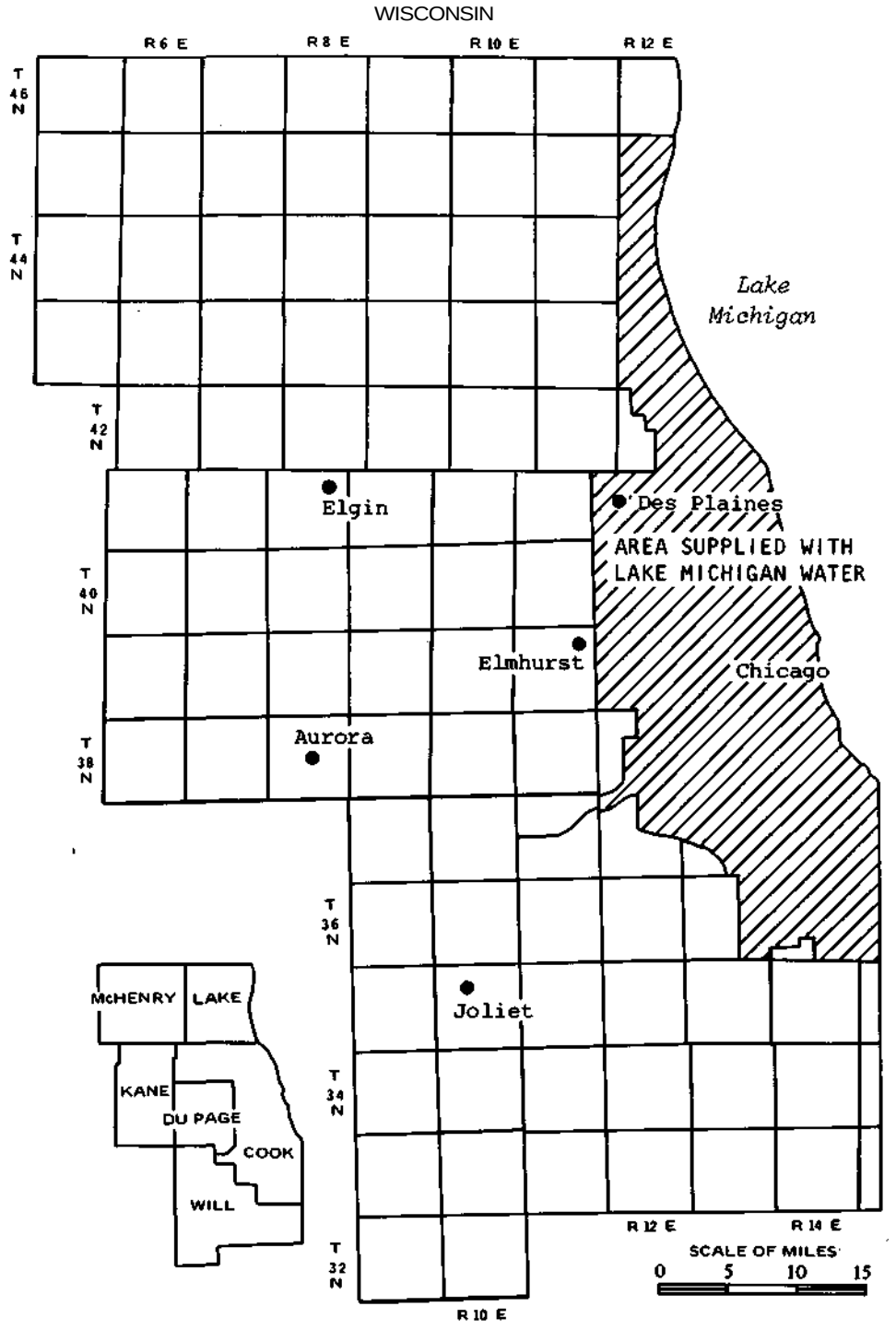

Figure 1. Location of study area

Ground rules were established by the Water Survey and Hittman Associates as follows:

1) Site — Aurora and DuPage County
2) Capacity — 1,5, and 10 mgd of product water
3) Capacity factor — 90 percent or 330 operating days per year
4) Pretreatment — acid injection
5) Interest rate — 5⅜ or amortization factor of 0.0678
6) Insurance — 0.25 percent of capital cost
7) Plant life — 30 years
8) Product salinity — 500 mg/l maximum
9) Power cost — calculated from data supplied by Commonwealth Edison Company of Illinois

SUMMARY AND CONCLUSIONS

The developing and desalting of large quantities of brackish water stored in the very deep Mt. Simon sandstone aquifer is considered as one alternative to aid in meeting projected water deficits forecast for the six counties in northeastern Illinois that compose the Chicago region.

The Mt. Simon aquifer is found at depths of 1500 to 1900 feet below ground surface and consists of fine- to coarse-grained sandstone. Many wells penetrate the upper 200 to 300 feet of the aquifer which generally contains potable water in the northern two-thirds of northeastern Illinois. It was estimated in 1971 that of the 151 mgd pumped from deep wells, 26 mgd was contributed by the Mt. Simon. Deteriorating mineral quality has been reported in many of these wells. Below the 200 to 300 foot level, the total dissolved minerals increase gradually with depth to almost 90,000 mg/l at the bottom of the aquifer. Chlorides increase to about 50,000 mg/l . The mineral quality varies with location as well as depth.

Groundwater in the aquifer occurs under artesian conditions. Hydrostatic heads in the Mt. Simon are reported to be more than 50 feet higher than heads in the overlying Cambrian-Ordovician aquifer. Groundwater movement is downdip from the recharge area in southeastern Wisconsin southward. On the basis of available core analysis and well tests, the average transmissivity and storage coefficient were estimated to be 10,000 gallons per day per square foot (gpd/ft^2) and 0.0004 respectively. The ratio of vertical to horizontal permeability is 0.5.

The yields of wells and the mineral quality of water withdrawn from wells are dependent primarily upon aquifer hydraulic properties and water quality-depth relationships. The Mt. Simon aquifer was modeled from existing data so that the hydraulic properties and the quality-depth profile could be determined for any given well field location. The flow in the Mt. Simon model was simulated by digital computer analysis to enable predictions of water quality and well field yields. A separate computer program was written to predict pH values. Analyses made indicated that the mineral concentration of water withdrawn from the Mt. Simon wells increases rapidly at first and then at gradually slower rates similar to drawdowns within a pumped well. The ultimate mineral concentration of the water withdrawn will depend not only on the well location but its depth of penetration. In a multiple-well system the ultimate concentration would also depend upon spacing and total pumpage.

Desalting plants with capacities of 1, 5, and 10 mgd were selected for study. The eastern part of Du Page County, an area of projected water deficiency, was selected as a site for the desalting plants. To aid in plant design, predictions of water quality of the Mt. Simon feedwater for different well field schemes were made by computer analysis. The important characteristics of the feedwater are its high hardness, high concentration of iron, and large amount of total dissolved minerals. For example, water from a well penetrating 50 percent of the Mt. Simon contains 40,000 mg/l TDM, exceeding seawater which has 35,000 mg/l TDM.

Five different desalting processes were considered: ion exchange (IE), electrodialysis (ED), reverse osmosis (RO), distillation, and freezing. The number of wells, each pumping at a rate of 1 mgd, needed to ultimately supply the desalting plants varied from 3 wells

(including standby) to supply a 1 mgd plant to 54 wells (including standbys) to supply a 10 mgd plant. Well penetrations into the aquifer were 20, 31, and 50 percent. Well fields were from 4 to 7 miles from the desalting plants.

The IE process was rejected because the high salinity water requires a very high chemical cost. The electrodialysis process was rejected because of the prohibitively high cost for electric power. The reverse osmosis process was applied only for 1 mgd plants with feedwater from wells with 20 or 50 percent aquifer penetration.

Evaluation of brine disposal methods led to selection of brine disposal by injection through wells open to the lower Mt. Simon aquifer. Depending upon the size of desalting plant and the desalting process, from 2 to 42 wells (including standbys) were required for disposal. Injection sites were at distances of less than 1 mile to 4 miles from desalting plants.

Costs of producing water for the 1 mgd RO plants ranged from 132.9¢/1000 gal for water from wells with 50 percent aquifer penetration to 136.4¢/1000 gal for 20 percent penetrating wells. Costs of producing water for 1 mgd freezing plants ranged from 138.6¢/1000 gal for water from wells with 50 percent penetration to 142.1¢/1000 gal for water from wells with 20 percent penetration. Costs of producing water for the 5 mgd distillation plants averaged 184.6¢/1000 gal. Costs of desalting water by the freezing process for 5 and 10 mgd plants were not estimated since the freezing process is still under development and it is difficult to estimate costs for plants larger than 1 mgd.

The costs are much higher than that of other alternatives but become more competitive when used in conjunction with the available fresh groundwater. The cost to one area in the region was estimated to be 74¢/1000 gal for a 15 mgd combined supply, in which 11 mgd was available from conventional groundwater sources and 4 mgd was supplied from a desalting plant.

Treated saline water from the Mt. Simon aquifer may be needed to aid in meeting projected water deficits in the Chicago region. Because of difficulties expected in operating a plant, a bench scale or pilot plant should be constructed to obtain data to be used as a guideline for future plants. Waste brine injection may have a harmful effect on the quality of water being withdrawn from existing wells open to both the Cambrian-Ordovician and the Mt. Simon aquifers. Any injection scheme should be approached with caution. A more practical approach to utilizing Mt. Simon water may be desalting water from wells open to both the Cambrian-Ordovician and the Mt. Simon aquifers.

DESCRIPTION OF MT. SIMON AQUIFER

GEOLOGY AND HYDROLOGY

The Mt. Simon sandstone derives its name from an exposure on Mount Simon near Eau Claire, Wisconsin (2). There, 234 feet of coarse-grained, partly conglomeratic sandstone overlies Precambrian granite and underlies a fine-grained, fossiliferous Eau Claire sandstone. In northeastern Illinois the Mt. Simon consists of fine- to coarse-grained, unfossiliferous sandstone underlying fossiliferous sandstone, shale, and dolomite of the Eau Claire (figure 2).

The Mt. Simon is present in all wells in northeastern Illinois that penetrate the base of the Eau Claire. Over most of the area it is found at a depth of 1500 to 1900 feet. Buschbach (2) estimated thicknesses of 1200 feet in northern McHenry County to 2800 feet in western Will County, based on data from outside the area as well as penetration data within the area (figure 3). One well subsequently has been drilled through the entire thickness of the Mt. Simon (2200 feet) in DuPage County. This thickness compares with the estimated 2500 plus foot thickness for that location (figure 3). A gas storage well in Kankakee County penetrated 2460 feet of Mt. Simon and ended in an arkosic zone.

The Mt. Simon is generally coarser, more poorly sorted, and more angular than sandstones of the other Cambrian or Ordovician formations in northeastern Illinois. Cores exhibit well developed cross-bedding, especially in the coarser grained beds. Red and green shales, a few inches to 15 feet in thickness, occur in the upper 300 feet and lower 600 feet, although they accounted for less than 5 percent of the total Mt. Simon sequence in any well studied by Buschbach (2). A few zones contain very fine quartz pebbles, and an arkosic zone is commonly found at the base of the Mt. Simon.

Although it is gradational into the overlying marine sediments of the Eau Claire, no marine fossils have been found in the Mt. Simon, suggesting its deposition in basins that had an influx of fresh water (2). The source of the sediments is believed to have been to the north, since the sandstones coarsen in that direction. Most of the Cambrian and Ordovician rocks are less dolomitic to the north, forming in southeastern Wisconsin a more or less continuous sandstone sequence from the Mt. Simon up through the St. Peter (Ordovician). This series of sandstones plus the overlying Galena dolomite are collectively referred to as the "sandstone aquifer" (4).

In northeastern Illinois the Mt. Simon sandstone and the lower incoherent sandstone of the Eau Claire Formation are hydrologically connected and considered as one unit, the Mt. Simon aquifer (5). In southeastern Wisconsin, the recharge area of the Mt. Simon, this aquifer is the lowermost unit of the "sandstone aquifer," which behaves hydrologically as one unit (6). Recharge to the sandstone aquifer (and, therefore, to the Mt. Simon) takes place as precipitation percolates down through the drift and, where present, overlying bedrock units. As one traces the sandstone aquifer southward into Illinois, the Eau Claire Formation becomes more shaley and dolomitic (2) and acts as a barrier between the Mt. Simon and the Cambrian-Ordovician aquifers. The top of the Mt. Simon generally dips northwest to southeast at 10 feet per mile.

Groundwater in the Mt. Simon occurs under artesian conditions because the Eau Claire

SYSTEM	SERIES	GROUP OR FORMATION	GRAPHIC LOG	THICKNESS (FEET)	DESCRIPTION	AQUIFERS
QUATERNARY	PLEISTOCENE			0 - 400+	Unconsolidated ice - and water-laid deposits, pebbly clay (till), silt, sand and gravel, generally discontinuous and interbedded; alluvial silts and sands commonly present along streams	Glacial drift aquifers
PENNSYLVANIAN				0 - 175	Shale; sandstones, fine grained; limestone; coal; clay	Shallow bedrock aquifers
MISSISSIPPIAN DEVONIAN *						
SILURIAN	NIAGARAN			0 - 400+	Dolomite, very pure to very silty, cherty; shale partings; thin shales and argillaceous beds frequently present in lower parts of Silurian dolomite.	
	ALEXANDRIAN			0 - 165	Upper and middle units - shale, light gray to green, plastic to brittle, some dolomite, silty; dolomite, mostly silty, argillaceous; minor limestone Lower unit - shale, dark gray, black, brown, plastic to brittle; some dolomite in upper part; silty, argillaceous.	
ORDOVICIAN	CINCINNATIAN	Maquoketa		0 - 250+		
	CHAMPLAINIAN	Galena Platteville		150 - 350+	Dolomite, cherty; sandy at base; limestone; shale partings.	Cambrian-Ordovician aquifer
		Glenwood St. Peter		75 - 650	Sandstone, fine to coarse grained; shale at top; locally cherty red shale at base.	
	CANADIAN	Prairie du Chien		0 - 340	Dolomite, sandy, cherty, interbedded with sandstone.	
CAMBRIAN	CROIXAN	Eminence Potosi		0 - 225	Dolomite, white, fine grained sandy at base; drusy quartz.	
		Franconia		45 - 175	Sandstone, dolomite, and shale, glauconitic, green to red, micaceous.	
		Ironton Galesville		103 - 275	Sandstone, fine to medium grained, well sorted, upper part dolomitic	
		Eau Claire		235 - 450	Shale and siltstone, dolomitic, glauconitic; sandstone, dolomitic, glauconitic; dolomite, sandy	
		Mt. Simon		2000±	Sandstone, coarse grained, white, red in lower half; lenses of shale and siltstone, red, micaceous.	Mt. Simon aquifer
PRECAMBRIAN					Not penetrated by wells in Chicago area. Nearby wells encounter red or gray granite or similar rocks.	

* Mississippian rocks present in Des Plaines Disturbance.
Devonian rocks present as crevice fillings in Silurian rocks.

after Hughes et at. (3)

Figure 2. Geologic column and aquifer description of northeastern Illinois

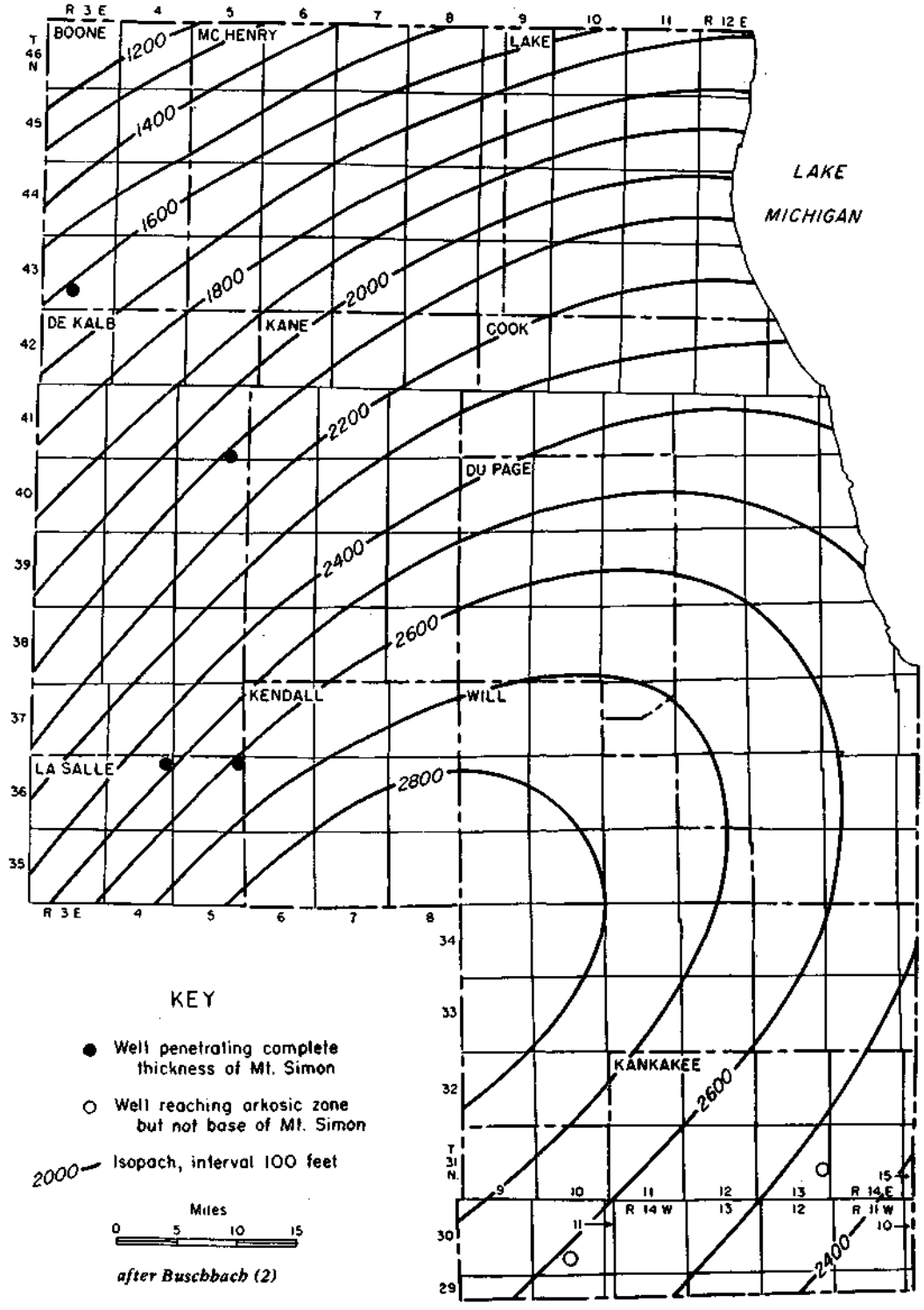

Figure 3. Thickness of Mt. Simon sandstone

Formation acts as a confining layer and head differences exist between the Mt. Simon and shallower aquifers. Walton and Csallany (7) reported that hydrostatic heads in the Mt. Simon were more than 50 feet higher than those in overlying aquifers along the Fox River in 1960. Groundwater movement is apparently downdip away from the recharge area and becomes increasingly vertical further southward as conditions become favorable for upward movement.

HYDRAULIC PROPERTIES

Although many Cambrian-Ordovician wells in northeastern Illinois also tap fresh water in the upper portion of the Mt. Simon aquifer, well test data from wells open exclusively to the Mt. Simon are scarce. Only one specific capacity value from such a well is available, all others being from multi-aquifer wells. Thus, the hydraulic properties of the Mt. Simon in the immediate study area could not be determined confidently from available data.

As described in the subsequent section, *Geohydrologic Model,* data from core analyses and well tests associated with underground gas storage projects outside the study area were collected and correlated with depth variables to describe a model of the hydraulic character of the Mt. Simon. On the basis of the application of this model to the geologic situation in the study area, average coefficients of transmissivity and storage were estimated to be 10,000 gpd/ft and 10^{-4}, respectively. The ratio of vertical to horizontal permeability is generally 0.5.

GROUNDWATER WITHDRAWALS

Pumpage from deep wells in northeastern Illinois began in Chicago in 1864 when an industrial sandstone well was drilled. Withdrawals from deep sandstone wells increased from 200,000 gpd in 1864 to 151 mgd in 1971 (8,9). Since many deep wells penetrate the top of the Mt. Simon aquifer, a portion of the pumpage from these wells comes from this unit. It is estimated that of the 151 mgd pumped from deep wells in 1971, 25.8 mgd was contributed by the Mt. Simon. Figure 4 shows the estmated growth of pumpage belived to be derived from the Mt. Simon between 1864 and 1971. Since 1960, pumpage from the Mt. Simon has increased approximately 4.4 percent each year. Pumpage derived from the Mt. Simon is concentrated in five major centers: Aurora, Chicago, Des Plaines, Elgin, and Elmhurst

WATER QUALITY

The mineral quality of water in the Mt. Simon aquifer of northeastern Illinois is only briefly discussed in the literature. The paucity of mineral data exists because this aquifer is either too deeply buried or too highly mineralized for extensive development to have taken place economically. The wells which have tapped the Mt. Simon have almost always been open to units of upper aquifers, resulting in blended water. Suter et al. (5) reported that a rapid increase in chloride concentration with depth was the most notable characteristic of Mt. Simon waters, and Zeizel et al. (10) observed that the average hardness in this aquifer was less than that of water from the Cambrian-Ordovician aquifer.

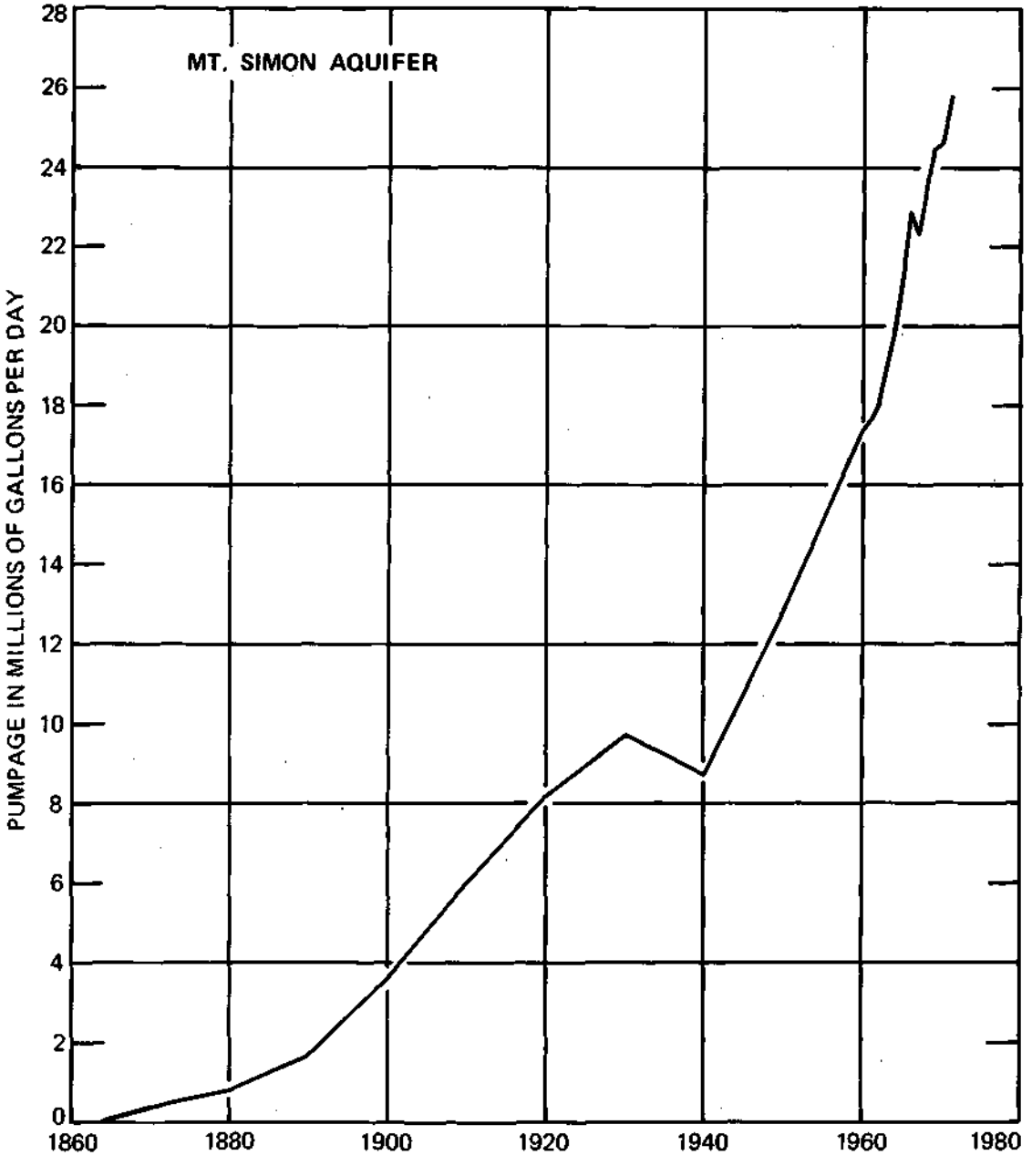

Figure 4. Growth of pumpage from Mt. Simon aquifer

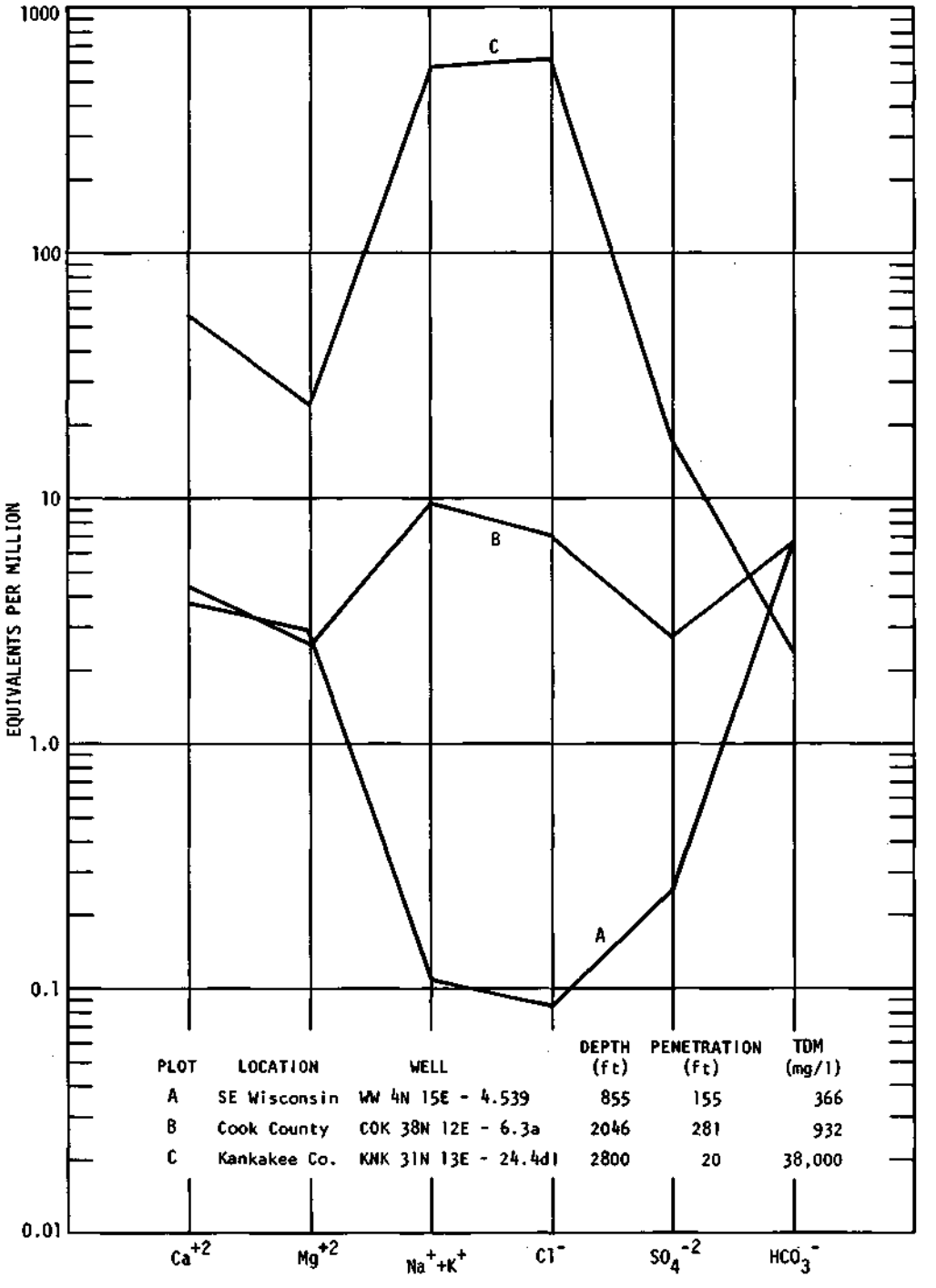

Figure 5. Variation of Mt. Simon water quality with location

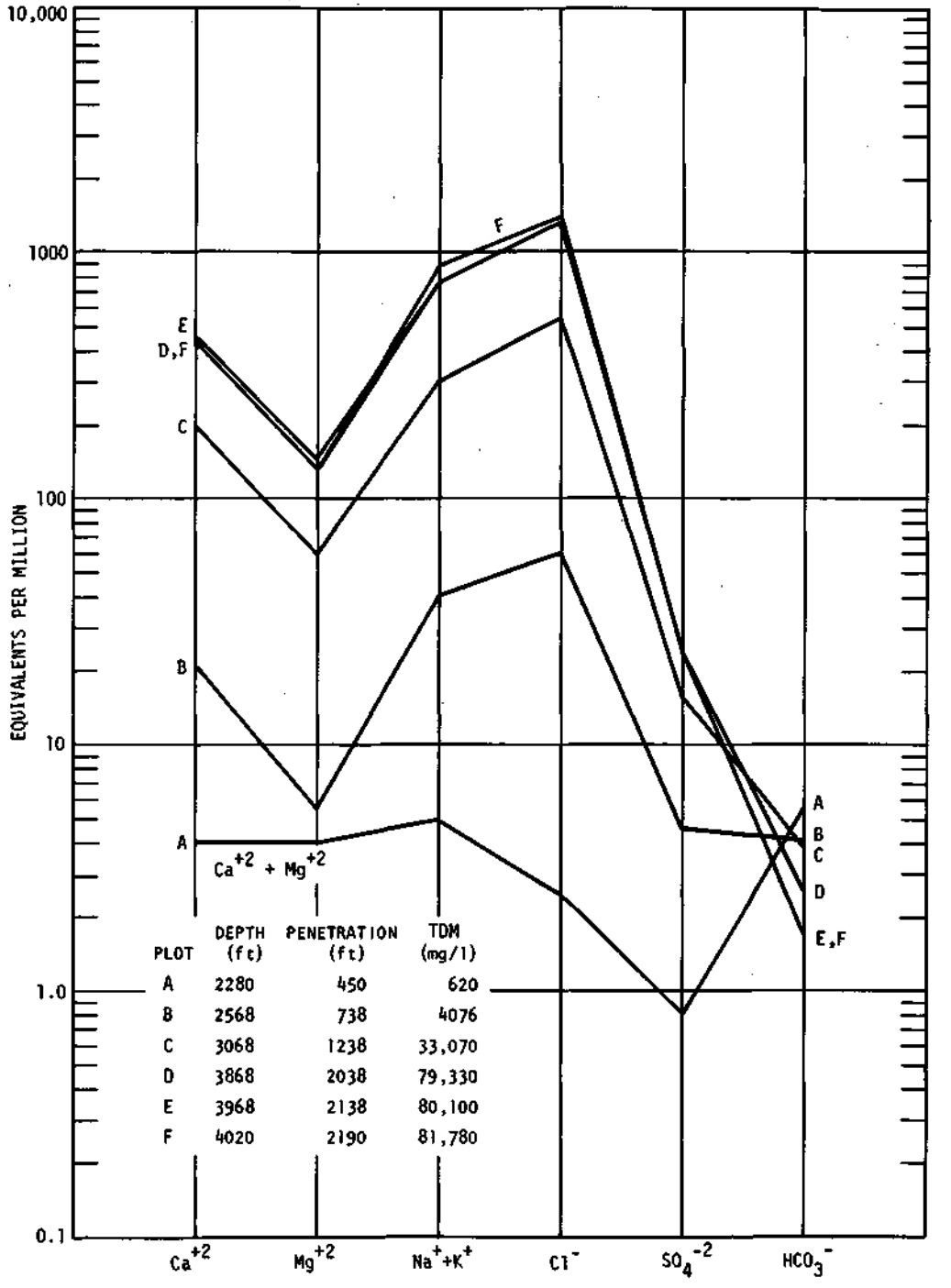

Figure 6. Variation of Mt. Simon water quality with depth

An example of the chemical character of water in the upper portion of the Mt. Simon in the Chicago area is given in figure 5, plot B. The sample was taken from a well which was cased to the top of the Mt. Simon and which penetrated 281 feet into the aquifer. This graphical presentation of equivalents of chemical constituents is referred to as a Schoeller diagram (11). The diagram reveals a feature of Mt. Simon waters in the area — the importance of $Na^+ + K^+$ and Cl^-. In this sample HCOi is also important, although generally it is a relatively minor constituent in deep wells. As a comparison, figure 5 also shows an analysis that is typical of water from the recharge area of the Mt. Simon aquifer in southeastern Wisconsin (plot A). The U-shaped Schoeller diagram is characteristic of these waters, since they are high in Ca^{+2}, Mg^{+2}, and HCO_3^- and low in Na^+, Cl^-, and SO_4^{-2}. As shown in plot C of figure 5, the character of Mt. Simon water to the south of the Chicago area (Well KNK31N13E-24.4dl) is, conversely, quite saline, with Na^+ and Cl^- ions predominating. The shapes of plots A, B, and C show a progression from recharge water, whose plot is typically U-shaped, to saline water with its dominant NaCl peak and steep right limb.

The variation of mineral content with depth and penetration into the Mt. Simon aquifer is illustrated in figure 6. Plots A to F represent analyses of samples taken at progressively deeper levels in a proposed waste disposal well in DuPage County (DUP 39N9E-9.2a). In plot A the Ca^{+2} and Mg^{+2} are lumped together from hardness data, since their individual concentrations were not known. As the sampling depth increased and the mineral concentration increased from a fresh water to a brine, the HCO_3^- content decreased, the anion side of the diagrams shifted to a steep limb (Cl/SO_4 ratio between 55 and 60), and the typical NaCl peak developed. The nearly constant slope of the Ca-Mg lines revealed that the Ca/Mg ratio remained essentially unchanged with depth, varying between 3.2 and 3.8. The Ca/Cl ratio is also one which remained very nearly constant, ranging from 0.31 to 0.37. Chloride became 60 percent by weight of the total mineral content, while the Na/Cl ratio approached 0.60 with depth. Table 1 shows the complete mineral analysis of the sample taken at a depth of 4020 feet (plot F).

Temperatures of Mt. Simon waters in the Chicago area are known only from two of the wells described above (COK38N12E-6.3a and DUP39N9E-9.2a). Temperatures of 51 and 55 F, respectively, were recorded from these wells. Temperatures in the "sandstone aquifer" of southeastern Wisconsin averaged about 50 F, while those from the upper portion of the Mt. Simon in LaSalle County (underground gas storage project) ranged rom 75 to 81 F.

TABLE 1
MINERAL ANALYSIS OF WATER SAMPLE FROM DUP39N9E-9.2a
TAKEN AT DEPTH OF 4020 FEET

		mg/l	epm			mg/l	epm
Iron (total)	Fe	129		Silica	$Si0_2$	4.5	
Manganese	Mn	9.9		Fluoride	F	18*	
Calcium	Ca	8,855	442.54	Boron	B	16	
Strontium	Sr	200	4.56	Chloride	Cl	50,500	1424.10
Magnesium	Mg	1,592	130.90	Nitrate	$N0_3$	1.4	0.02
Ammonium	NH_4	0.0	0.00	Sulfate	$S0_4$	1,133	23.57
Sodium	Na	19,500	847.83	Alkalinity	(as $CaC0_3$)	84	1.68
Potassium	K	393	10.05				
Copper	Cu	0.05					
Zinc	Zn	1.5					
Chromium	Cr	0.15					
Turbidity (Jtu)		890		Hardness	(as $CaCO_3$)	28,900	578.00
Color		10					
Odor		Ch					
pH(in lab)		6.0		Total dissolved minerals		81,780	

*Distilled

WATER QUALITY MODEL

Basic to the selection of a suitable desalting process is the quality of feedwater which is processed. An understanding of the variation in water quality with depth and location throughout the Mt. Simon is essential, if one is to predict the transient nature of that quality during pumping periods. A water quality model of the Mt. Simon is necessary — one which defines the chemical character of the aquifer at any site in terms of a quality-depth profile.

This section describes the collection and computer analysis of Mt. Simon water quality data and the resulting regression equations which constitute the water quality model used in this study.

SAMPLING

As pointed out in the previous section, two of the wells described — COK38N12E-6.3a and DUP39N9E-9.2a — are the only known wells in the Chicago area for which water sample analyses from the Mt. Simon are available. Additional analyses of water samples for study were available from wells outside the Chicago area in southeastern Wisconsin and to the south and southwest of Chicago in Kankakee, LaSalle, Livingston, and McLean Counties. Analyses were also available from a well in Champaign County and a well in Putnam County. Water quality data from south and southwest of Chicago, with the exception of the Putnam County analysis, were obtained from analyses of water samples collected during gas storage reservoir test borings. Samples were taken at specified depths by utilizing inflatable packers to seal off upper and lower waters. The Putnam County analysis is for a sample collected in a waste disposal well open to the entire Mt. Simon sequence above the well bottom-hole depth. Data from southeastern Wisconsin represent samples taken from the "sandstone aquifer" in the recharge area of the Mt. Simon.

Practically all of the water quality data, with the exception of the Cook and DuPage County analyses, are from the "end points" of the water quality sequence which finds Mt. Simon water "beginning" as a calcium-magnesium bicarbonate type and progressing to a predominantly sodium chloride type.

Sample Distribution. A total of 68 mineral analyses of water samples from the Mt. Simon aquifer were available. Figure 7 shows the distribution of samples by county and type. The largest group of samples, 47, came from gas storage test boreholes, with 23 from McLean County. Thirteen samples were from the recharge area, whereas only 7 samples (from 2 wells) came from the Chicago area.

Sampling Technique. The compilation of mineral analyses was made by a search of available data, thus no control was exercised over the collection of samples. Most of the samples were collected during the early 1960s; however, the Wisconsin samples were collected between the mid-1940s and the late 1960s. As described earlier, most Illinois samples were point samples, wherein casing or inflatable packers isolated a specified collection point depth. One sample from Putnam County represents water collected at the bottom of a well which was open to all of the Mt. Simon penetrated to that point. The Wisconsin samples generally represent water from the entire sequence of the "sandstone aquifer"; however, the

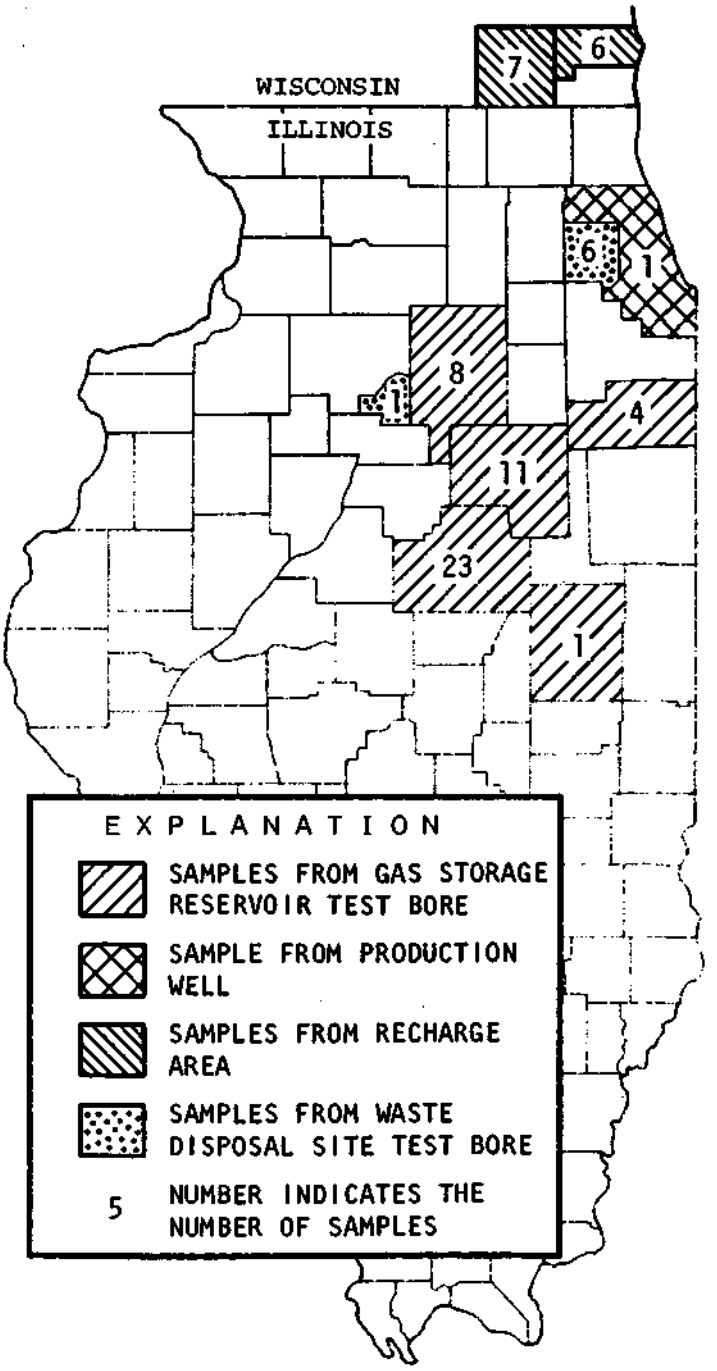

Figure 7. Locations of water samples from the Mt. Simon aquifer

variation of mineral quality with depth is not as great in the recharge area as it is in Illinois, so each of these samples should be fairly representative of water quality at its sampling location.

Analyses of storage reservoir samples were conducted by Bradford Laboratories, Evansville, Indiana. All other Illinois samples were analyzed by the Illinois State Water Survey. Wisconsin samples were analyzed by the U.S. Geological Survey Water Resources Division in Madison, Wisconsin.

Number of Samples. The detail of analysis from sample to sample was not uniform; some constituents and physical properties were determined in some samples and not in others. A summary of these analyses is presented in table 2.

TABLE 2
RESULTS OF SAMPLE ANALYSES
(Chemical constituents in milligrams per liter)

Constituent or property	Number of samples	Range of values
$Na^{*}+K^{+}$	68	2 to 24,569 (as Na^{+})
Ca^{+2}	66	59 to 9023
Mg^{+2}	66	16 to 1713
Cl^{-}	68	0 to 52,000
SO_4^{-2}	68	1 to 2050
Alkalinity	67	26 to 336 (as $CaC0_3$)
Hardness	68	202 to 29,800 (as $CaC0_3$)
Fe^{+2}	67	0 to 460
Mn^{+2}	43	0 to 10.8
Total dissolved minerals (TDM)	68	276 to 87,985
CO_2	40	4 to 96
pH	63	5.7 to 8.2
Temperature, °F	10	51 to 81F
Specific gravity	42	1.0040 to 1.0617

Although CO_2 and pH have been included in the presentation and analysis of available data, it is conceded that inherent difficulties exist in determining these two variables, such as loss of CO_2 with time and the effects of time and temperature on pH. Caution should be exercised, therefore, to avoid a strict interpretation of these data.

DATA ANALYSIS

In order to attempt a definition of the chemical character at any given location and depth of Mt. Simon waters, it was necesary to determine the relationships between the mineral constituents and physical properties (dependent variables) and the spacial distribution of the samples (independent variables). The dependent variables have been outlined in table 2, while the independent variables were: well depth, bottom-hole elevation, elevation of the top of the Mt. Simon, and penetration into the Mt. Simon. Values of each of these independent variables were obtained for each of the 68 locations where water samples were collected. Independent-variable data were from reports prepared for gas storage hearings conducted by the Illinois Commerce Commission and from the U.S. Geological Survey,

Madison, Wisconsin. The ranges in value of the independent variables are shown in table 3.

TABLE 3
RANGES IN VALUE OF INDEPENDENT VARIABLES

Variable	Range in value (ft)
Depth	855 to 4843
Bottom-hole elevation	-35 to -4316
Mt. Simon elevation	235 to -3195
Penetration	20 to 2190

Preliminary graphical analysis of the relationship between certain dependent variables, such as TDM and Cl^-, and bottom-hole elevation revealed a good correlation for most variables, prompting a more detailed investigation into the interrelationship between the independent and dependent variables.

A step-wise multiple regression analysis was done using the four independent variables and each dependent variable separately. The step-wise multiple regression is an analysis whereby each independent variable is entered into the regression equation successively. The desired response is to reduce the standard error of estimate, which is the measure of the scatter or departure of the data points from the regression line, that is, the variance about the regression. The F-ratio is the measure of that variance with respect to a particular independent variable. If an F-ratio of 1.0 or less is obtained, the reduction in the standard error of estimate is no more than what one would expect from the introduction of a purely random independent variable into the regression analysis.

The relationship of each mineral constituent to the independent variables — depth, bottom-hole elevation, Mt. Simon elevation, and penetration — was investigated by means of the step-wise multiple regression technique described. Regression coefficients A_1-A_4, corresponding to the independent variables X_1-X_4, respectively, were computed, as were the Y-intercepts, the multiple-correlation coefficients, and standard errors of estimate. The results of the regression analyses are summarized in table 4. Missing coefficients correspond to independent variables which were eliminated by one or more of the criteria: the F-ratio fell below a specified level (usually 2.0), the multiple correlation was not significantly improved by the additional variable, or the standard error of estimate was not significantly improved by the additional variable.

Examples of regression equations generated by the results are given by the dependent variables $Na^+ + K^+$ and Cl^-. $Na^+ + K^+$ (expressed as Na^+) showed the following relationship to the independent variables:

$$Na^+ = 20.77X_1 + 12.94X_2 - 2.32X_4 - 22{,}541$$

Two variables were required to define Cl^-:

$$Cl^- = 56.42X_1 + 39.33X_2 - 60{,}446$$

None of the regression equations required the use of all four independent variables. In the case of iron, only bottom-hole elevation was found to be significant. Most equations required three independent variables, with X_1 and X_2 (depth and bottom-hole elevation) being the most commonly selected variables. With the exceptions of iron and CO_2, the multiple

TABLE 4

SUMMARY OF RESULTS OF STEP-WISE MULTIPLE-REGRESSION ANALYSIS

Dependent variable	Regression coefficients A_1	A_2	A_3	A_4	Dependent variable intercept		Multiple correlation coefficient	Coefficient of determination (%)	Standard error of estimate
$Na^{+}+K^{+}$	20.77	12.94		-2.32	-22,541	mg/l	0.95	90.2	2632 mg/l
Ca^{+2}	10.68	7.28	1.06		-11,117	mg/l	.0.92	84.6	1077 mg/l
Mg^{+2}	2.10	1.49	0.14		-2,146	mg/l	0.90	81.0	236 mg/l
Cl^{-}	56.42	39.33			-60,446	mg/l	0.94	88.4	6215 mg/l
SO_4^{-2}	1.50	1.21	-0.34		-1,573	mg/l	0.95	90.2	197 mg/l
Alkalinity	-0.18		-9.55×10^{-2}	0.13	488	mg/l	0.87	75.7	48 mg/l
Hardness	34.77	23.72	3.34		-36,202	mg/l	0.92	84.6	3532 mg/l
Iron (total)		-2.47×10^{-2}			-6.22	mg/l	0.29	8.4	88.6 mg/l
Manganese	3.40×10^{-3}	2.79×10^{-3}		4.24×10^{-3}	-4.51	mg/l	0.94	88.4	0.95 mg/l
TDM	94.53	65.76			-100,756	mg/l	0.94	88.4	10,204 mg/l
CO_2	0.31		0.31	-0.32	-166	mg/l	0.57	32.5	22.7 mg/l
pH	-3.00×10^{-3}	-2.39×10^{-3}			10.56		0.88	77.4	0.32
T,°F		-1.97×10^{-2}	-2.54×10^{-2}		-1.75F		0.91	82.8	5.1 F
Specific gravity	2.92×10^{-5}			-1.44×10^{-5}	0.9360		0.99	98.0	0.00325

correlation coefficients were high, ranging from 0.87 to 0.99 for alkalinity and specific gravity, respectively. Manganese, which one might expect to behave somewhat similarly to iron, had a correlation coefficient of 0.94, more than three times that for iron. Despite its small sample size, temperature had a multiple correlation coefficient of 0.91.

When the multiple correlation coefficient is squared, one obtains the coefficient of determination expressed in percent, which is the variation explained by the regression line with respect to the dependent variable.

As may be noted, the standard error of estimate in many instances is substantial in proportion to the lower end of the expected range of values for those constituents. Because of these relatively large standard errors, it is quite probable that the regression equations would have limited applicability in areas where mineralization is low.

Some measure of the predictability of the regression equations can be obtained by observing the fit of the measured data to the equations. For example, the equation for total dissolved minerals was used, along with the appropriate independent variables, to compute a TDM value corresponding to each sample. The computed and measured TDM values were then compared to determine how well the regression equation was able to predict TDM. As expected, the predictability of the TDM equation was quite poor in the case of samples from southeastern Wisconsin, because of the large standard error in proportion to the low mineral content of those samples. The predictability of TDM generally improved with depth. Of the Chicago area samples, the Cook County sample (2046-foot depth) had the smallest error in prediction, 22.7 percent. The greatest accuracy (least error) of the equation occurred at depths greater than 3000 feet, although 10 of the 17 samples from depths between 2000 and 3000 feet had computed TDM values within 25.3 percent of observed values. All of the 28 samples from depths below 3800 feet had computed values within 25.4 percent of measured values, and 22 of these were predicted with errors smaller than 9 percent.

A similar level of predictability was observed in the regression equations for the other dependent variables.

GEOHYDROLOGIC MODEL

The availability of saline water from the Mt. Simon aquifer in northeastern Illinois is dependent upon the hydraulic character of the aquifer as well as the density and viscosity of the water. These latter two properties vary with solute concentration and temperature and can be estimated for given conditions with appropriate tables. The hydraulic properties which govern the flow of such waters — hydraulic conductivity and storage coefficient — must also be determined, however, before reasonable estimates of expected water quality and quantity can be made.

The hydraulic properties of the Mt. Simon were evaluated from three sources of information on file at the State Water Survey: drill core analyses, well tests, and specific capacity data.

DRILL CORE ANALYSES

The most detailed data came from laboratory analyses of 45 drill cores from test holes at nine underground gas storage projects in northern Illinois (figure 8). Two additional core tests were made on cores from an industrial waste disposal well in Putnam County and a waste disposal test hole in DuPage County. All core analyses were conducted by private core testing laboratories utilizing constant-head permeameters. Data for gas storage areas were obtained from Illinois Commerce Commission testimony, while disposal well data were filed with permit applications to the Illinois Sanitary Water Board, now the Illinois Environmental Protection Agency. Copies of all the above data are on file at the State Water Survey.

Cores from the gas project test holes were taken from 48 to 598 feet into the Mt. Simon, averaging 210 feet, while the Putnam County well core sampled 274 feet from several intervals and the DuPage County well core sampled the lower 167 feet. All cores were tested for porosity and horizontal permeability, and all but the disposal well cores were also tested for their vertical permeability.

Permeability is a term often used synonymously with hydraulic conductivity. In this report permeability refers to a constant which is characteristic of the aquifer and which has the dimensions of length squared. It varies with the square of the mean grain diameter and with a dimensionless constant that depends upon porosity and on the character and packing of the grains (12). Permeability is a measure of the ease with which fluids can permeate the aquifer in a given direction. The most commonly used units in the oil and gas industry are the darcy and the millidarcy.

Hydraulic conductivity is a term which is dependent upon both the properties of the aquifer (permeability) and those of the fluid (specific gravity and viscosity). It is defined as the flow of a given fluid (usually water) in volume per unit of time through a unit cross section of aquifer under a unit hydraulic gradient. Hydraulic conductivity has the dimensions of velocity and the commonly used units of gallons per day per square foot.

Examination of the permeability data for each core revealed no apparent correlation

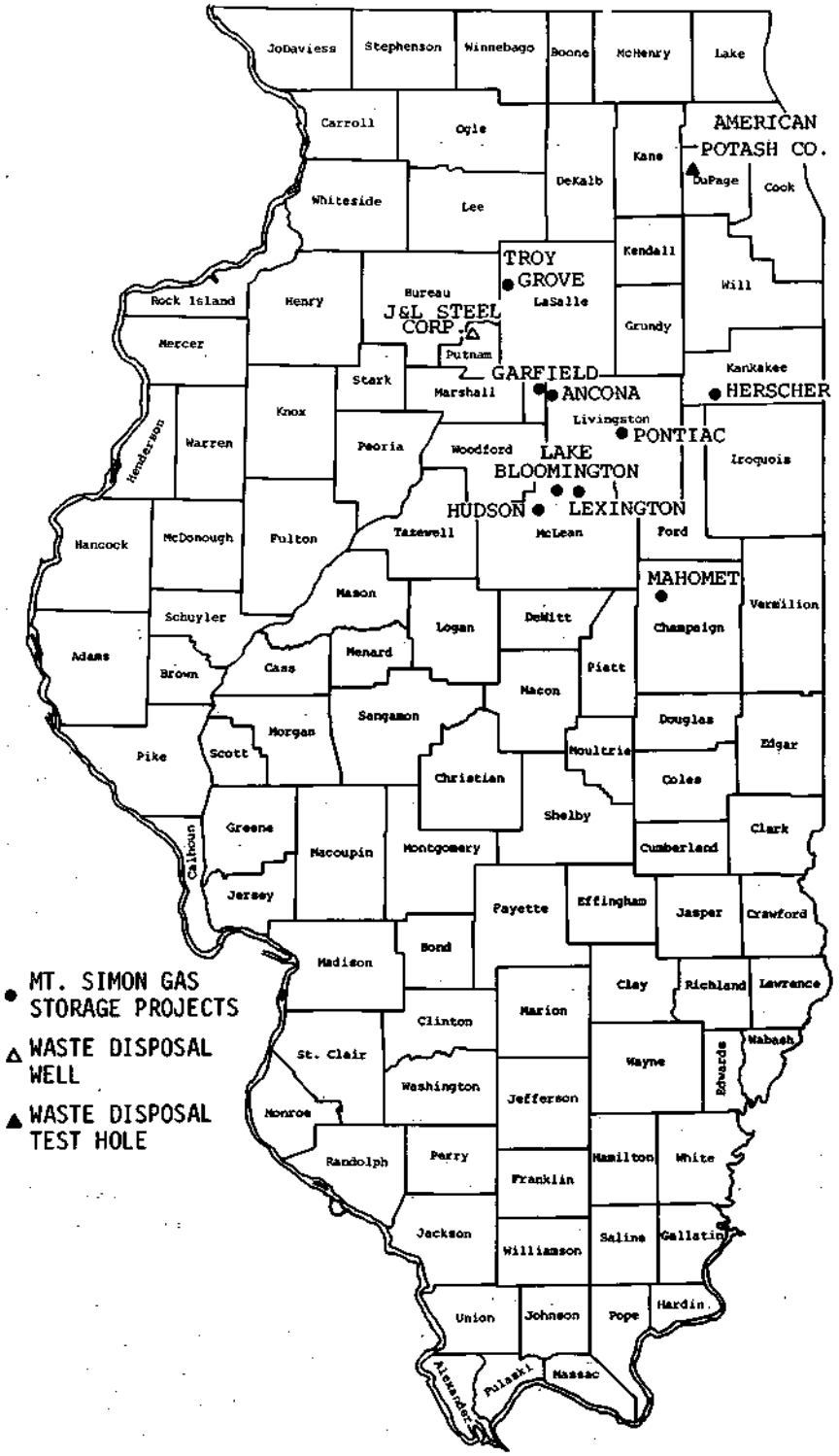

Figure 8. Locations of drill cores from Mt. Simon aquifer

with depth; permeabilities varied from 10^{-3} to 10^{3} millidarcies in a seemingly random fashion. It was assumed, therefore, that the most meaningful quantitative measure for each core would be an average value of permeability. Lovelock (13) suggested that the geometric mean $[\bar{x} = (x_1 \cdot x_2 \cdot x_3 \cdot \ldots x_n)^{1/n}]$ is the most representative mean value to use under such conditions. The geometric mean permeability was computed for each of the cores with the results shown plotted versus mean sea level elevation in figure 9. The line represents the regression equation for all cores, while the points represent the averages of the data at each gas field (but actual values for the waste disposal sites).

The ratio of vertical to horizontal permeability (P_v/P_h) was also computed for each core by dividing their geometric mean values by one another. These results are shown plotted versus mean sea level in figure 10, where the line again represents the regression equation for all the data and the points show the averages at each gas field.

Figures 9 and 10 suggest that on a regional basis there is an apparent relationship of these variables with depth. Correlation coefficients, however, were only 0.68 and 0.53 for horizontal permeability and P_v/P_h, respectively. In addition, the scatter of data points (not shown) about the regression lines was considerable, as evidenced by the standard errors of estimate for these two variables —12.5 millidarcies and 0.13, respectively.

PUMPING TEST ANALYSES

Pumping test data from the Mt. Simon aquifer were available from three long-term tests conducted in 1962,1965, and 1969 at gas storage project sites. The tests were conducted at pumping rates of 80, 45, and 56 gpm for periods of 48, 40, and 18 days, respectively. At least five observation wells were available at each site; however, because of the partial penetration effects caused by the great thickness of the Mt. Simon aquifer, data from distant (greater than 1.5 times the aquifer thickness) observation wells were given preference to those from wells closer to the pumped well, in order to avoid distortions in data caused by partial penetration of wells.

Data from the distant observation wells were analyzed by graphical techniques described by Walton (14). The results are summarized below.

Gas storage site	General location	Average transmissivity (gpd/ft)	Average storage coefficient
Ancona	NW LaSalle Co.	10,600	1.8×10^{-4}
Pontiac	Central Livingston Co.	1,635	1.3×10^{-4}
Hudson	NW McLean Co.	980	5.2×10^{-5}

For comparison one can, by assuming an aquifer thickness of 2500 feet and using estimated field temperatures, convert the above values of transmissivity into permeabilities of 180, 22.4, and 12.3 millidarcies, respectively. These compare with the geometric means determined from cores at these sites of 39.6, 4.2, and 16.5 millidarcies, respectively. The permeabilities compare reasonably well only at Hudson, whereas those at Ancona and Pontiac are larger by factors of 4.5 and 5.3, respectively. The permeabilities are shown plotted versus mean sea level elevation in figure 11. An additional test was reported in Illinois

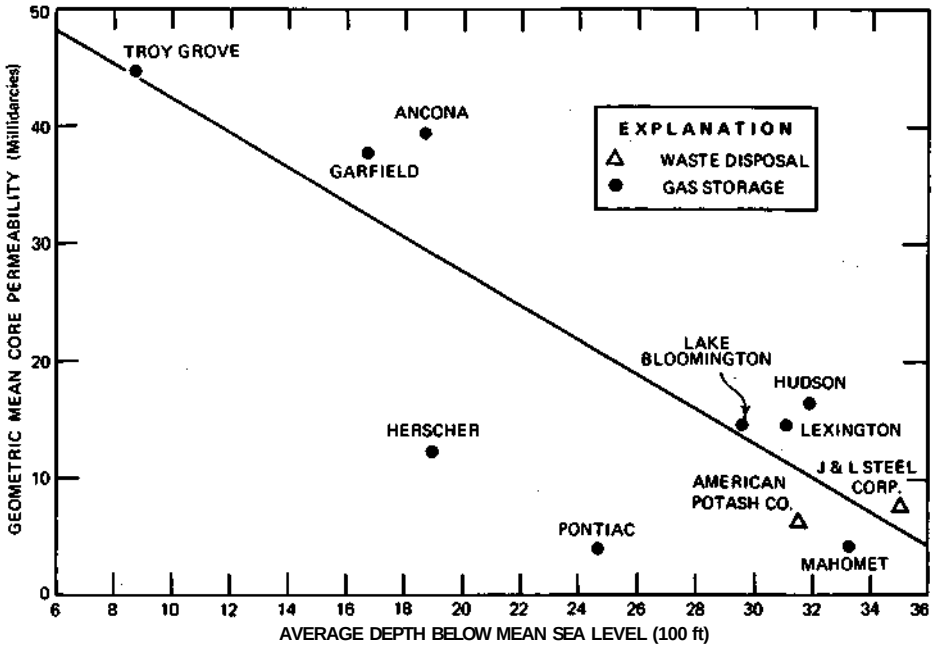

Figure 9. Horizontal permeabilities determined for drill cores from the Mt. Simon aquifer

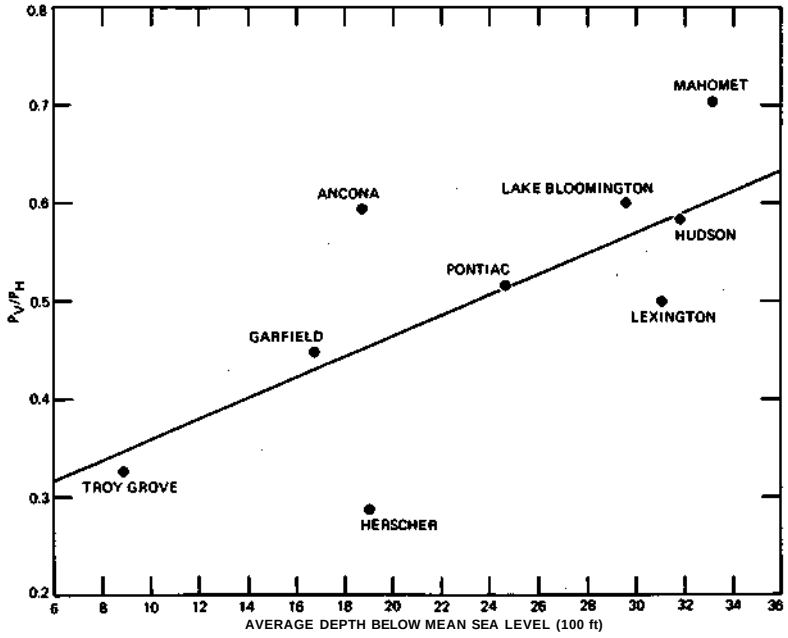

Figure 10. Ratios of vertical to horizontal permeabilities for drill cores from the Mt. Simon aquifer

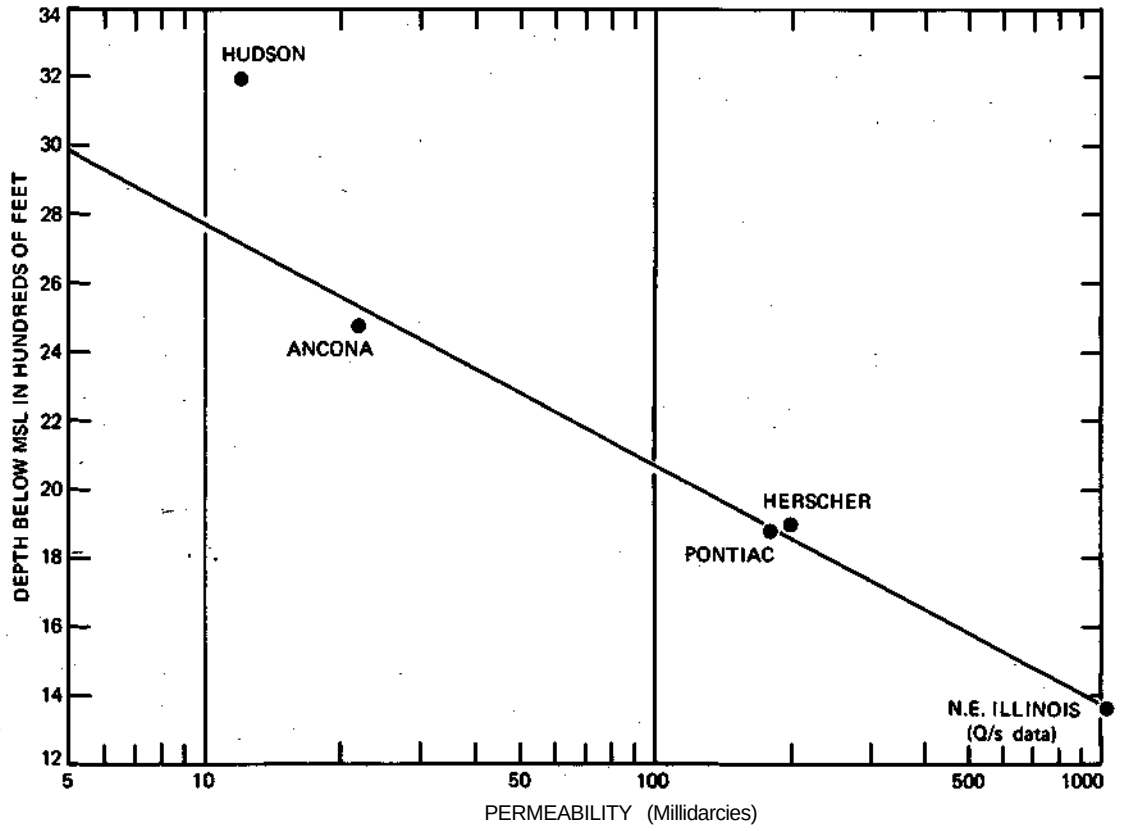

Figure 11. Permeabilities determined from well tests and specific capacity data

Commerce Commission testimony for the Herscher field in 1957. The permeability computed from the test was reported to be 200 millidarcies and is included in figure 10.

SPECIFIC CAPACITY ANALYSES

Specific capacity data can often be useful for estimating aquifer transmissivity and, therefore, hydraulic conductivity. The technique of constructing graphs of specific capacity versus transmissivity for various values of time, well radius, and storage coefficient is described by Walton (14). Application of such graphs transforms specific capacity data into estimates of aquifer transmissivity.

In the four-county area of Cook, DuPage, Kane, and Will Counties, 38 values of specific capacity were estimated from data in Water Survey files for wells penetrating the top of the Mt. Simon aquifer. Only one specific capacity was for a well open only in the Mt. Simon. The remaining specific capacities were for wells open to both the Mt. Simon and to various higher bedrock units. The average depth of Mt. Simon penetration in these wells was 270 feet.

Walton and Csallany (7) estimated yields of individual units of the Cambrian-Ordovician and Mt. Simon aquifers to selected wells in the Chicago area. Their estimates were applied to the specific capacity data in the Chicago area and used in conjunction with the specific capacity-transmissivity graph technique (14) to estimate the transmissivity of the Mt. Simon aquifer at these well sites. Transmissivity was then divided by the depth of penetration at the well to determine a coarse estimate of the hydraulic conductivity. No attempt was made to correct these computed values for partial penetration; horizontal flow lines were assumed, since P_v/P_h values for this area are rather low (0.3 to 0.4).

Values of hydraulic conductivity derived in this manner ranged from 1.2 to 450 gpd/ft^2 and averaged 68.1 gpd/ft^2. Their geometric mean was 18.9 gpd/ft^2, which is in close agreement with the value of 16 gpd/ft^2 estimated by Walton and Csallany (7) for the Mt. Simon in northern Illinois. The geometric mean value, 18.9 gpd/ft^2, corresponds to a permeability of 1040 millidarcies. This value is plotted on figure 11, using the average elevation for the wells described which is minus 1350 feet.

Analyses of the three sets of permeability data described above produce two main findings. One is the apparent regional trend of decreasing permeability with depth, and the other is the noticeable discrepancy between core permeabilities and permeabilities determined from well production and specific capacity tests.

Figures 9 and 11 show that for both core and well tests, the permeabilities decrease as the depth increases. Core permeabilities show a decrease of nearly 15 millidarcies for each 1000 feet of elevation loss, while well test permeabilities (plotted on semilog paper) decrease approximately 1.4 log cycles per 1000 feet of elevation loss. The data in figure 11 are admittedly sparse and, therefore, not conclusive; however, the depth-related trend is evident.

The discrepancy between core data and well tests is most reasonably accounted for by a consideration of the lithology involved. Discussions held with geologists associated with the Mt. Simon and other coring projects have resulted in general agreement concerning the

matter. The cores may not be truly representative of the total thickness of the Mt. Simon or even necessarily of the intervals sampled. Because of the lithologic character of the Mt. Simon involving thin zones of silty material in the upper portion of the sandstone, and the non-continuous nature of the coring, two things are believed to occur which could affect the sampling. The more permeable zones of the Mt. Simon tend to be friable and are frequently not amenable to coring. These zones are not included in the core intervals analyzed by laboratory processes but are studied by stratigraphers from a descriptive standpoint. Thus, the sampling would tend to be weighted toward the more cohesive (and less permeable) zones, since coring would likely be more complete there. It is also possible that permeabilities from cores differ from those of well tests, because cores might not reflect the weighted aquifer properties (because of their non-continuous sampling) to the extent that flow toward a well does.

Since well tests tend to reflect actual performance characteristics, it seems reasonable to place more weight on permeabilities derived from these tests rather than on those found in laboratory tests of cores. Core data are probably most useful for providing estimates of P_v/P_h ratios for areas of interest by using figure 10 along with appropriate mean sea level elevations.

DIGITAL COMPUTER MODEL

A digital computer model which has the capability of simulating pumping from wells or well fields and tracing the movement of 14 different chemical constituents as a result of changing pressures in the aquifer was developed for the Mt. Simon aquifer.

The digital model is based upon a finite difference approach to solve the equations governing the flow of groundwater. The finite difference approach first involves replacing the continuous aquifer system parameters by an equivalent set of discrete elements. In working with digital computers both the space and time variables are treated as discrete parameters. Secondly, the equations governing the flow of groundwater in the discretized model are written in finite difference form. Finally, the resulting set of finite difference equations is solved numerically with the aid of a digital computer.

In the Mt. Simon digital model the aquifer is subdivided by a finite-difference grid into a two-dimensional cross section network with radial symmetry as shown in figure 12. Thus the digital model is in effect a three-dimensional representation of the aquifer. The finite-difference grid is variable in dimensions in the horizontal direction, with a fine spacing near the well or well field and progressively larger spacings with distance from the center of pumping. The finite-difference grid, in the vertical direction, is broken down into 20 separate layers. Each of these layers initially represents l/20th of the thickness of the aquifer and is assigned a category number as shown in figure 12. The horizontal finite-difference grid lines represent isochemical and constant aquifer property lines.

It should be noted that the vertical scale of figure 12 is greatly reduced compared with the horizontal scale. For example, if the aquifer thickness equals 2600 feet and the well radius equals 1.0 feet then the ratio of the vertical to horizontal scales is 52 to 1.

The equations governing the flow of groundwater in a discretized model such as that discussed above have been given previously by Prickett and Lonnquist (15) and will not be repeated here; however, explanations will be provided where conditions are greatly different.

The following main assumptions have been made in designing the computer model. These are based mainly upon the hydrogeologic and water quality studies described earlier.

1) All pumped water is derived from storage by the compaction of the aquifer and its associated beds and by the expansion of the water itself, and as such no recharge is included.
2) The vertical chemical profile within the cone of influence of pumping is everywhere initially the same.
3) No chemical reactions take place as a result of water flowing in the aquifer system.
4) The effects of dispersion and diffusion on the chemical profile are negligible as a result of the changing flow pattern over that existing initially.
5) No heat is exchanged between the flowing water and the aquifer as a result of pumping.
6) The entire aquifer system is initially under steady state conditions.

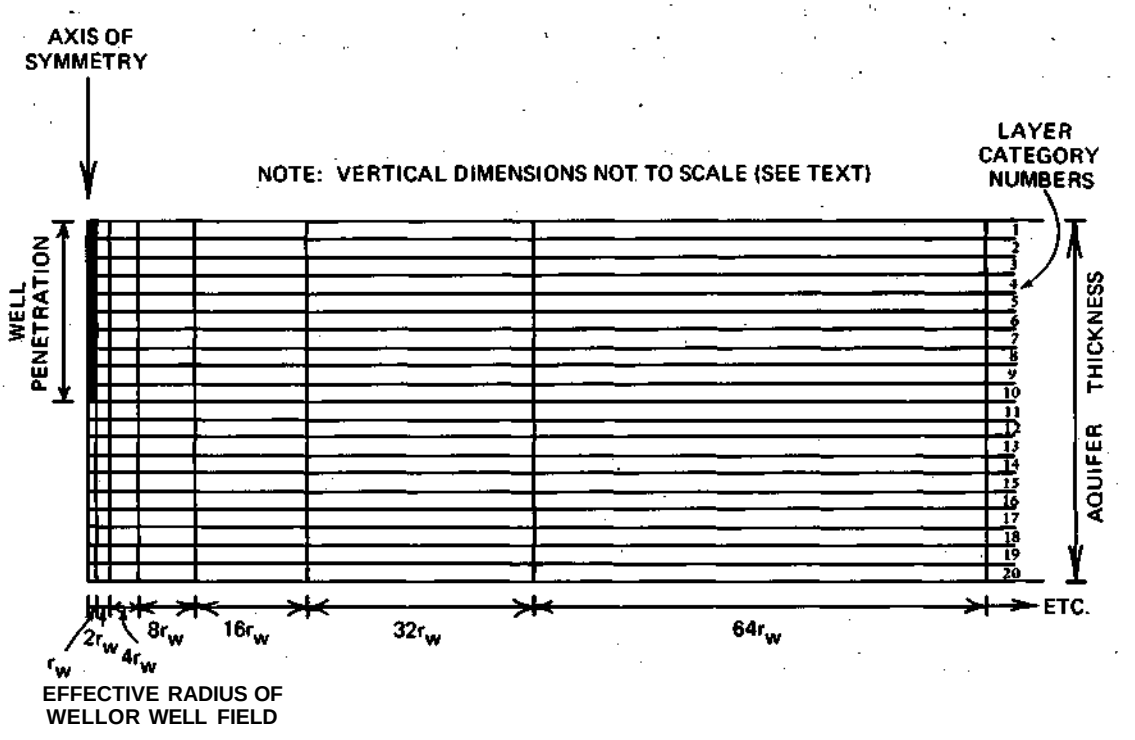

Figure 12. Initial finite-difference grid for Mt. Simon aquifer model

PROGRAM OPERATIONAL SEQUENCES

A brief description of the operation of the computer model follows. The flow chart is shown in figure 13 and the example finite-difference grid in figure 14.

The program is composed of five main sections. In the first section the characteristics of the well or well field are defined and chemical quality and aquifer property data are assigned to each of the 20 layers of the model. During the entire simulation, the chemical quality within each model layer stays the same. However, as will be explained later, the layers are allowed to move vertically and to change size.

In the second section the pressure distribution in the aquifer is calculated as a result of pumping for a given time interval. The iterative alternating direction implicit (IADI) method described by Prickett and Lonnquist (15) was used to compute the pressure distribution. As water is removed by pumping and pressures decline, the chemical quality distribution in the aquifer changes. This can be seen, for example, in figure 14. Near the well or well field the lines of constant chemical quality begin to converge toward the point of discharge. Water at the bottom of the aquifer is drawn mainly upward toward the well, whereas water at the top of the aquifer moves laterally toward the well.

The third main section of the computer program computes the locations of the horizontal grid lines of the model due to changing pressures and water movement in the aquifer. Under ordinary circumstances the finite grid of groundwater models is regarded as fixed in space. However, the computer model for the Mt. Simon aquifer incorporates grid lines which are allowed to move in accordance with water movement. Only the horizontal lines are allowed to move whereas the vertical lines remain fixed. This procedure was used mainly because the prime interest of this project was to trace movement of waters of varying chemical quality, and from a numerical standpoint, the moveable grid allows a much simpler way of programming. In fixed grid line models it would be necessary to carry along two sets of grids, one for the calculations of pressures and another one for tracing the movement of isochemical lines. In the moveable grid model the pressures are calculated along a single set of isochemical lines.

The fourth section of the program integrates the water quantity contributions from individual layers of the model to the well or well field. Since the chemical quality of each layer is known, the resultant chemical quality mixture of the pumped water can be calculated.

The last main section of the program adjusts the model aquifer properties to fit the changes in size of the individual layers as time progresses. Some layers enlarge in size during pumping (those at the bottom of the aquifer near the well) and others contract (those at the top of the aquifer). The layers that enlarge in size have larger thicknesses than initially defined and therefore are capable of transmitting and storing more water. The reverse is true for the layers that contract. Before proceding to another time interval in the simulation, adjustments in individual layer transmissivities and storage properties are made.

The total process of pumping, calculating pressure distribution, moving layer boundary lines, computing chemical quality of pumped water, and adjusting model aquifer properties is repeated for the total number of time increments desired.

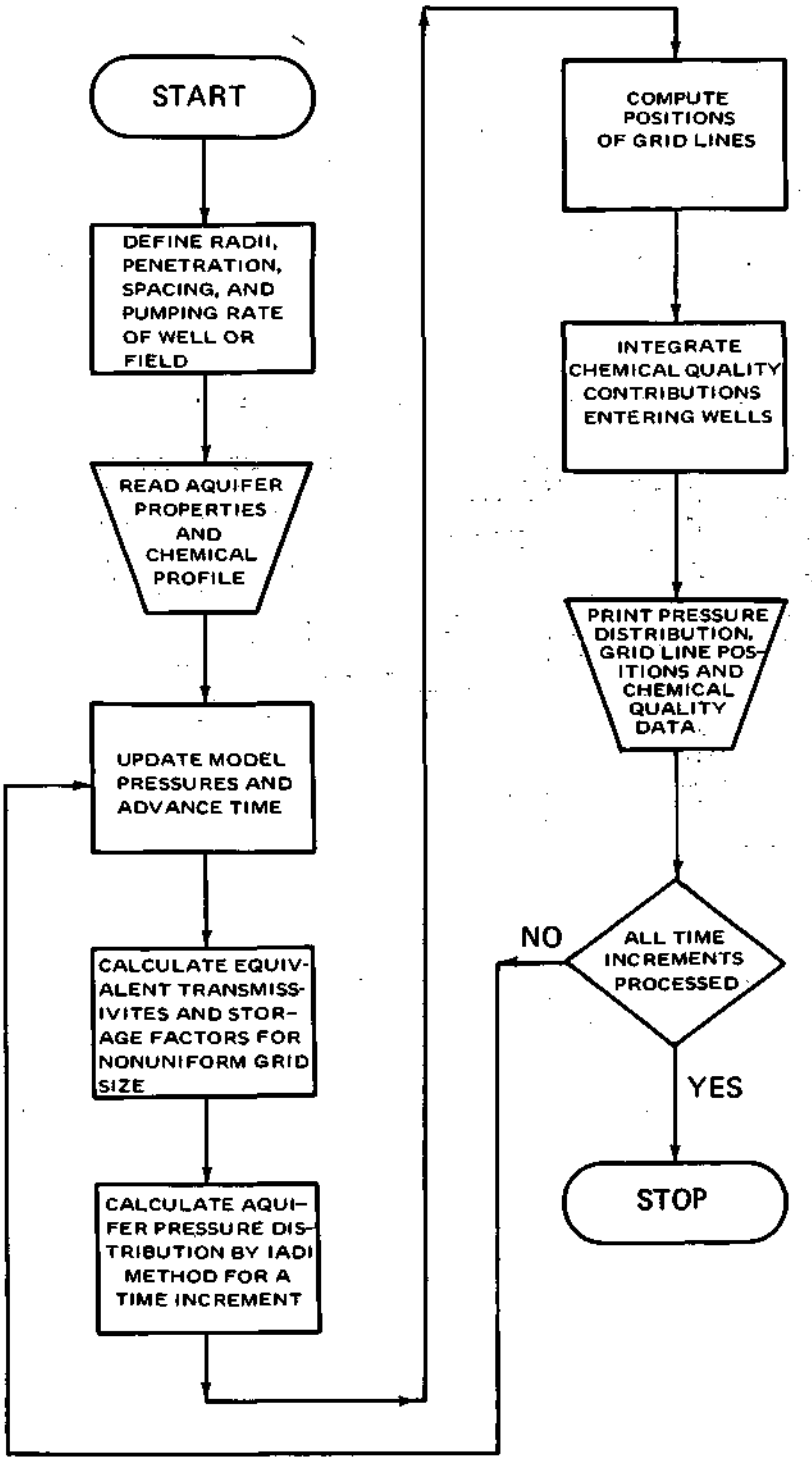

Figure 13. Flow chart for Mt. Simon aquifer model

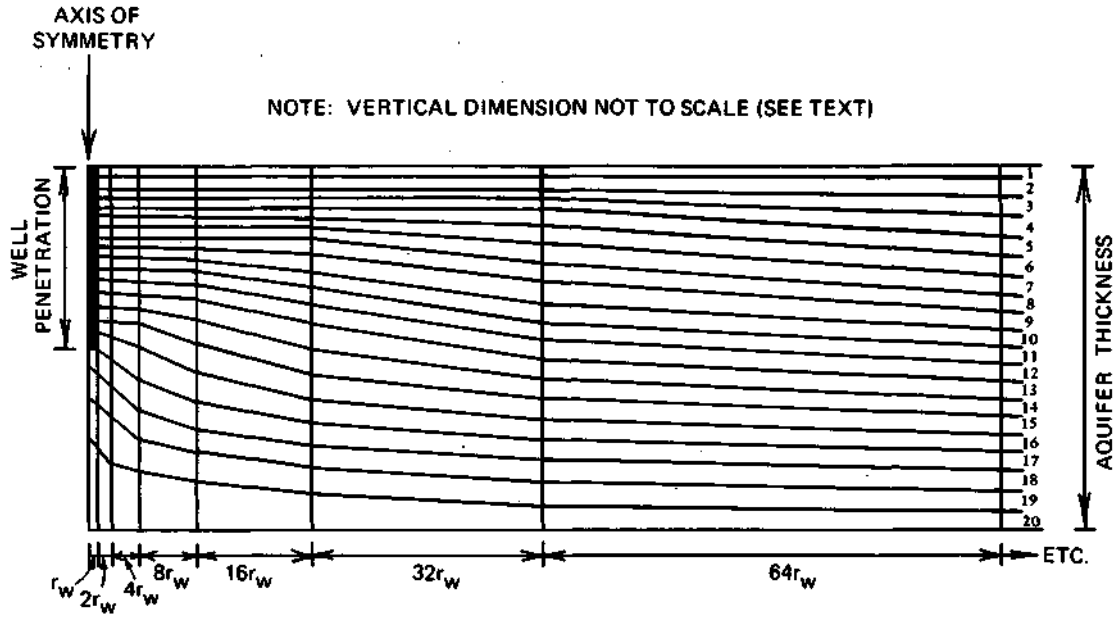

Figure 14. Example of finite-difference grid as a result of pumping

THEORETICAL AND CASE HISTORY MODEL RESPONSE TO PUMPING

Several computer runs were made to check the validity of the programming. Unfortunately, very few comparisons of theoretical solutions versus computer simulations could be made since, except for relatively simple cases, theoretical solutions are nonexistent. Therefore, the model response was checked against two known theoretical solutions for uniform aquifer conditions; comparisons were made between aquifer response under uniform conditions and model simulated distributions of specific gravity and temperature; and finally a comparison was made between a model simulated and an actual field case history.

The first comparison between model response and theory is shown in figure 15. In this case a fully penetrating well was pumped at a constant rate of 694 gallons per minute (gpm) in an aquifer of uniform properties of transmissivity equaling 10,000 gpd/ft at 68.4 F, specific gravity equaling 1, and an aquifer storage coefficient of 2.8×10^{-4}. An analysis made of the model response to pumping under the above conditions is shown in figure 15. The agreement with theory is excellent. By using a 100 percent penetrating well in this comparison, all water flow is radial. Thus for this first comparison there was no vertical movement of layer boundaries and a separate check was needed.

Figure 16 shows the model response resulting from pumping a 31 percent penetrating well in an aquifer that has a vertical to horizontal hydraulic conductivity ratio of 0.5. Again the comparison of output response is in excellent agreement with theory.

In this case, a great deal of vertical flow is prevalent near the pumped well and therefore individual layer boundaries change significantly during the simulation. Thus, this simulation is an independent check on the method of adjusting layer flow properties as a result of the changing size of the finite-difference grid.

The reader will notice the fluctuations of the computer data around the solid line for the pumped well curve of figure 16. These fluctuations (less than about 1 percent of the total drawdown) are due to two phenomena; i.e., the slight inaccuracies in the assumptions made in phasing in individual layers to the pumped well as time progresses and the effects of discretizing time. The layers begin moving upward toward the well when pumping starts. As pumping continues, some layers begin contributing water to the well, whereas initially they were located at some depth below the bottom of the well. As these layers move upward they eventually become connected to the well. However, the layers, as they come into the well, are themselves partially penetrated. Thus until a layer is fully contributing to the well an extra adjustment must be included. This flow adjustment was somewhat empirical but was based primarily on standard partial penetration corrections given in groundwater text books. Considerable effort was made to take care of this effect properly.

It should be realized that the accuracy of the computations is dependent upon the number of model layers. The more layers included in the model, the better the accuracy (and the less fluctuation of output data). However, large numbers of model layers increase the cost of the computer runs significantly. A reasonable compromise between accuracy and cost had to be made.

The discretization of time also causes some fluctuations in drawdowns of the computer model, and the only way found to minimize these was to reduce the time increments to an acceptable size.

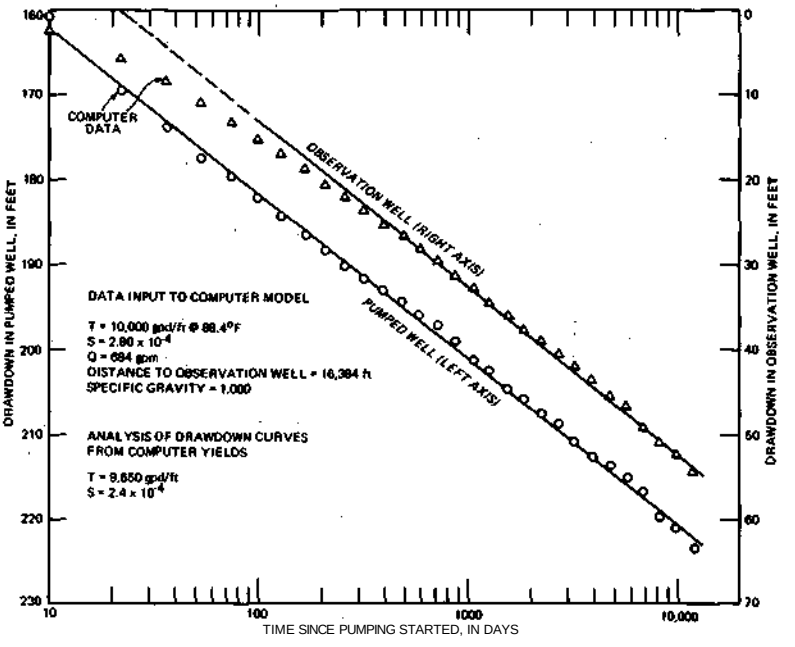

Figure 15. Comparison of model response and theoretical response for a 100 percent penetrating pumped well

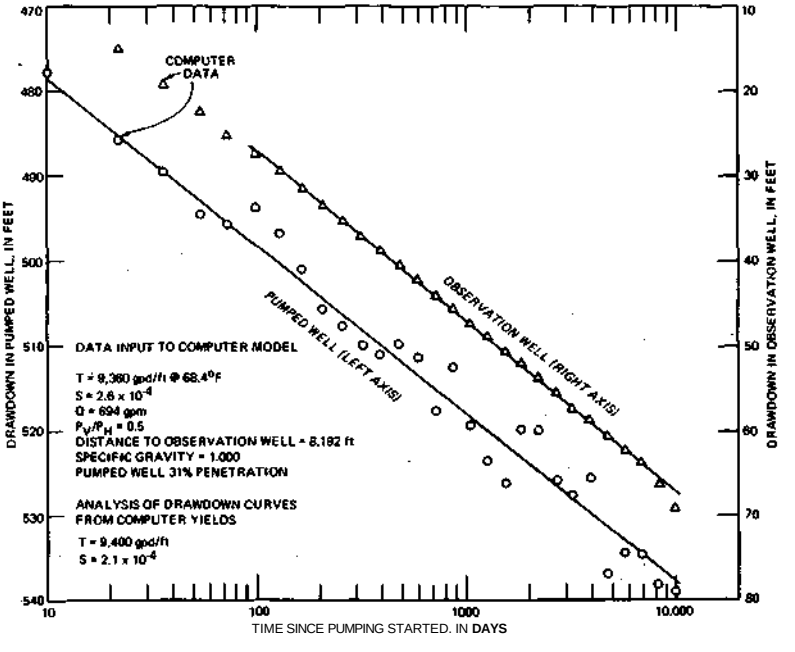

Figure 16. Comparison of model response to theoretical response for a 31 percent penetrating pumped well

A third simulation run was made to check the model response for the effects of interaction of various temperatures in the model layers. The hydraulic conductivity of the aquifer parts is a function of temperature (because it affects the viscosity of the flowing fluid) and incorporating this feature in the model is not difficult. The temperature profile of table 5 was assigned to the model layers for this problem. Even though the theory is available to describe fluid flow in the individual model layers, there is no known theoretical solution to this problem for the entire aquifer to compare with the computer simulation. However, a comparison can be made with the results of the pumped well response given in figure 16 since the only difference here is that a temperature profile was added over and above that included in the simulation shown in that figure. Figure 17 shows the comparison of drawdowns and the temperature of the pumped water. A line was drawn through the computer drawdown data. The exact position of that line is somewhat ill defined but the trend is obvious. At the beginning of pumping, the water pumped from the well was colder than the constant 68.4 F curve of figure 16, so the viscosity is greater causing a greater drawdown. However, as time progresses the water becomes warmer, the viscosity decreases, and the time rate of decline in water levels decreases.

The fluctuations in water levels in figure 17 are again evident. However, the fluctuations are still about only 1 percent of the total drawdown and are considered acceptable. Even though the drawdown data are fluctuating, the temperature curve is smooth, as shown in figure 17. At this point it can be realized how insensitive the chemical quality of the pumped water will be to the instantaneous head in the pumped well. It is only the long-term heads that will affect water quality since there is a tremendous amount of water in storage in the aquifer and it takes considerable time for water to travel from place to place in the system.

A fourth comparative analysis was made of the effects of a specific gravity distribution imposed on the computer model. Here again, there is no known theoretical solution to compare with the computer response. The specific gravity profile of table 5 was assigned to the model layers, and the computer model response to pumping is shown in figure 18 in comparison with the pumped well response of figure 16. All other coefficients of the two simulations are the same. As indicated in figure 18 the specific gravity of the pumped water is initially greater than 1.000, so a greater drawdown than in figure 16 is realized. As time progresses, the specific gravity of the pumped water steadily increases and causes greater and greater drawdown in the well as would be expected with the heavier water.

Although the above theoretical and simulation comparisons lend confidence to the validity of the computer model, an attempt was made at computer simulating past histories of chemical quality changes under field conditions in a well field at Aurora, Illinois. This well field consists of four wells which penetrate both the upper portion of the Mt. Simon aquifer (about 500 feet) and the entire overlying Cambrian-Ordovician aquifer. Thus, pumpage from this field represents a mixture of waters from the two aquifers. A study of individual yields of wells penetrating these aquifers indicates that about 25 percent of the total pumpage from this Aurora well field is derived from the Mt. Simon aquifer and the remainder from the Cambrian-Ordovician aquifer. Pumpage from this well field began in the early 1900s when the first two wells were drilled and generally increased with time. Two additional wells were added to the field in the early 1930s. Pumpage records indicate that between 1941 and 1968 pumpage rates, as a total, from the well field stabilized at about 2.8 mgd. However, consider-

TABLE 5

CHEMICAL PROFILE FOR MT. SIMON AQUIFER AT AURORA

Model layer	T°F	Specific gravity	TDM	Na+K	Mg	Cl	SO_4	Ca	Alkalinity ($CaCO_3$)	Hardness ($CaCO_3$)	Fe	Mn	Inverseof viscosity	pH	P_v (@68.4 F)	P_h (@68.4 F)
1	60	1.000	500	50	30	100	120	90	280	145	1	0.1	0.90	7.90	1.8	3.6
2	63	1.000	1,000	200	40	500	122	100	275	450	5	0.2	0.93	7.75	1.8	3.6
3	64	1.001	1,500	250	45	650	126	140	269	600	8	0.3	0.94	7.62	1.8	3.6
4	65	1.002	3,500	800	60	2,000	142	350	250	900	18	0.9	0.95	7.48	1.8	3.6
5	67	1.004	6,200	1,500	80	3,500	168	470	235	1,200	29	1.1	0.98	7.38	1.8	3.6
6	68	1.007	11,500	2,800	90	6,500	205	520	215	2,500	36	1.7	0.99	7.26	1.8	3.6
7	71	1.012	19,500	4,800	250	11,500	320	1,320	205	4,200	42	2.5	1.02	7.03	1.8	3.6
8	73	1.016	25,500	6,300	420	14,700	420	2,200	195	7,200	46	3.1	1.08	6.90	1.8	3.6
9	74	1.020	30,500	7,600	580	17,700	500	3,000	187	9,800	50	3.8	1.10	6.80	1.8	3.6
10	76	1.024	35,500	8,800	720	21,000	570	3,700	175	12,000	54	4.4	1.13	6.72	1.8	3.6
11	78	1.027	39,500	9,800	850	23,000	630	4,300	170	14,200	57	4.9	1.16	6.64	1.8	3.6
12	80	1.033	46,500	11,600	1020	27,500	740	5,400	160	17,500	61	5.8	1.19	6.59	1.8	3.6
13	82	1.037	51,500	12,800	1150	30,500	820	6,100	147	19,800	63	6.3	1.22	6.54	1.8	3.6
14	84	1.042	58,000	14,400	1260	34,500	920	7,100	135	22,700	67	7.2	1.25	6.53	1.8	3.6
15	85	1.045	62,000	15,500	1350	36,700	980	7,700	130	24,600	69	7.8	1.26	6.51	1.8	3.6
16	87	1.048	65,500	16,300	1420	39,000	1030	8,200	125	26,700	71	8.2	1.29	6.47	1.8	3.6
17	89	1.054	73,000	17,800	1550	43,000	1150	9,200	108	29,700	75	9.1	1.32	6.43	1.8	3.6
18	91	1.057	77,000	18,600	1680	45,200	1220	9,800	100	32,700	78	9.6	1.35	6.39	1.8	3.6
19	93	1.062	83,000	19,900	1730	48,700	1320	10,600	90	33,700	81	10.3	1.37	6.34	1.8	3.6
20	95	1.066	88,000	21,000	1950	52,000	1400	11,500	80	36,700	85	11.0	1.40	6.30	1.8	3.6

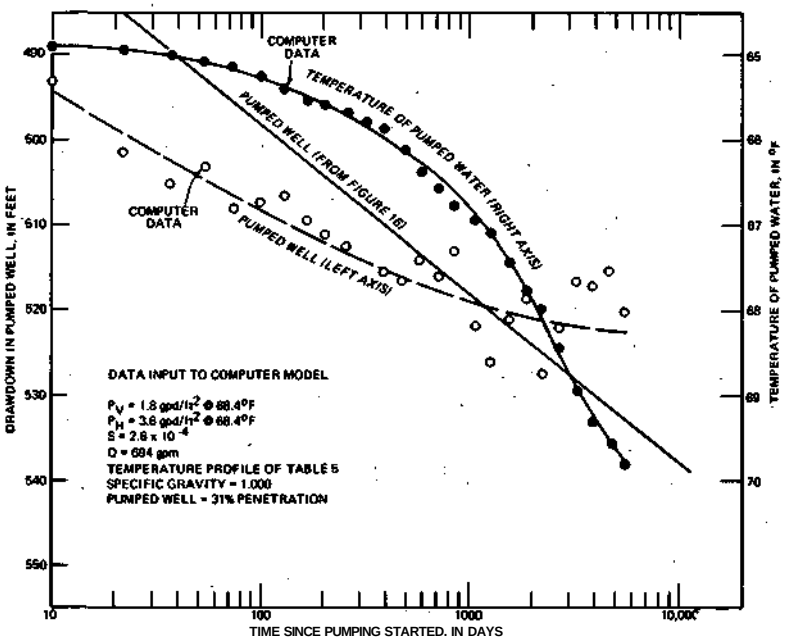

Figure 17. Comparison between model response with temperature profile and uniform temperature model

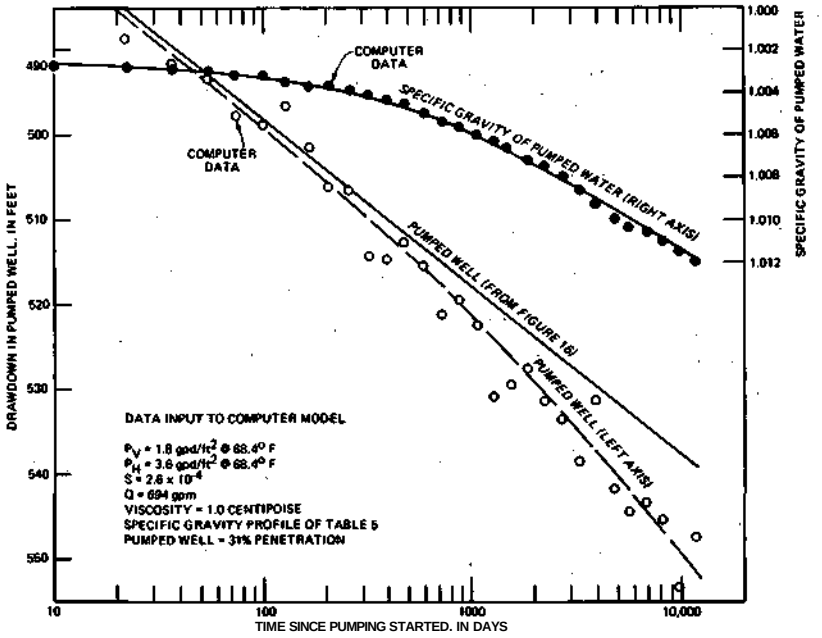

Figure 18. Comparison between model response with specific gravity profile and uniform specific gravity model

able alternating of pumpage among the wells was practiced. Chemical quality analyses of water pumped from the four wells have been conducted somewhat erratically over the years, but a definite characteristic of increasing total dissolved minerals and chlorides has been noted. In recent years total dissolved minerals of over 4000 mg/l and chlorides consistently over 1000 mg/l have been measured. In the early 1940s chemical analyses showed TDM values around 600 mg/l and chloride contents about 220 mg/l .

A computer simulation was set up for the above well field situation. The vertical chemical profile for the Mt. Simon aquifer shown in table 5 was used as the main input data to the computer model. The characteristics of the well field were taken into account and an average pumpage rate of 700,000 gpd (25 percent of total pumping rate as explained above) was used for the 27-year period between 1941 and 1968. The simulation was carried out with the following results.

Total dissolved minerals ranged from about 900 mg/l initially to 4600 mg/l at the end of 27 years of pumping. The chloride content varied from 350 mg/l initially to about 2400 mg/l at the end of pumping. In mixing the Mt. Simon water with the Cambrian-Ordovician water it was assumed that the latter water had a TDM content equal to 300 mg/l and a chloride content of 10 mg/l and remained constant over the period of the simulation. The comparison between measured and simulated TDM and chloride levels for this case history is encouraging in light of the lafge number of estimates needed as input to the computer model.

WELL FIELD DESIGN

Several studies were made initially to find a set of well and well field characteristics that possibly would be reasonable and practical. Since the individual well drawdowns and chemical quality output were not known in advance, a series of various well and well field schemes were designed on the basis of theoretical estimates. Originally three different well schemes were chosen for each of three constant feedwater rates of 1, 5, and 10 mgd. Thus altogether nine different schemes were studied. As will be outlined later, these nine basic schemes, in various combinations, were used to provide variable feedwater rates required as a result of continuously declining desalinization plant efficiencies, which in turn were due to the increasing TDM of the feedwater with time.

The nine well and well field schemes are as follows. First, the 1 mgd feedwater rate can be supplied by a single well having a penetration into the Mt. Simon aquifer of 20, 31, or 50 percent of the aquifer's total thickness. The three simulated 5 mgd feedwater supplies are made up of five 1 mgd wells having identical penetrations of 20, 31, or 50 percent. The spacing of the five wells for the three penetrations is the same, as shown in figure 19A. The three 10 mgd feedwater supplies are made up each of ten 1 mgd wells having identical penetrations, again of either 20, 31, or 50 percent penetration with a spacing as shown in figure 19B. All wells of all schemes are designed to yield 1 mgd and have the characteristics shown in a later section in figure 43.

WATER QUALITY PREDICTIONS

The process by which the final water quality predictions were made (the results are shown in tables 9 through 11) can be summarized by using the constant rate 5 mgd 31 percent

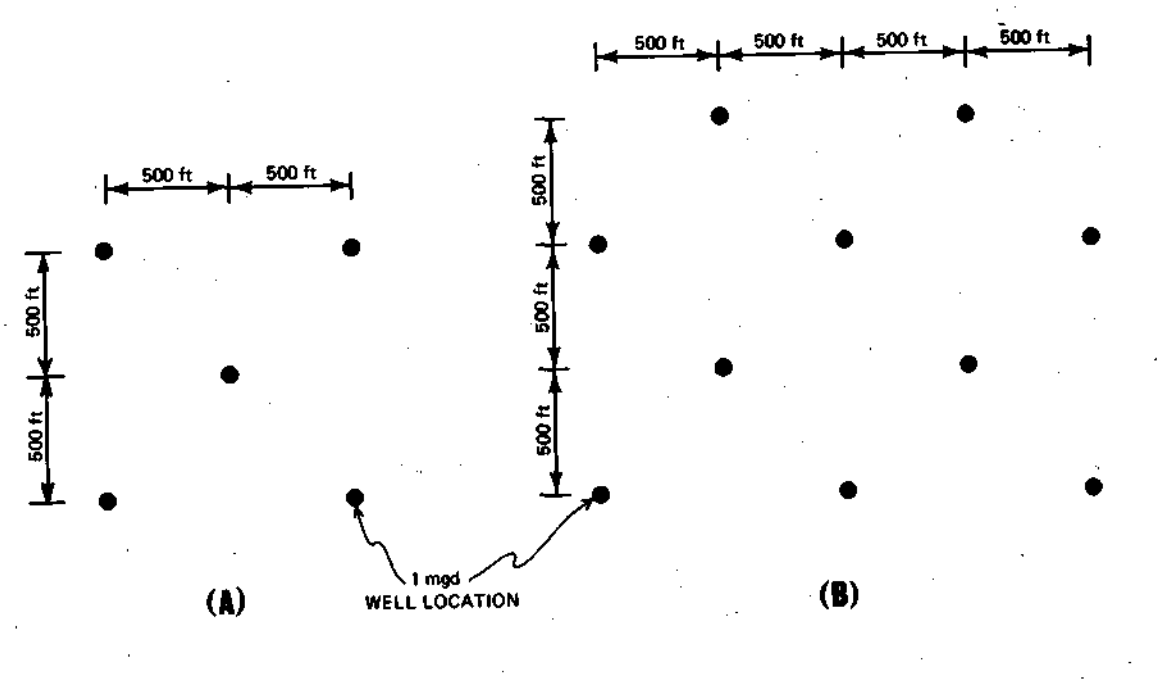

Figure 19. Well spacing schemes for 5 mgd feedwater rate and 10 mgd feedwater rate

penetration well scheme as an example. First, as with all simulations, the chemical profile of table 5 was used as the main input data. The characteristics of the 5 mgd well spacing and penetration were entered and the computer model simulation of 30 years of constant pumping was carried out. Initially graphs were prepared of the variation in chemical quality of the pumped water based on the computer output data for all constituents of interest except pH. (A separate computer program was written, on the basis of modified equations derived by Trussell and Thomas (16), for the predictions of pH values resulting from water mixtures.)

An example of TDM variation with time for the above 5 mgd 31 percent penetration scheme is shown in table 6. As time proceeds the TDM values increase as waters of high mineral content are progressively drawn up into the well field. As the mineral content of the pumped feedwater increases, the ratio of brine waste water to product water increases. The end effect is that increasing mineral content of the constant rate feedwater input results in a decreasing output rate of the product water (see discussion in the section on *Desalting Processes).*

TABLE 6
INITIAL TDM PREDICTION OF MT. SIMON AQUIFER
FEEDWATER FOR CONSTANT PUMPING 5 MGD
31 PERCENT WELL FIELD SCHEME

Years of pumping	TDM (mg/l)
0	9,000
1	15,400
2	19,200
3	22,000
4	24,000
5	25,400
10	30,000
15	32,800
20	34,400
25	35,600
30	35,900

The main goal of this feasibility report is based upon a constant product water rate. Therefore a variable feedwater rate, increasing with time, must be supplied to the desalinization plant to maintain the desired constant output. Unfortunately, a variable feedwater rate changes the chemical quality of the feedwater and in turn changes the ratio of product to brine water rates which results in a different needed feedwater rate, etc. etc.

The reader should realize that the needed feedwater rates were unknown until the desalinization plant designers analyzed the water quality curves. Therefore the Water Survey and Hittman initiated an iterative exchange of predicted chemical quality curves for various feedwater rates and needed feedwater rates for constant product water and continued this exchange until a satisfactory stable solution to the problem was achieved. In this process, two of the original nine basic schemes were eliminated from consideration, i.e., the 10 mgd 20 percent scheme, for lack of available drawdown, and the 1 mgd 31 percent scheme for lack of convergence of chemical analysis results.

Continuing with an explanation of the constant feedwater rate of the 5 mgd 31 percent scheme, an initial set of chemical quality curves was sent to Hittman for analysis and the iterative scheme described above began. The final variable feedwater rate chemical quality values for all constituents are given later in tables 9 through 11. The final variable feedwater rates for all schemes are given in table 7.

TABLE7

VARIABLE FEEDWATER RATES NEEDED FOR CONSTANT PRODUCT WATER RATES

(Feedwater rates in million gallons per day)

Years of pumping	20 Percent well penetration		31 Percent well penetration		50 Percent well penetration		
	1 mgd	5 mgd	5 mgd	10 mgd	1 mgd	5 mgd	10 mgd
0	1.1	6.7	7.3	15.4	1.7	9.3	20.4
1	1.1	8.0	8.8	21.2	1.7	11.7	26.2
2	1.2	9.1	9.8	24.1	1.8	13.5	30.0
3	1.2	9.9	10.5	26.4	1.8	14.4	32.5
4	1.3	10.5	11.0	28.2	1.9	15.3	34.4
5	1.3	10.9	11.4	29.3	1.9	15.9	36.3
10	1.5	12.3	12.3	33.4	2.0	18.1	39.0
15	1.6	12.9	13.0	34.0	2.1	18.6	40.0
20	1.6	13.4	13.3	34.5	2.2	18.9	40.8
25	1.7	13.6	13.6	35.0	2.2	19.1	41.3
30	1.8	13.9	13.9	35.7	2.3	19.3	41.7

Data in table 7 and other geohydrologic data indicate that *multiple well fields* are needed to produce the variable feedwater rates. This is primarily due to a lack of available drawdown for pumping rates much in excess of 10 mgd in a single field with reasonable well spacings. In addition, geographically concentrated pumpage results in excessive mineral content of the feedwater. A description of the multiple well field schemes follows in the next section.

MULTIPLE WELL FIELD LAYOUT AND OPERATION

The scheme for 5 mgd product water with 50 percent penetrating wells will be given in detail as an example of the operation of the multiple well fields. As shown in table 7, feedwater rates have to vary from 9.3 mgd initially to 19.3 mgd after 30 years of pumping. Four 5 mgd well fields were selected to provide a source of the feedwater. The spacing of these well fields (see figure 44 in a later section) was chosen on the basis of minimizing chemical content of the feedwater, minimizing pumping lifts, and leaving sufficient space for construction of possible injection well fields centered near the desalinization plant.

Since a feedwater rate of 9.3 mgd is necessary at the start, well field number 1 is initially made fully operational and field number 2 is nearly at full capacity. At a time of slightly less than one year from the beginning of pumping, well fields number 1 and 2 are fully operational and well field number 3 begins to be phased into the total until fully operational at about four years. Well field number 4 then is phased into operation as the needs for increased feedwater rates continue during the remainder of the 30 year plant life. Similar phasing of pumpage is carried out in well fields for all other schemes.

Well field spacing layouts for the variable feedwater rates for the 5 mgd and 10 mgd schemes of table 7 are shown in figures 20 and 21. The well layouts for the 1 mgd schemes are composed of single wells spaced 4 miles on either side of the desalinization plant. Spacing of individual wells within the well fields was shown in figure 19.

The total number of feedwater wells in any scheme is the sum of the 1 mgd wells necessary to supply the ultimate feedwater requirement plus standby wells (a 20 percent standby factor was utilized). Thus, the simplest scheme, requiring a 2 mgd feedwater supply, uses two wells plus a single standby or a total of three wells; and the largest scheme, requiring 45 mgd of feedwater, uses 45 wells plus 9 standbys or a total of 54 wells.

PUMPING LEVEL PREDICTIONS WITHOUT INJECTION

Tables were prepared of estimated water level declines in pumped wells that would result from the variable feedwater rate demands and field spacings outlined above.

This was done by measuring the distances between well fields, preparing time-water level decline graphs for these distances from the computer output data, and applying the principle of superposition to account for the time-phasing of pumpage and mutual interference effects between well fields. As an example, table 8 shows a water decline listing with time for the individual well fields of the scheme for 5 mgd constant product water with 50 percent penetrating wells.

The water level declines in table 8 do not include the effects of turbulent well losses. Total pumping lifts to the land surface were calculated from a series of tables such as table 8 for all schemes by adding in turbulance losses and the distance between the land surface and the original static level.

TABLE 8
ESTIMATED AVERAGE WATER LEVEL DECLINE FOR 5 MGD
50 PERCENT SCHEME WITHOUT INJECTION
(In feet below original static level)

Years of pumping	Field 1	Field 2	Field 3	Field 4
0.27	560	540	70*	70*
1	640	638	160*	160*
2	730	729	460	260*
3	790	790	680	380*
4	850	850	805	560
5	910	910	880	730
10	1140	1140	1120	1100
15	1260	1260	1250	1230
20	1340	1340	1335	1315
25	1400	1400	1395	1385
30	1440	1440	1435	1425

*These water level declines are due only to inference from the other well fields, as pumpage here has not started yet.

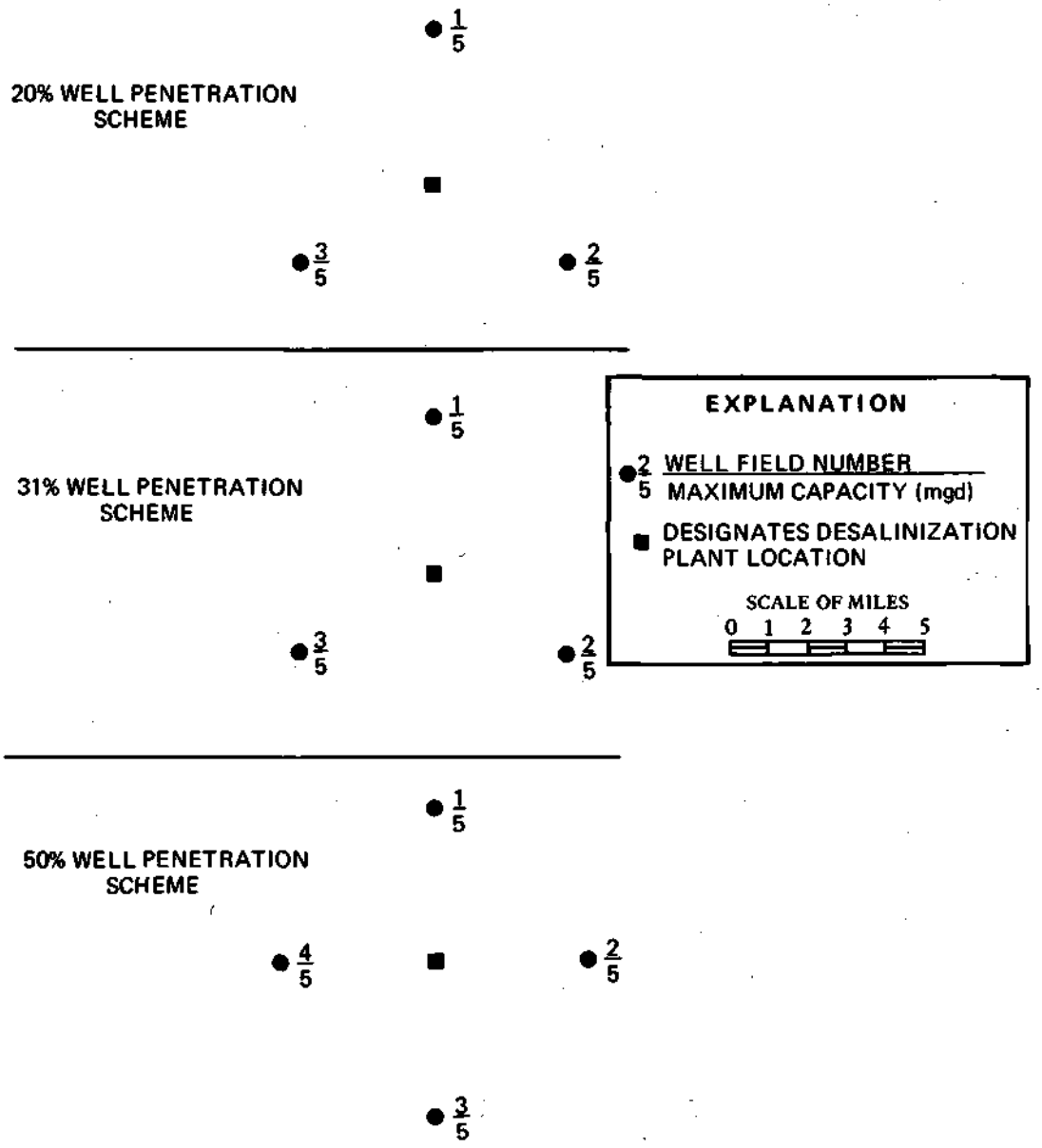

Figure 20. Multiple well field schemes for variable feedwater rates for constant 5 mgd product water

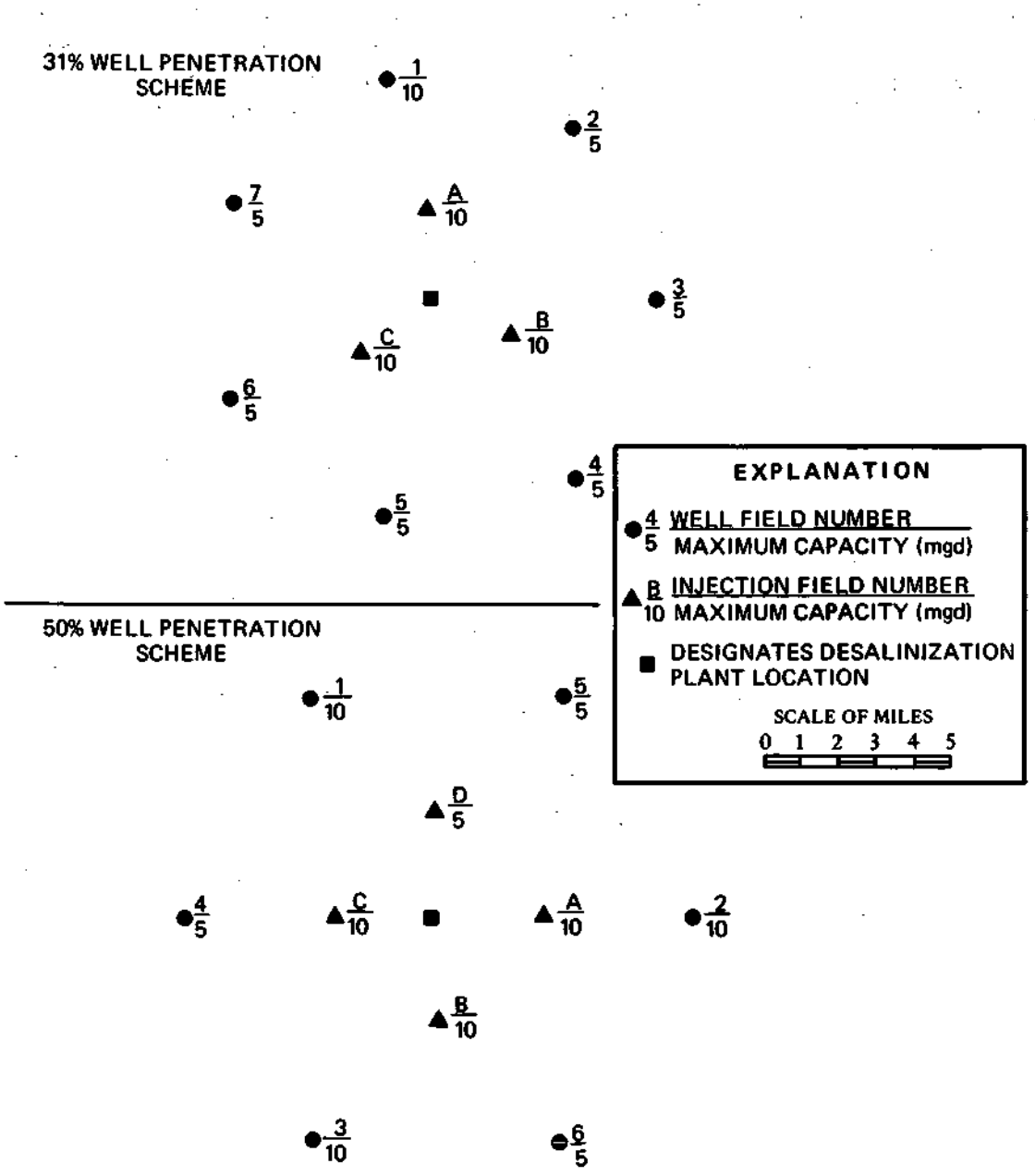

Figure 21. Multiple well field schemes for variable feedwater rates for constant 10 mgd product water

It should be noted here that no effects of any injection scheme on the above pumping levels were included in this first set of pumping level calculations. The effects of injection of waste brine water were added in later when it was shown that deep well injection appeared to be the most efficient way of brine waste disposal. An explanation of the injection schemes and different pumping levels will be given later in the section on *Brine Disposal.*

FEEDWATER QUALITY

Chemical analysis data supplied by the Water Survey indicated that the amount of dissolved minerals in the water increases with increasing depth of well penetration into the aquifer and with increasing drawdown as time goes on. The important characteristics of the water from the Mt. Simon aquifer are its high hardness, high concentration of iron, and large amount of total dissolved minerals. For example, the 40,000 mg/l TDM water from a 50 percent penetrating well at the end of 30 years exceeds even that of seawater which has about 35,000 mg/l TDM.

Figure 22 presents an example of the change of TDM with time for different desalting plant production rates at 50 percent penetration in the Mt. Simon aquifer. The figure also shows that the largest increase of TDM would occur during the first 10 years, after which the rate of change would gradually diminish. Figure 23 was generated from the Mt. Simon aquifer data. In this figure, the TDM value is presented as a function of production rate with withdrawal year as a parameter. The changing water characteristic is clearly shown. [Note: The desalting plant production rates and the well withdrawal rates are related by recovery ratios determined by iteration of process and well data. See table 25 for final recovery ratios.]

The high concentration of Ca^{+2} ions in the water can cause scale formation in certain desalting processes. The removal of a large proportion of the calcium content by chemical pretreatment is not practical because of the cost of chemicals. The practical method to desalt the water is to select and design processes to operate under conditions such that the precipitation of calcium salts will not occur. This restricts the choice of processes. Detailed discussion is presented later.

Another problem is the high content of iron and manganese. Iron is frequently present in well water in the ferrous state which is more soluble than the ferric state. If iron is precipitated, it will deposit on metal surfaces, thereby increasing frictional resistance to flow through pipes, and requiring costly cleaning procedures. Therefore, iron must either be removed from the water by oxidation to change from the ferrous to the ferric state before entering the desalting process, or be retained in the water with suitable measures taken to prevent precipitation, such as avoidance of oxidation or addition of antiprecipitation agents. The choice of the proper method depends on the technical feasibility and the comparative cost analysis. This also is discussed in later sections.

The characteristics of the Mt. Simon aquifer water can be listed as follows:

- The TDM content varies in a very large range, from 2000 mg/l at 20 percent penetration, 1 mgd and 0 year, to 40,000 mg/l at 50 percent penetration, 10 mgd and 30 years.
- The concentrations of all ions (except alkalinity) increase as the withdrawing time increases. The rate of increase is very large during the first 10 years, then gradually diminishes, so that the concentration approaches a constant value.
- For the same withdrawal rate, the deeper the penetration the more concentrated the water.
- The water is relatively neutral. The pH value varies in the range of 6.5 to 7.5.

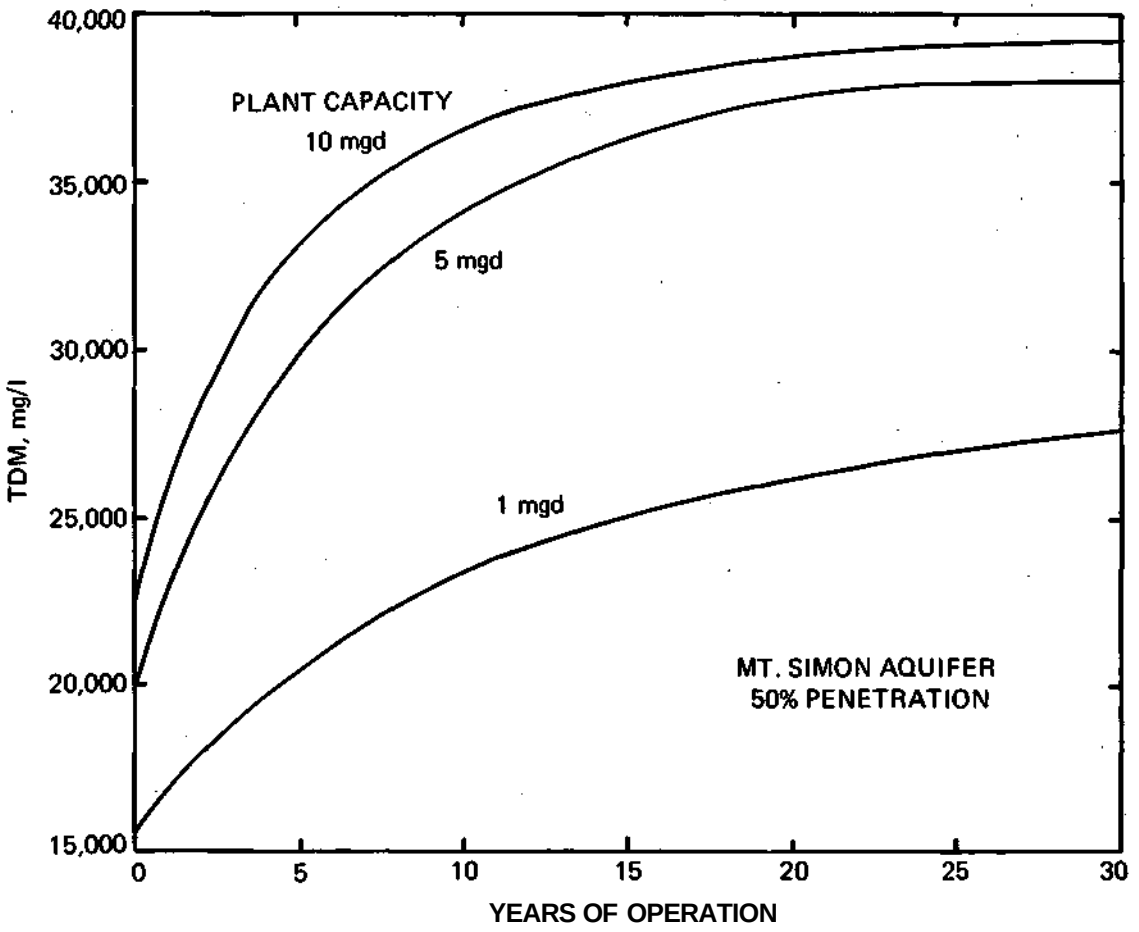

Figure 22. Variation of TDM with time for different plant capacities

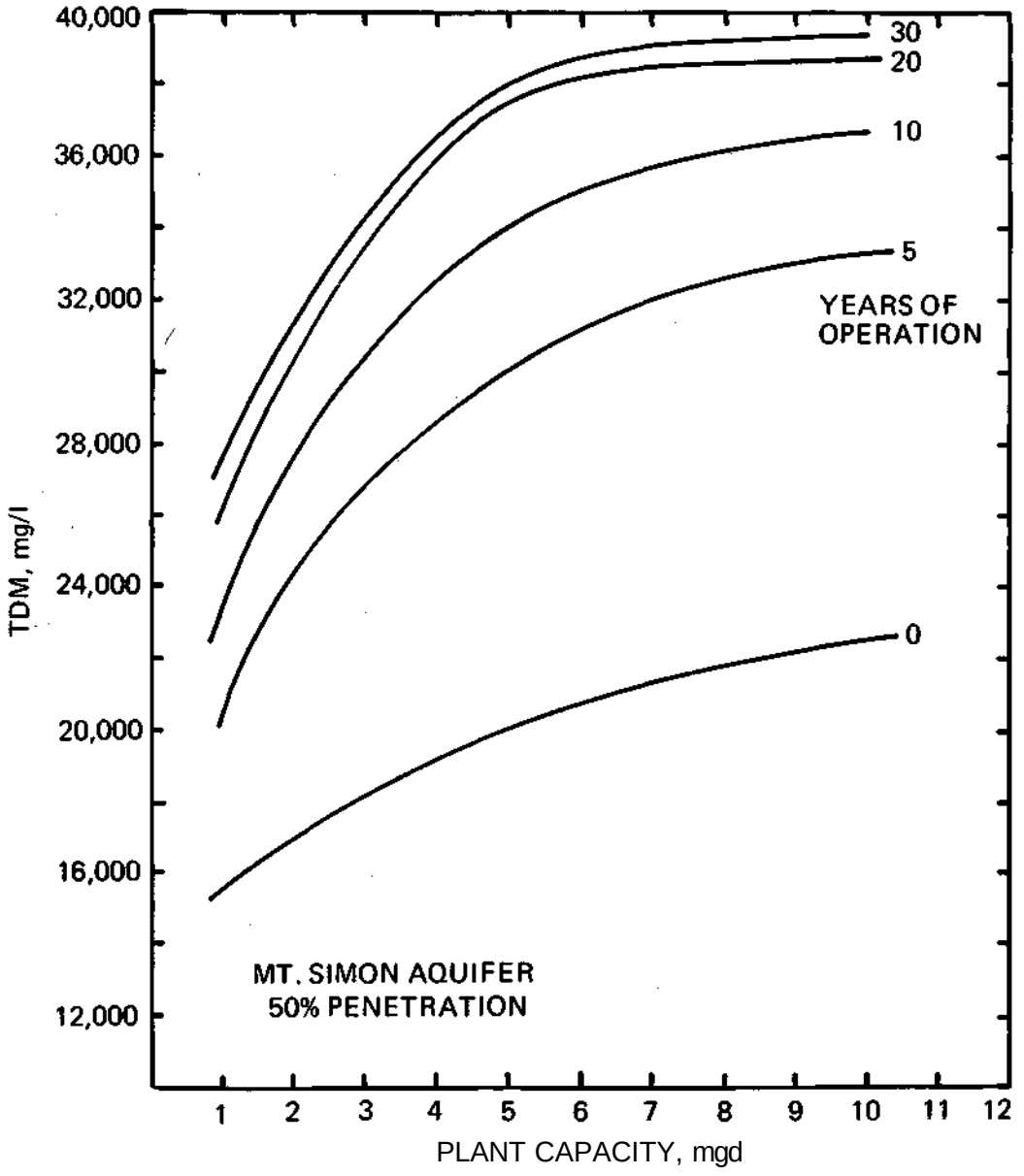

Figure 23. Variation of TDM with plant capacity at different years of operation

- The pH value decreases as the withdrawal time increases; the water is gradually changed to acidic with time.
- Water temperature increases with aquifer depth.
- The iron content is high.

Tables 9, 10, and 11 present detailed water analyses for different penetrations, production rates, and years. The ever-increasing concentration of the constituents in the water with time shows that the scale formation tendency increases and the recovery ratio decreases as time goes on. Since the change in water quality is so great and it is impractical to refinance after only a few years operation of a plant, it is suggested that the plant be designed and financed on the basis of the 30th year water quality. In this case the plant would be operated with low feed rate in the first few years, followed by a gradual increase in the feed rate until the 30th year.

TABLE 9

WATER ANALYSIS OF MT. SIMON AQUIFER AT 20 PERCENT PENETRATION

Years of pumping	TDM	T°F	Fe	Mn	Na + K	Mg	Ca	SO_4	Cl	Alkalinity ($CaCO_3$)	Hardness ($CaCO_3$)	pH
1 mgd Product*												
0	2,000	63.4	9.2	0.40	400	43	180	130	1,000	267	650	7.56
1	3,600	64.2	14.4	0.65	800	60	280	145	2,000	256	1,000	7.30
2	5,200	64.9	18.0	0.85	1,200	80	390	160	3,000	250	1,450	7.18
3	6,400	65.5	20.0	0.95	1,500	94	480	175	3,800	246	1,700	7.10
4	7,600	66.0	22.0	1.10	1,700	110	570	180	4,500	243	2,000	7.04
5	8,400	66.5	23.2	1.23	1,970	130	660	200	5,000	240	2,280	7.00
10	11,900	67.9	27.2	1.68	2,850	207	980	248	7,100	230	3,630	6.90
15	13,800	68.3	29.5	1.92	3,400	250	1,200	275	8,200	226	4,020	6.86
20	15,100	68.7	30.9	2.05	3,760	275	1,360	295	8,800	224	4,550	6.79
25	16,000	69.1	32.0	2.16	4,020	298	1,480	308	9,400	221	4,950	6.77
30	17,000	69.4	33.0	2.26	4,220	314	1,580	320	9,700	220	5,300	6.76
5 mgd Product*												
0	5,000	64.2	15	0.80	1,200	90	440	165	2,800	255	1,800	7.06
1	8,800	66.0	20	1.25	2,000	165	850	210	5,000	247	3,400	7.00
2	11,400	67.2	23.7	1.57	2,600	225	1,150	245	6,600	241	4,400	6.96
3	13,600	68.2	26.4	1.81	3,100	270	1,370	276	7,800	236	5,200	6.92
4	15,500	68.8	28.3	2.00	3,500	300	1,560	305	8,800	232	5,600	6.89
5	17,200	69.4	29.8	2.14	3,800	330	1,730	330	9,600	229	6,100	6.86
10	23,000	71.2	35.2	2.70	4,900	415	2,350	430	12,600	214	7,800	6.74
15	27,200	72.4	38.8	3.14	5,700	465	2,800	485	14,900	204	9,200	6.66
20	30,700	73.5	41.5	3.50	6,700	545	3,150	520	16,700	196	10,200	6.62
25	32,500	74.4	43.5	3.83	7,400	620	3,420	540	18,300	191	11,200	6.59
30	33,400	75.1	45.0	4.15	8,100	670	3,660	550	19,700	186	12,000	6.57

*See table 25 for recovery ratios.

TABLE 10

WATER ANALYSIS OF MT. SIMON AQUIFER AT 31 PERCENT PENETRATION

Years of pumping	TDM	T°F	Fe	Mn	Na + K	Mg	Ca	SO_4	Cl	Alkalinity ($CaCO_3$)	Hardness ($CaCO_3$)	pH
5 mgd Product*												
0	9,000	66.5	23.0	1.30	2,200	140	800	210	5,000	240	2,500	6.92
1	12,600	67.7	27.5	2.00	3,400	290	1,500	280	8,400	227	4,500	6.85
2	16,000	68.8	1.0	2.35	4,300	360	1,870	330	10,500	220	6,000	6.79
3	18,800	69.6	33.8	2.65	5,000	420	2,170	370	12,200	214	7,000	6.75
4	21,000	70.3	35.8	2.85	5,500	460	2,420	400	13,400	210	7,700	6.72
5	22,800	70.9	37.2	3.00	5,900	495	2,630	420	14,400	206	8,300	6.69
10	28,000	72.8	41.5	3.53	6,800	575	3,250	480	16,800	194	10,200	6.64
15	31,200	73.9	43.8	3.85	7,700	622	3,630	520	18,200	186	11,300	6.60
20	33,300	74.6	45.1	4.07	8,100	660	3,820	550	19,100	183	12,000	6.58
25	34,600	75.2	46.0	4.20	8,300	682	3,920	560	19,700	181	12,500	6.57
30	35,400	75.5	46.5	4.32	8,400	710	3,950	570	20,200	181	12,800	6.56
10 mgd Product*												
0	11,000	67.1	25.4	1.50	3,100	200	1,000	240	6,800	232	3,500	6.88
1	18,800	70.3	34.5	2.50	5,000	375	1,950	335	11,300	218	6,500	6.81
2	22,200	71.5	38.0	2.90	5,900	450	2,370	390	13,600	210	7,900	6.75
3	24,600	72.4	39.5	3.25	6,400	505	2,670	430	15,200	204	8,900	6.71
4	26,400	73.0	41.0	3.50	6,800	548	2,900	455	16,300	200	9,700	6.67
5	27,800	73.5	41.8	3.77	7,100	578	3,070	480	17,200	198	10,300	6.65
10	32,000	74.8	44.5	4.17	7,900	668	3,650	520	19,400	186	12,000	6.59
15	34,400	75.5	46.1	4.30	8,400	703	4,000	565	20,200	176	12,600	6.56
20	36,000	76.1	47.1	4.50	8,800	735	4,250	600	20,600	175	13,100	6.54
25	37,200	76.5	47.8	4.65	9,200	770	4,400	620	21,200	174	13,900	6.53
30	38,200	76.8	48.0	4.80	9,400	800	4,600	640	21,700	172	14,500	6.52

*See table 25 for recovery ratios.

TABLE 11

WATER ANALYSIS OF MT. SIMON AQUIFER AT 50 PERCENT PENETRATION

Years of pumping	TDM	T°F	Fe	Mn	Na + K	Mg	Ca	SO_4	Cl	Alkalinity ($CaCO_3$)	Hardness ($CaCO_3$)	pH
1 mgd Product*												
0	15,600	69.0	31.6	2.10	3,850	290	1,400	298	9,000	223	4,700	6.85
1	17,400	69.4	32.5	2.25	4,160	310	1,600	310	9,800	221	5,300	6.82
2	18,300	67.4	33.3	2.35	4,460	330	1,770	326	10,500	218	5,740	6.80
3	19,000	70.1	34.0	2.45	4,700	355	1,910	340	11,000	217	6,130	6.77
4	19,700	70.4	34.8	2.55	4,880	375	2,000	352	11,500	215	6,480	6.76
5	20,500	70.7	35.4	2.65	5,050	390	2,090	365	11,900	214	6,780	6.74
10	23,400	71.6	37.8	2.94	5,700	459	2,400	410	13,300	208	7,770	6.70
15	25,000	72.2	39.4	3.20	6,220	507	2,720	440	14,800	203	8,670	6.67
20	26,100	72.6	40.4	3.37	6,550	530	2,880	460	15,500	201	9,270	6.66
25	27,100	73.0	41.2	3.50	6,750	550	2,990	474	16,000	199	9,680	6.65
30	27,600	73.3	41.8	3.57	6,910	566	3,080	482	16,400	198	9,950	6.64
5 mgd Product*												
0	20,000	70.7	36.0	2.65	5,000	400	2,000	370	11,800	213	6,700	6.75
1	23,200	72.0	38.2	3.03	6,000	460	2,500	410	14,200	207	8,100	0.73
2	25,600	72.7	40.2	3.29	6,600	520	2,850	440	15,600	202	9,300	6.70
3	27,400	73.1	41.6	3.50	7,000	560	3,080	470	16,800	198	10,000	6.68
4	28,800	73.4	42.8	3.65	7,200	590	3,250	495	17,600	195	10,500	6.66
5	30,000	73.7	43.5	3.78	7,400	620	3,420	515	18,200	193	10,900	6.65
10	34,000	74.8	46.7	4.25	8,200	710	3,940	570	20,000	185	12,400	6.59
15	36,400	75.6	48.5	4.53	8,700	765	4,230	595	21,000	177	13,400	6.55
20	37,500	76.2	49.5	4.70	9,100	7%	4,420	620	21,500	174	14,000	6.53
25	38,000	76.6	49.9	4.80	9,300	812	4,520	640	21,800	173	14,400	6.52
30	38,000	77.0	50.0	4.90	9,500	820	4,570	660	21,900	172	14,900	6.52
10 mgd Product*												
0	22,500	71.5	30.0	2.9	5,500	450	2,400	400	13,200	209	7,600	6.71
1	26,200	73.0	38.5	3.4	6,700	540	2,850	460	16,200	204	9,600	6.67
2	28,600	73.7	41.8	3.7	7,300	600	3,180	490	17,400	199	10,700	6.65
3	30,400	74.3	43.2	3.9	7,700	640	3,420	520	18,200	196	11,400	6.63
4	32,000	74.8	43.8	4.1	7,900	670	3,600	540	18,900	192	11,900	6.62
5	33,200	75.1	44.3	4.25	8,100	690	3,750	555	19,400	190	12,400	6.60
10	36,600	76.0	46.3	4.6	8,800	750	4,170	613	20,900	181	13,800	6.56
15	38,000	76.5	48.0	4.75	9,100	770	4,450	650	21,400	175	14,500	6.53
20	38,700	76.9	49.2	4.96	9,400	790	4,620	667	21,800	172	15,000	6.51
25	39,100	77.1	50.2	5.05	9,700	830	4,720	680	22,300	170	15,400	6.50
30	39,300	77.3	51.2	5.10	9,900	855	4,800	690	22,500	168	15,700	6.50

*See table 23 for recovery ratios.

DESALTING PROCESSES

Five different desalting processes are discussed in this section. They are electrodialysis (ED), ion exchange (IE), reverse osmosis (RO), vapor compression-vertical tube evaporation-multistage flash (VC-VTE-MSF), and freezing processes. On the basis of data supplied by the Water Survey, both technical and economic aspects of the processes were studied and some recommendations have been made for each process. Because of the salinity increase with time of the Mt. Simon aquifer water, the ED and IE processes were found to be unsuitable.

In the RO process, two desalting stages were used with a salt rejection ratio of 90 percent in each stage. The RO process is still under rapid development and it is expected that, in the future, a one-stage process may be available for the water salinity range encountered in this study.

The choice of the VC-VTE-MSF distillation process was based on the following:

- It has relatively high thermal efficiency.
- Energy sources other than steam (for example: electricity) can be used.
- Communication with Commonwealth Edison Company indicated that no steam will be available for purchase from their plants in the area.

Although there has been some commercial operation of freezing plants, freezing processes are still in the development stage. They have the advantage of operating at low temperatures where most scale formation can be avoided. This is of particular importance for the Mt. Simon aquifer water which has a high content of scale-forming compounds in solution.

ELECTRODIALYSIS

Electrodialysis (ED) has been established as an efficient and reliable method for desalting brackish water. At present, there are many plants in commercial operation throughout the world, the largest ED plant in the United States being a 1.2 mgd plant located at Siesta Key, Florida. The cost of water produced by an ED system is very sensitive to the water salinity since the power consumption increases rapidly with an increase in feed salinity. Figure 24 shows typical electrodialysis process power costs as a function of feed salinity (17). The rapid increase of power cost with increasing feed salinity is clearly indicated in this figure.

Process Description

Electrodialysis is a process which, under the influence of electric potential, extracts salts from water by using ion exchange membranes that are permeable either to positively charged ions or to negatively charged ions. They are called cation or anion membranes. The membranes are installed in alternating fashion in a stack. When a voltage is imposed across the stack, ions migrate toward the electrode opposite in charge to their own through the membrane which is permeable to them. Alternate compartments are then enriched or

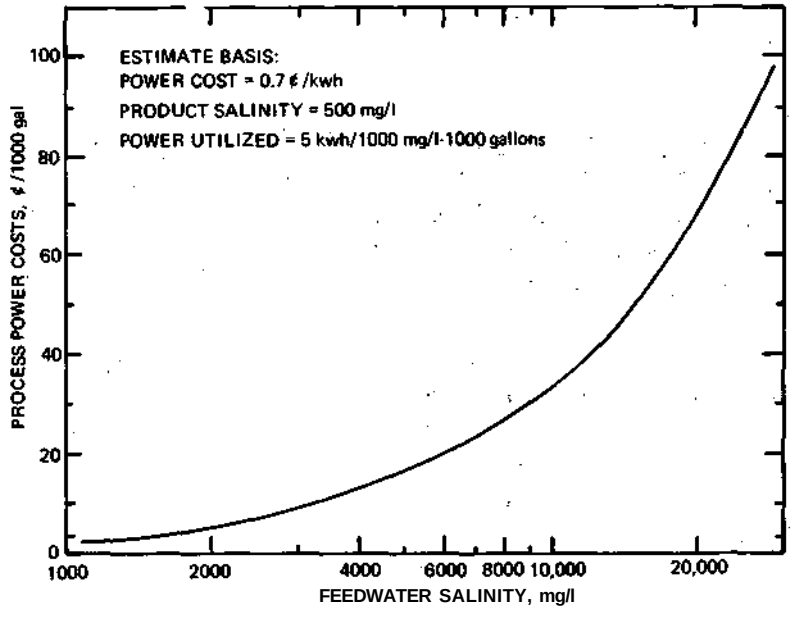

Figure 24. Typical electrodialysis process power costs

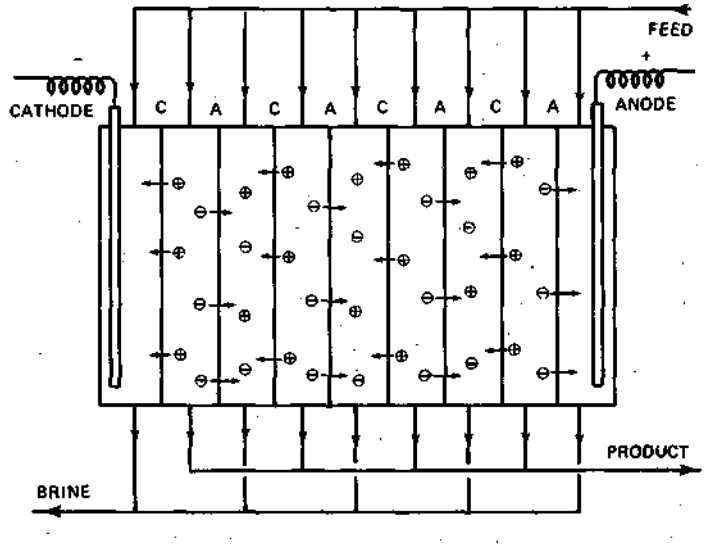

Figure 25. Principle of electrodialysis

depleted in ions. The depleted compartment produces desalted water and the enriched compartment produces a brine stream. The principle of electrodialysis is shown in figure 25.

The desired characteristics of ion exchange membranes used in ED plants include:

1) High ion permeability and low water transfer
2) High electrical conductivity
3) Homogeneous quality and low degree of swelling
4) High mechanical strength
5) Chemical stability in different solutions
6) Low deflection under pressure

Of all the membrane properties, the most important one is electrical conductivity. A membrane with high electrical conductivity can transport more ions by its high electrical current density, but there are upper limits on current density for an ED stack. Concentration polarization on the surface of the membrane and the heating of the membrane play major roles in limiting the current density.

The ions are transported to the membrane surface from the bulk solution by electrical current and also by natural diffusion. As the current density in the electrodialysis stack is increased, the rate of transfer of ions through the membrane increases, until a point is reached at which the rate of transfer through the membrane is greater than the rate of arrival of ions at the interface between membrane and solution. The solution film next to the membrane then becomes depleted of ions and electrical resistance increases sharply in this region. This phenomenon is called polarization. The large voltage drop across the ion depleted film may cause dissociation of water molecules, and hydroxyl and hydrogen ions may be formed. The formation of hydroxyl and hydrogen ions increases the precipitation of calcium carbonate and magnesium hydroxide scale. The scale will cause additional electrical resistance.

The membrane usually contributes a large part of electrical resistance in the stack. Therefore, most of the voltage drop across an electrolysis stack goes into heating the membranes. The current density must be limited at a certain value which does not overheat the membrane.

. Scale formation on the surface of the membrane causes a decrease in stack efficiency and an increase in pumping power requirement. To minimize the scale formation, an increase of turbulence is usually employed. The effect of turbulence on an ED system can be listed as follows:

1) Turbulence decreases the thickness of the stagnant fluid sublayer.
2) Turbulence increases the rate of diffusion of ions toward the membrane. This allows a high current density to be used in the process.
3) Turbulence washes the membrane surfaces and holds precipitates in suspension until discharge from the stack.

High fluid velocities and specially designed membrane separators are used to ensure turbulence in the fluid streams. These separators typically have flow deflectors, either in the form of mesh or regularly spaced obstructions which break up flow profiles to establish a high degree of turbulence for any given fluid velocity.

Application to the Mt. Simon Aquifer

The ED process is very sensitive to the water salinity. When the concentration of feedwater is low, the process is competitive with other processes. With high salinity feedwater, two restrictions may make the ED system both technically and economically inapplicable. These restrictions are power cost and scale formation.

Power Cost., As shown in figure 24, the power cost would be prohibitively high as feed salinity increases above 10,000 mg/l. The chemical analysis of Mt. Simon aquifer water shows that the salinity is mostly higher than 10,000 mg/l . For the most favorable case of 20 percent penetration and 1 mgd plant capacity, figure 26 gives the power cost as a function of withdrawal year. A sample calculation is shown in Appendix A. The figure shows that the power cost rises to more than 6¢/1000 gal within 10 years of plant operation and approximately 9¢/1000 gal at 30 years. The high power cost makes the ED process noncompetitive with other processes.

Scale Formation. An ED plant can be operated without extensive scale control pretreatment if the calcium concentration in the brine discharge is less than 440 mg/l (18). Also, the calcium concentration in the brine discharge can be increased to 900 mg/l with the addition of a sequestering agent such as sodium hexametaphosphate. The water analyses given in tables 9, 10, and 11 show that the calcium concentration in the feedwater already exceeds this calcium limitation. Extensive chemical treatment would be necessary to reduce calcium concentration, resulting in high chemical costs.

These two factors, high power cost and scale formation, indicate that the ED process is not practical for desalting Mt. Simon aquifer water.

Application to Low Salinity Water

For very low salinity water, the ED process is competitive with other processes. As an example, the cost of using the ED process to desalt a groundwater in the Aurora area, which has the analysis presented in table 12, was computed to be 40 to 5¢/1000 gal. The process and economic calculations were performed by use of References 18, 19, and 20. Plant capacities of 1, 5, and 10 mgd were assumed. Figure 27 gives the unit water cost as a function of plant capacity. In the calculation, 500 mg/l product salinity and 1.25¢/kwh power cost were assumed.

TABLE 12
GROUNDWATER ANALYSIS FROM AURORA AREA

Ion	mg/l	Ion	mg/l
Fe^{+2}	0.6	SO_4^{-2}	80
Mn^{+2}	0.2	Alkalinity	254
Ca^{+2}	155	Hardness	552
Mg^{+2}	40	TDM	2001
NH_4^-	0.7	pH	7.3
Na^+	351	Temperature	65 F
Cl^-	694		

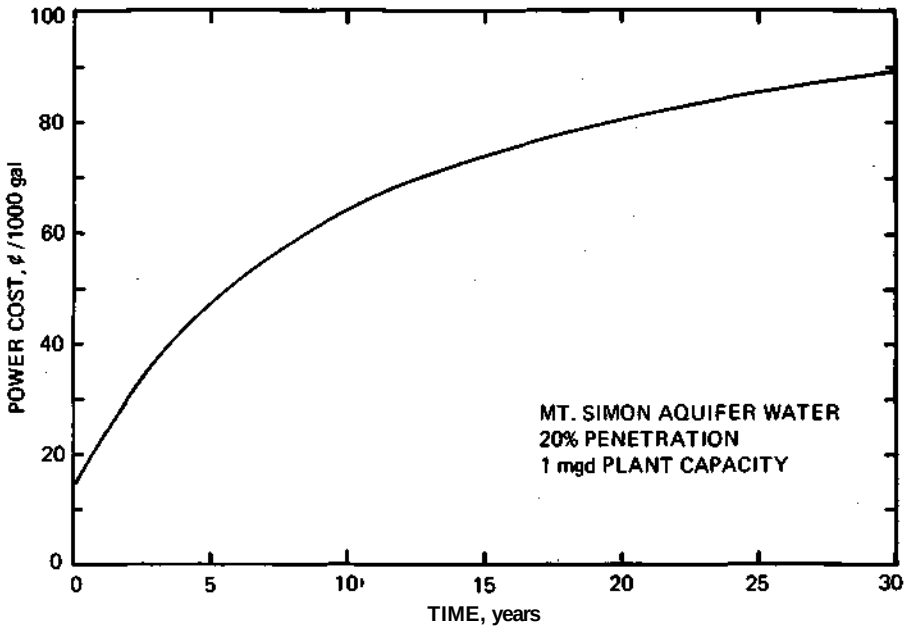

Figure 26. Power cost for ED plant

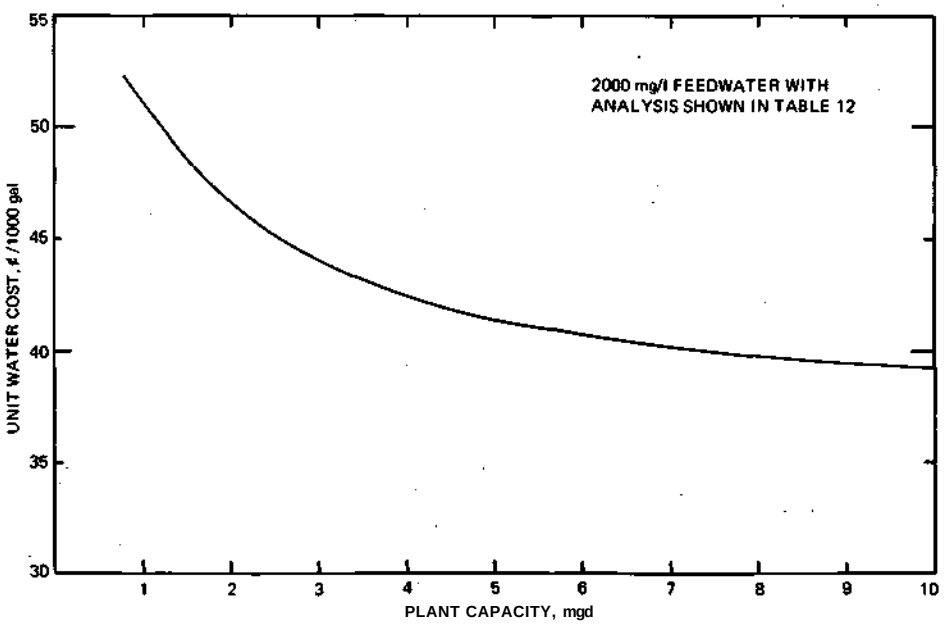

Figure 27. Unit water cost as a function of plant capacity for electrodialysis process

ION EXCHANGE

Ion exchange (IE) is not a new process. It has been used for many years in softening hard water. The most important example is the use of zeolite to remove calcium and magnesium hardness from water, the regeneration being done with common brine.

As the need for low cost, high quality, potable water increases, the ion exchange process may be considered as a water desalting method in addition to its use in softening hard water. Today resin manufacturers can produce resins tailor-made for specific applications, so the ion exchange process may be competitive with distillation, reverse osmosis, electrodialysis, and other desalting processes for some feedwaters. The choice of a favorable process involves many factors. One of the most important factors is, of course, the unit water cost of the process.

The ion exchange process is very sensitive in its economics to water quality. Since each plant is an individual case, it is impossible to generalize on the economics of the ion exchange process, but generally the lower the total dissolved minerals the more economical the ion exchange process becomes.

Process Description

Ion exchange resins are synthetic polymers which can remove salts from solution in water. These polymers are of two types, those which remove positive ions such as sodium, calcium, and magnesium, and those which remove negative ions such as chloride, sulfate, and bicarbonate. If saline water is passed through beds of both types of resin, most of the dissolved ions can be removed from the water. Very pure water can usually be produced with this process.

The resins eventually become exhausted, but they can be quite simply regenerated by chemical treatment, in which the cation exchanger is washed with acid solution and the anion exchanger with alkali. The chemical consumption is proportional to the amount of impurity removed from the water, but the resins may be used an infinite number of times, except that a certain amount of loss by attrition must be replaced.

Several ion exchange processes have been characterized as practical for water demineralization. In general, all the processes can be put into two categories: fixed-bed systems and moving-bed systems. The most important feature of the ion exchange process is the choice of resins. As an example, a three unit fixed-bed system is analyzed to show the chemical reactions in an ion exchange process.

The basic process consists of three units in series (21). The first unit is the alklinization unit and contains resin of the bicarbonate form. As the influent passes through the unit, all the anionic constituents are converted to the bicarbonate salts of sodium, calcium, and magnesium. The reaction in the unit takes place in accordance with the following equation:

$$(R\text{-}HN)HCO_3 + NaCl \rightarrow (R\text{-}HN)Cl + NaHCO_3 \quad (1)$$

The second unit, called the dealkalinization unit, contains weak acid resins in the hydrogen form. The bicarbonate salts produced in the first exchanger are converted to carbonic acid in the reaction:

$$(R\text{-}COOH) + NaHCO_3 \rightarrow (R\text{-}COONa) + CO_2 + H_2O \quad (2)$$

The third unit is the carbonate unit. It contains resin of the free base form. This resin absorbs the carbonic acid effluent from the previous unit and converts it to the bicarbonate form as shown in the equation:

$$(R\text{-}N) + CO_2 + H_2O \rightarrow (R\text{-}HN)HCO_3 \quad (3)$$

The last unit now contains resin in the bicarbonate form which is identical to the anion exchanger at the beginning of the treatment process. Therefore, a reverse flow is possible except for the second exchanger which must be regenerated to the hydrogen form again and the first exchanger which must be regenerated to the free base form.

The regeneration reactions are:

$$(R\text{-}HN)Cl + NH_4OH \rightarrow (R\text{-}N) + NH_4Cl + H_2O \quad (4)$$

and

$$2(R\text{-}COONa) + H_2SO_4 \rightarrow 2(R\text{-}COOH) + Na_2SO_4 \quad (5)$$

The regenerants used here are ammonium hydroxide and sulfuric acid respectively. After the regeneration, the flow pattern can be reversed for the next cycle (i.e., through the third unit first), the third unit now acting as the alkalinization unit and the first unit now acting as the carbonation unit. A schematic flow sheet of the process is shown in figure 28.

Application to the Mt. Simon Aquifer

As in the case of the electrodialysis process, the cost of ion exchange desalting is also very much dependent on the salinity of the feedwater. Both the chemical cost and capital cost increase with increasing water salinity. Figure 29 presents the capital cost of the ion exchange process as a function of water salinity (21). When the total salinity is increased from 2000 mg/l to 4000 mg/1, the capital cost is also doubled. Of course, the concentration of different ions in the water also plays an important role in determining the capital cost. TDM alone cannot very accurately determine the capital cost. Therefore, figure 29 gives only an approximation of capital cost.

The chemical cost plays an important role in determining the water cost in the ion exchange process. Since ion exchange is essentially a process of chemical substitution, each mole of certain constituents removed from water requires a mole of chemical regenerants in the regeneration cycle. Therefore, the chemical cost varies approximately linearly with the salinity of the feedwater. Appendix B gives a sample calculation of the chemical cost for 20 percent penetration, 1 mgd, and 30 years withdrawal. The chemical cost is approximately $4.13/1000 gal at the end of 30 years. The chemical cost alone makes the ion exchange process impractical for application to Mt. Simon aquifer water.

Application to Low Salinity Water

For very low salinity water, the chemical cost of the ion exchange process may be in the range which makes the process competitive with other processes. Again, the groundwater analysis in the Aurora area as presented in table 12 was used to determine the water cost by the ion exchange process.

Figure 30 presents the unit water cost as a function of plant capacity. The costs are in the range of 50 to 60¢/1000 gal. The calculations were based on data presented in References

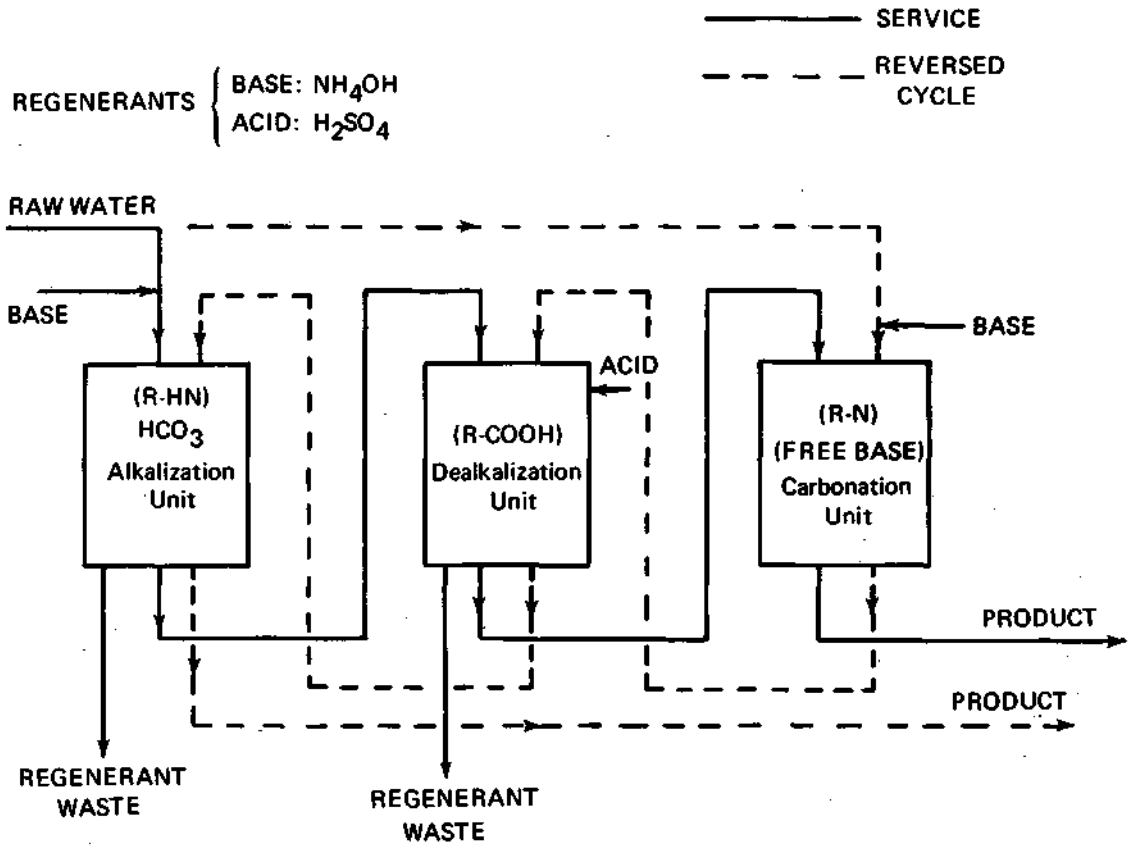

Figure 28. Three-unit desalination ion exchange process

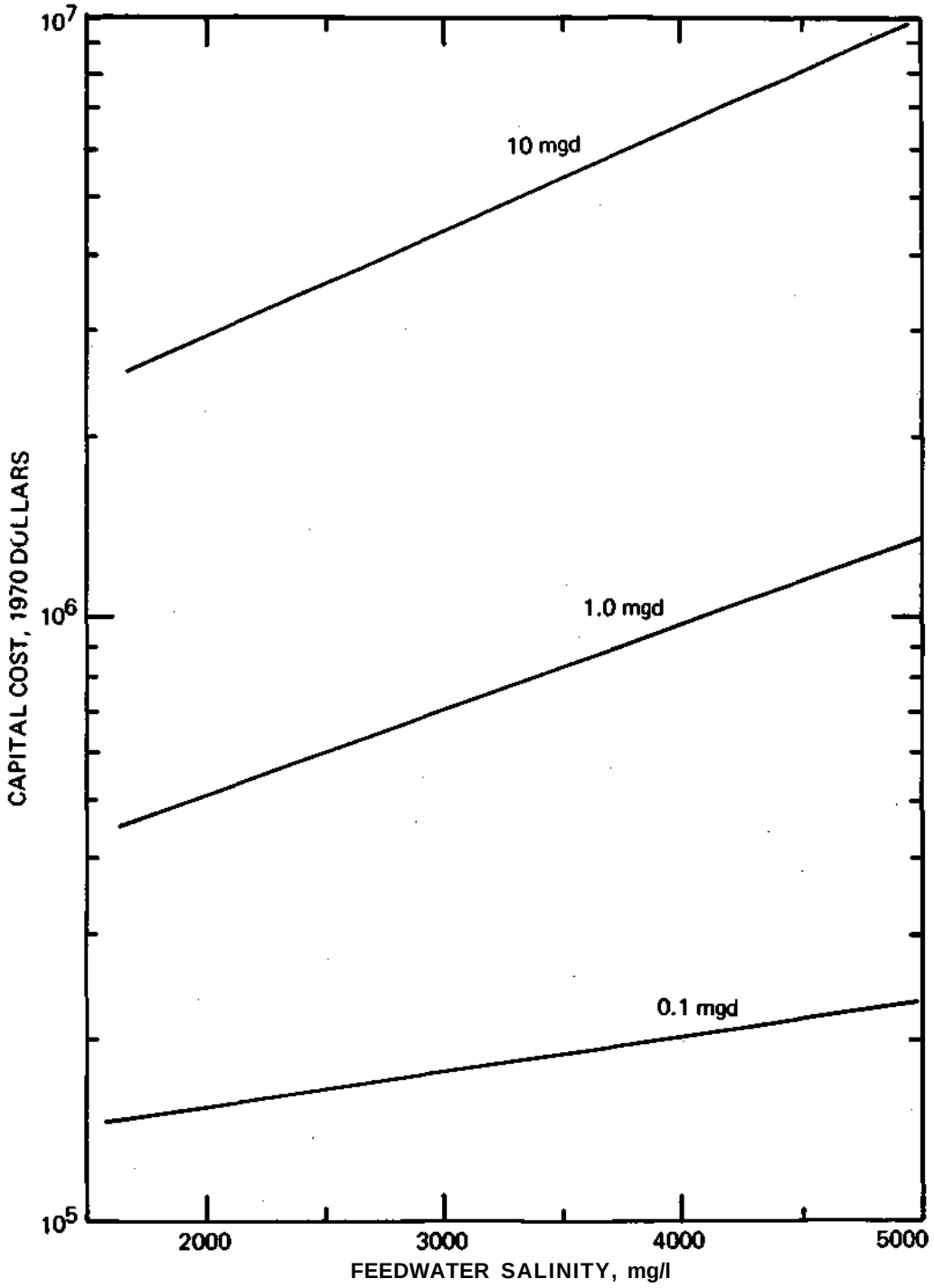

Figure 29. Capital cost as a function of feedwater salinity for fixed-bed ion exchange process

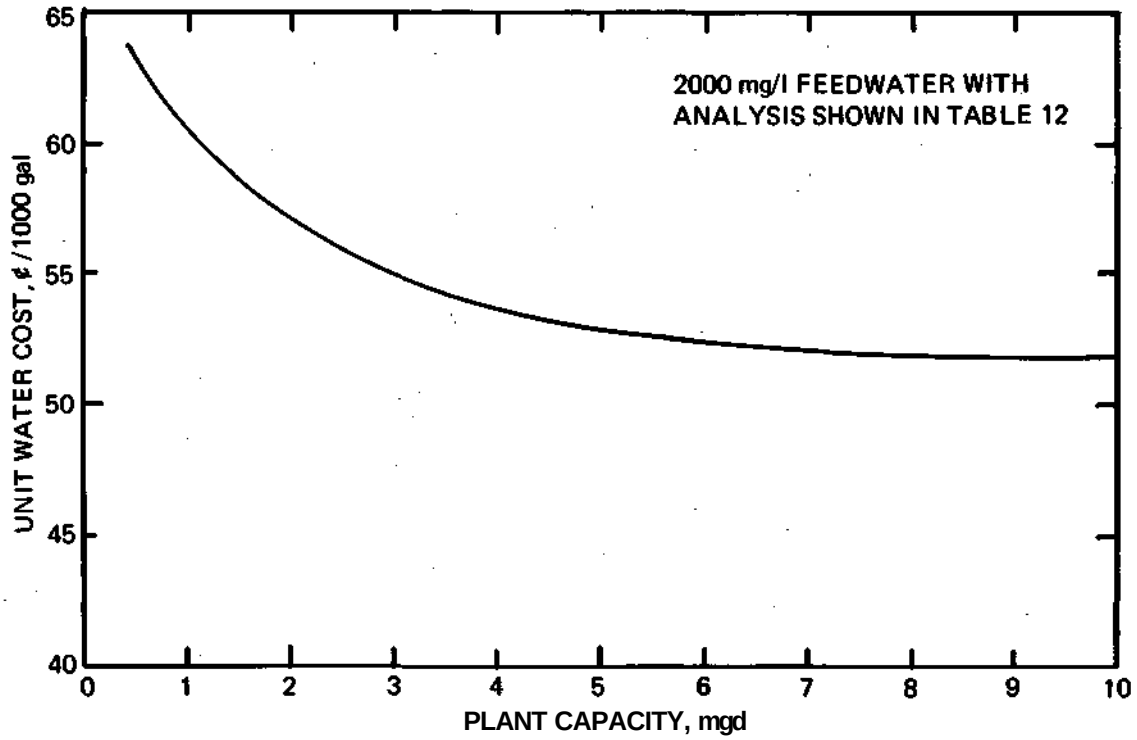

Figure 30. Unit water cost as a function of plant capacity for ion exchange process

21 and 22. The costs of NH_3 and H_2SO_4 were assumed to be $62.55/ton and $34.60/ton respectively.

REVERSE OSMOSIS

Reverse osmosis (RO) is a relatively new process. At present (1972), the salt rejection of the membranes is not high enough to desalt very high salinity water, such as seawater or the Mt. Simon aquifer water, in a single stage. Therefore, a two-stage RO process has been assumed for desalting the Mt. Simon aquifer water. However, research on membranes for seawater desalting is in progress and it is expected that a single-stage RO process for desalting very high salinity water will be available in the future.

Process Description

Osmosis and reverse osmosis processes depend on a membrane that selectively controls the components of a solution which can pass through it. In the case of saline water, the water can pass through the membrane but the salt ions cannot. This property of the membrane is known as semipermeability. When a semipermeable membrane is used to separate fresh water from saltwater, there will be a tendency to equalize the salt concentrations by a flow of water from the fresh water side into the saltwater. This flow of water is called osmosis. If a pressure is gradually applied to the salt side, it will first impede the flow and finally the flow stops at certain applied pressure which is called osmotic pressure. When the applied pressure exceeds the osmotic pressure, the flow is reversed so that water flows from the saltwater into the fresh water, thereby accomplishing desalting of the saltwater.

The rate of water production in the RO process depends on the applied pressure, the osmotic presure, and the membrane characteristics. A simple mathematical expression for the process is (23, 24):

$$W_p = K(\Delta p - \Delta \pi) \qquad (6)$$

where K is the membrane constant which is a function of pressure; Ap is the applied pressure across the membrane; and An is the net osmotic pressure. The value of osmotic pressure depends on the concentration difference across the membrane — the higher the concentration of the feed water, the higher the osmotic pressure in the system. According to the above equation, the applied pressure must be greater than the osmotic pressure in order to produce low salinity water. Therefore, high pressure systems must be used for high salinity water.

A simplified model of the RO process is shown below to demonstrate the relationship between feed, product, and brine:

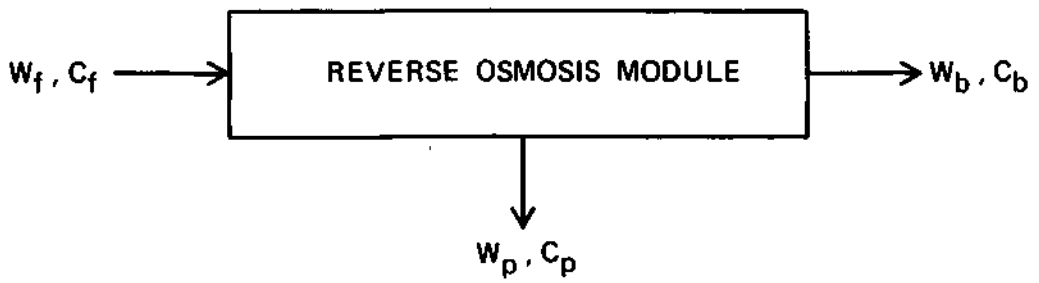

In this model, W and C represent flow rate and concentration respectively. The subscripts f, p, and b indicate feed, product, and brine respectively. The feedwater in the model is gradually concentrated along the length of the flow passages since product water is extracted along the length of the module. Therefore, the osmotic pressure is not constant in the system. An average value of concentration is usually adopted for practical use and it is defined as:

$$C = \frac{C_f + C_b}{2} \tag{7}$$

A set of equations based on the above equation has been developed as follows:

$$\Delta C = \frac{\eta}{2}(C_f + C_b) \tag{8}$$

$$C_p = \frac{1-\eta}{2}(C_f + C_b) \tag{9}$$

$$\Delta\pi = 0.0115\Delta C \tag{10}$$

$$C_b = C_f \frac{1 + R + \frac{1-\eta}{2}R}{1 + \frac{1-\eta}{2}R} \tag{11}$$

where η is the salt rejection ratio which is defined as the fraction of salt rejected by the membrane and R is the ratio of the product flow rate to the brine flow rate (W_p/W_b). The recovery ratio is defined as $W_p/W_f = R/R + 1$.

Pretreatment

The feedwater for a reverse osmosis desalting plant requires some form of pretreatment to prevent fouling of the membranes which would seriously decrease the quality and quantity of the product water. The treatment costs could add a significant amount to product water costs. Therefore, only the required minimum pretreatment should be performed.

The water analysis of the Mt. Simon aquifer indicates that deterioration of the reverse osmosis membrane performance may be expected because of the presence of the following substances:

1) Iron and manganese which form oxides that deposit on the membrane surfaces
2) Scale-forming constituents, primarily calcium sulfate and calcium carbonate

Iron and Manganese Control. The concentrations of iron and manganese in the water are initially very high and they also increase with withdrawal time. Two different methods are considered here to avoid the precipitation of iron and manganese oxides. One is to remove the iron and manganese from the water; the other is to prevent the entry of oxygen into the system to avoid the oxidation of iron and manganese. [Note: The method to treat manganese is essentially the same as to treat iron; therefore, only iron is mentioned hereafter.]

1) *Aeration, Sedimentation, and Filtration.* Aeration is a process which consists of intimately mixing water and air to accelerate the oxidation of the iron in the water with precipitation of the highly insoluble ferric hydroxide. The chemical reaction is illustrated by the following equation:

$$4Fe(HCO_3)_2 + O_2 + 2H_2O \rightarrow 4Fe(OH)_3 + 8CO_2 \tag{12}$$

Iron is frequently present in well water in the ferrous state which is more soluble than is the ferric state. Therefore, complete iron removal requires oxidation of the ferrous iron to the ferric state.

Since the precipitation is not instantaneous, a retention or sedimentation tank following the aerator is necessary to provide time for the precipitation and settling of ferric hydroxide.

A low pH value of the water usually prevents the precipitation of ferric hydroxide even with an adequate supply of oxygen. For effective iron removal by aeration, the pH should be at least approximately 7.5. The release of carbon dioxide during aeration tends to increase the pH of the water, but the increase is not enough to accelerate the precipitation. The supplemental feed of an alkali is sometimes required to complete the precipitation of ferric hydroxide after aeration.

It is convenient to follow the aeration by lime softening. As the pH of the water is increased by the feeding of lime, oxidation of the iron is rapid. Precipitation and sedimentation can take place in the same unit, followed by filtration. Lime treatment can accelerate the iron precipitation and partially improve the quality of the water as well.

2) Iron Retention. The alternative to iron removal is iron retention. As mentioned before, iron in well water is in the ferrous state which is soluble in water. If the entry of oxygen into the system is avoided, the oxidation from the ferrous to the ferric state cannot take place. Because of the relatively high solubility of the ferrous state, the iron is retained in the solution without precipitation. Figure 31 shows the solubility of Fe^{+2} in water as a function of the pH value (25). Points in the area below or to the left of the solubility line represent unsaturated solutions of Fe^{+2}, whereas points in the area above or to the right represent temporary conditions of supersaturation that will result in precipitation until the concentration is reduced to some point on the line. For example, at a pH value of 7.5, the solubility of Fe^{*2} can be 550 mg/l . Data for the Mt. Simon aquifer water show that its pH value is always less than 7.5 and its iron concentration is in the range of 9.2 to 52 mg/l . The concentration of iron in the ferrous state is well below the solubility limit in the water provided no oxidation occurs to change from the ferrous to ferric state.

The operation of an RO system is under high pressure, so it is not possible for air to leak into the system. If an airtight system, including the pipelines from the well field and to the brine disposal well, is maintained in the plant, iron retention in the water can be successfully achieved without difficulty. To ensure the retention of iron in the system, a small amount of polyphosphate may be added. A complex is formed between iron and the added polyphosphates. This complex formation prevents or delays any iron precipitation.

Comparing the above two methods, iron retention is preferable as iron control for the RO process. The reasons for this choice are:

1) The investment in equipment for iron removal is avoided.
2) The disposal of large amounts of iron sludge is avoided.
3) The iron concentration increases with the withdrawal time. This would make the design and process control difficult for an iron removal system.
4) The iron concentration and pH value of the water are in the range in which no ferrous precipitation is possible.
5) The RO system is a high pressure system, so that there is no leakage of air into the plant and consequently no iron precipitation.

Prevention of Scale Formation. The major scale-forming components in the water are $CaCO_3$ and $CaSO_4$ due to the high concentration of calcium. Two methods for controlling the scale are considered here. One is to inject acid into the feed water for alkaline scale control and then operate the plant at the recovery rate which will avoid $CaSO_4$ precipitation. The other is to use a lime or lime-soda process to remove part of the calcium and magnesium.

1) *Acid Injection.* The acid injected into the water reacts with bicarbonate according to the following equations:

$$H_2SO_4 + 2HCO_3^- \rightarrow SO_4^{-2} + 2CO_2 + 2H_2O \quad (13)$$

$$HCl + HCO_3^- \rightarrow Cl^- + H_2O + CO_2 \quad (14)$$

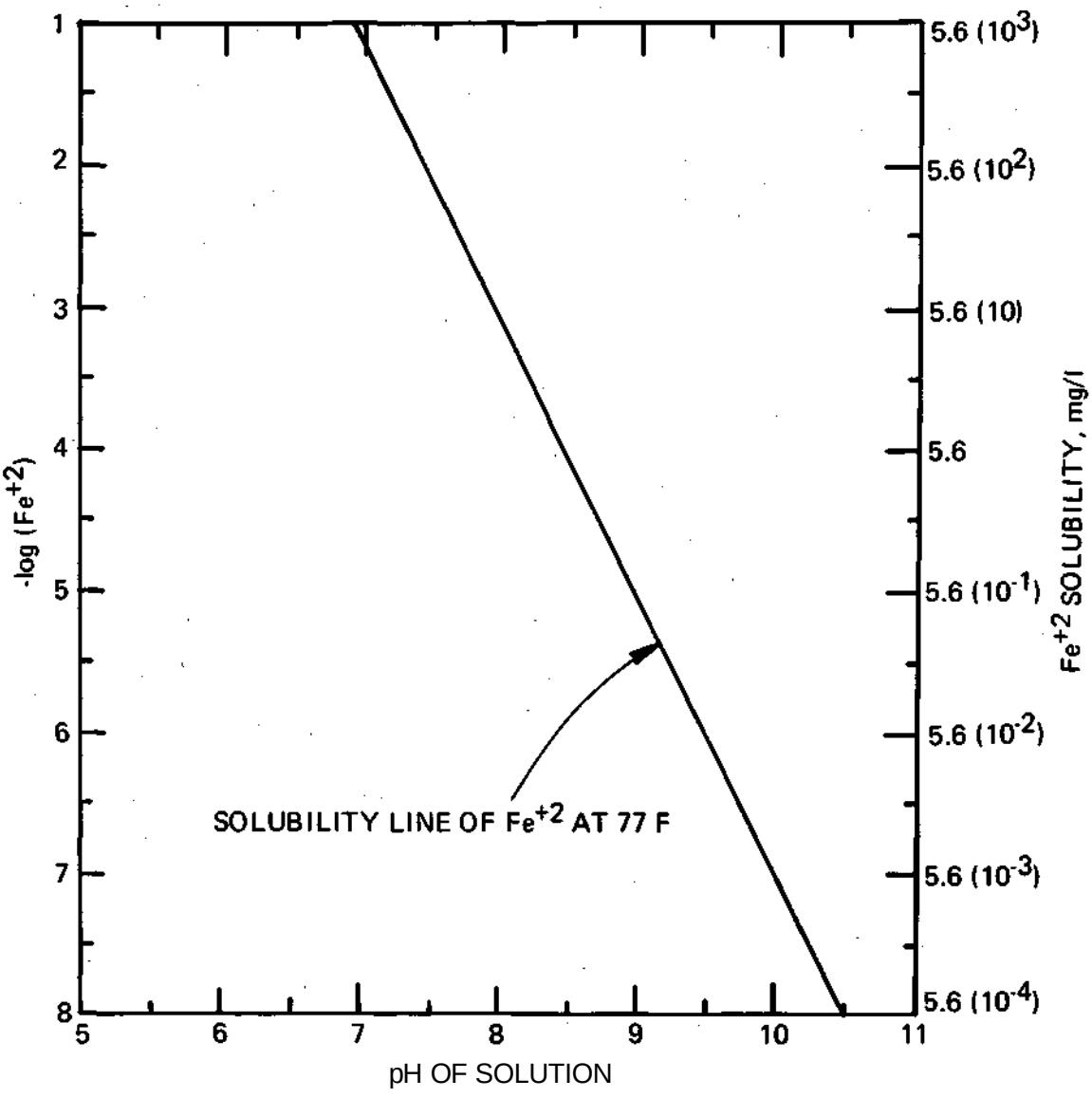

Figure 31. Solubility of Fe^{+2} as a function of pH value

Here either H_2SO_4 or HCl can be used for the removal of HCO_3^- from the water. However, the addition of H_2SO_4 will increase the SO_4^{-2} concentration which in turn will increase the possibility of $CaSO_4$ precipitation and decrease the recovery ratio in the RO process. For example, in the case of 20 percent penetration and 1 mgd plant capacity, the recovery ratio is 40 percent compared with 54.5 percent recovery ratio for HCl injection. The HCl removes bicarbonate without increasing the SO_4^{-2} concentration. Therefore, HCl is the preferable choice as the chemical for acid injection pretreatment. Tables 13 and 14 present comparisons of the raw water and pretreated water after acid injection.

TABLE 13
COMPARISON OF CANDIDATE RAW WATER
AND H_2SO_4 INJECTION PRETREATED WATER
(At 20% penetration and 1 mgd)

	0 Year		30 Years	
	Raw water	Treated water	Raw water	Treated water
Mg^{+2}	43	43	314	314
Na^+	400	400	4220	4220
Ca^{*2}	180	180	1580	1580
Cl^-	1000	1000	9700	9700
SO_4^{-2}	130	384	320	531
Alkalinity (as $CaCO_3$)	267	0	220	0
Fe^{+2}	9.2	9.2	33.0	33.0
Mn^{+2}	0.4	0.4	2.3	2.3

TABLE 14
COMPARISON OF CANDIDATE RAW WATER
AND HCl INJECTION PRETREATED WATER
(At 20% penetration and 1 mgd)

	0 Year'		30 Years	
	Raw water	Treated water	Raw water	Treated water
Mg^{+2}	43	43	314	314
Na^+	400	400	4220	4220
Ca^{+2}	180	180	1580	1580
Cl^-	1000	1189	9700	9856
SO_4^{-2}	130	130	320	320
Alkalinity (as $CaCO_3$)	267	0	220	0
Fe^{+2}	9.2	9.2	33.0	33.0
Mn^{+2}	0.4	0.4	2.3	2.3

After acid injection, the bicarbonate concentration in the water is essentially equal to zero. Therefore, the $CaCO_3$ scale is avoided. The precipitation of $CaSO_4$ then becomes the limiting factor on the operation of an RO system. On the basis of the data of Marshall and Slusher (26), figure 32 was plotted to show the solubility product of $CaSO_4$ (gypsum) as a function of ionic strength. The solid line is the solubility product (Ksp) of Ca and SO_4 at saturation. The dotted line represents the maximum allowable bulk stream molarity product of Ca and SO_4 to avoid precipitation at the membrane due to concentration polarization. The ratio between wall concentration and bulk concentration is taken as 1.43 for $CaSO_4$ (27). The curve of Ksp' = 0.5 Ksp is derived from this value.

During concentration of the feedwater in an RO system, the ionic strength and molal calcium sulfate product increase along a line with a slope of 1/2 as plotted in figure 32. The intercept of such a line with the solubility product saturation curve then gives the ionic strength at saturation. The ratio of the ionic strength at saturation to the initial ionic strength gives the concentration ratio which can be achieved without $CaSO_4$ scale formation. As an example, at 20 percent penetration, 1 mgd, and 0 year, the total ionic strength after HCl pretreatment is 0.04 and the solubility product is 6.075×10^{-6}. This is

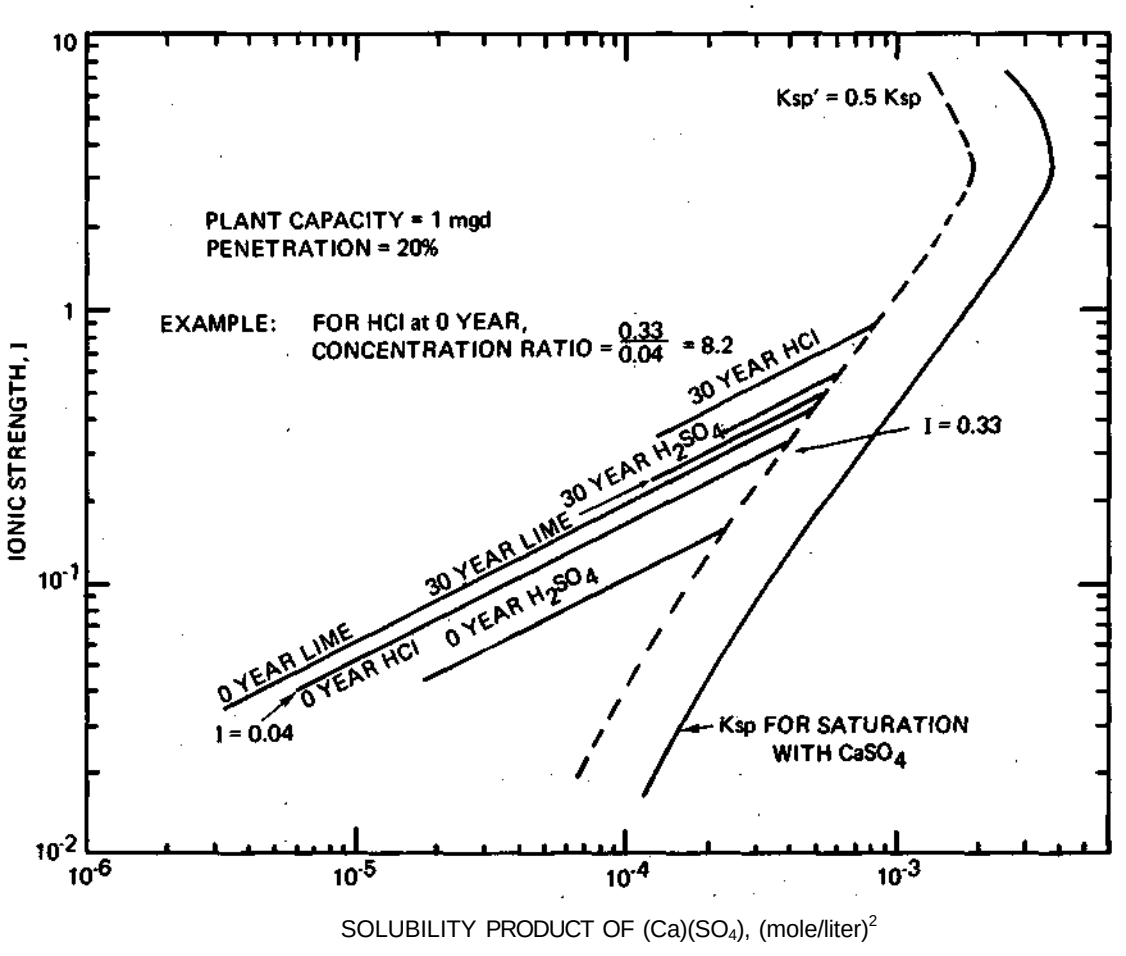

Figure 32. Determination of concentration ratios for different pretreatment methods at 0 and 30 years

the starting point in figure 32. During concentration, the ionic strength and the solubility product increase along a line with a slope of 1/2 until intercepting the dotted line of Ksp'. The interception gives an ionic strength of 0.33. The ratio of this ionic strength at maximum concentration to the original ionic strength gives a concentration ratio (C_b/C_f) of 8.2. From equation 11, the recovery ratio, R, is approximately 0.92 if the salt rejection ratio, η, is 0.9. Table 15 gives a sample calculation for 20 percent penetration and 1 mgd plant capacity by the interception method.

TABLE 15
THE DETERMINATION OF CONCENTRATION RATIO BY THE INTERCEPTION METHOD FOR HCl PRETREATMENT WATER
(20% penetration, 1 mgd)

	mg/l	Ionic strength (x 10^3)	Total ionic strength (x 10^3)	Molarity (x 10^3)	$(Ca)(SO_4)$ (x 10^6)	Intercept I x 10^3	Molar concentration ratio
0 Year							
Mg	43	3.2		1.8			
Na	400	8.7		17.4			
Ca	180	9.0	40.3	4.5	6.075	330	8.19
Cl	1189	16.7		33.5			(88%)
SO_4	130	2.7		1.55			
30 Years							
Mg	314	25.8		12.9			
Na	4220	91.75		183.5			
Ca	1580	79	341.71	39.5	131.5	750	2.3
Cl	9856	138.5		277			(56%)
SO_4	320	6.66		3.33			

2) *Lime or Lime-Soda Treatment.* The cold lime process is a proven method for removal of calcium and magnesium hardness as well as iron and manganese. One advantage of this treatment is that it is possible to be selective and precipitate the calcium and/or magnesium to the desired level by controlling the type and amount of chemical added. The basic chemical reactions are as follows:

Removal of calcium bicarbonate:

$$Ca(HCO_3)_2 + Ca(OH)_2 \rightarrow 2CaCO_3 + 2H_2O \quad (15)$$

Removal of magnesium bicarbonate:

$$Mg(HCO_3)_2 + 2Ca(OH)_2 \rightarrow Mg(OH)_2 + 2CaCO_3 + 2H_2O \quad (16)$$

Removal of calcium noncarbonate hardness:

$$CaSO_4 + Na_2CO_3 \rightarrow Na_2SO_4 + CaCO_3 \quad (17)$$

$$CaCl_2 + Na_2CO_3 \rightarrow CaCO_3 + 2NaCl \quad (18)$$

Removal of magnesium noncarbonate hardness:

$$MgSO_4 + Na_2CO_3 + Ca(OH)_2 \rightarrow Mg(OH)_2 + CaCO_3 + Na_2SO_4 \quad (19)$$

$$MgCl_2 + Na_2CO_3 + Ca(OH)_2 \rightarrow Mg(OH)_2 + CaCO_3 + 2NaCl \quad (20)$$

The cost of soda ash is higher than that of lime and its dosage to remove magnesium noncarbonate hardness is large; therefore, it is economical to remove only the absolutely necessary amount of hardness.

The water analysis of the Mt. Simon aquifer shows relatively low concentration of alkalinity, so most of the hardness is of the noncarbonate form. To remove a large amount of hardness, a costly lime and soda treatment is necessary since lime is used to remove carbonate hardness and soda to remove noncarbonate hardness.

Table 16 presents a comparison of raw water and lime treated water at 20 percent penetration and 1 mgd capacity. Table 17 is constructed on the basis of these data. In figure 32, operation lines for the lime treated water are shown. At 0 year, the recovery ratio is 0.96 for lime treatment compared with 0.92 for HC1 treatment. The results for other cases are shown in Appendix C.

TABLE 16

COMPARISON OF CANDIDATE RAW WATER AND LIME TREATMENT WATER

(20% penetration, 1 mgd)

	" Raw water (after coagulant correction)	Treated water
0Year		
Fe	9.2	0
Mn	0.4	0
Ca(as $CaCO_3$)	180 × 2.5=450	450+35-258=227
Mg(as $CaCO_3$)	43 × 4.12=177	177 × 0.9=160
Na	400	400
Cl	1000	1000
SO_4 ($CaCO_3$)	130 × 1.04=135+9=144	144
Alkalinity (as $CaCO_3$)	267-9=258	35
30 Yeats		
Fe	33	0
Mn	2.3	0
Ca (as $CaCO_3$)	3950	3950 +35 - 211 =3774
Mg (as $CaCO_3$)	1290	1160
Na	4220	4220
Cl	9700	9700
SO_4 (as $CaCO_3$)	333 +9 =342	342
Alkalinity (as $CaCO_3$)	220-9=211	35

TABLE 17

THE DETERMINATION OF CONCENTRATION RATIO BY THE INTERCEPTION METHOD FOR LIME PRETREATMENT WATER

(20% penetration, 1 mgd)

	mg/l	Ionic strength ($\times 10^3$)	Total ionic strength ($\times 10^3$)	Molarity ($\times 10^3$)	$(Ca)(SO_4)$ ($\times 10^6$)	Intercept I x 10^3	Molar concentration ratio
0 Year							
Ca	90.8	4.54		2.27			
Mg	39	3.2		1.6			
Na	400	8.7		17.4			
			33.75		3.24	410	12.1
Cl	1000	14.1		28.2			(96% recovery)
SO_4	137	2.86		1.43			
HCO_3	42.7	0.35		0.7			
30 Years							
Ca	1510	75.48		37.74			
Mg	282	23.2		11.6			
Na	4220	91.75		183.5			
			234.94		125.7	495	2.15
Cl	9700	137.5		275			(55% recovery)
SO_4	329	6.66		3.33			
HCO_3	42.7	0.35		0.7			

By comparison of the above two methods, it is suggested that HC1 pretreatment be chosen as scale control for the RO process. The reasons for this choice are:

1) The investment in equipment for lime tratment, which is much more expensive than acid injection equipment, is avoided.
2) The disposal of large amounts of lime sludge is avoided.
3) Water analysis shows that the alkalinity decreases and calcium concentration increases with the withdrawing time, so that HC1 pretreatment would become less costly and lime pretreatment more costly as time goes on.
4) The recovery ratios for both pretreatment methods are essentially the same.

Application to the Mt. Simon Aquifer

Since the water quality changes with penetration, with plant capacity, and with time in the Mt. Simon aquifer, the practicality of applying the RO process to these different waters must be considered. Table 18 presents the recovery ratios (RR) at different penetrations and different plant capacities. The detailed graphical method to obtain the results is shown in Appendix C.

TABLE 18
MAXIMUM RECOVERY RATIOS AT DIFFERENT PENETRATIONS AND PLANT CAPACITIES FOR RO PROCESS

Penetration	1 mgd		5 mgd		10 mgd	
	Years	RR	Years	RR	Years	RR
20%	0	0.92	0	0.82	Not applicable	
	30	0.56	5	0.22		
31%	Not applicable		0	0.74		
			30	0.13	30	<0.10
50%	0	0.60				
	30	0.44	30	<0.10	30	<0.10

From table 18, it can be seen that the recovery ratios decrease rapidly as the feedwater becomes more concentrated at deeper penetrations and higher plant capacities. Thus, the RO process appears to be practicable only for 1 mgd plants since the lower recovery ratios at other capacities make the process impractical for a 30-year plant.

Two-Stage RO Process

Because of the high concentration feedwater, a one-stage RO process cannot be employed to produce potable water which meets the 500 mg/l TDM standard. A two-stage RO system must be used. A flow diagram for a two-stage RO plant is shown in figure 33. The feedwater from the well field first undergoes a pretreatment prior to passing through the desalting section. The pretreatment, as suggested before, is HC1 injection. The feedwater, W_{f1}, from the well field is then pressurized and mixed with the recycle brine from the second RO stage. The mixed feedwater, Wf, then enters the first RO stage. The brine, W_{b1}, from the first stage is sent through a filter to the brine disposal well field. The product water, W_{f2}, from the first RO stage is again pressurized and sent to the second RO stage as feedwater. In

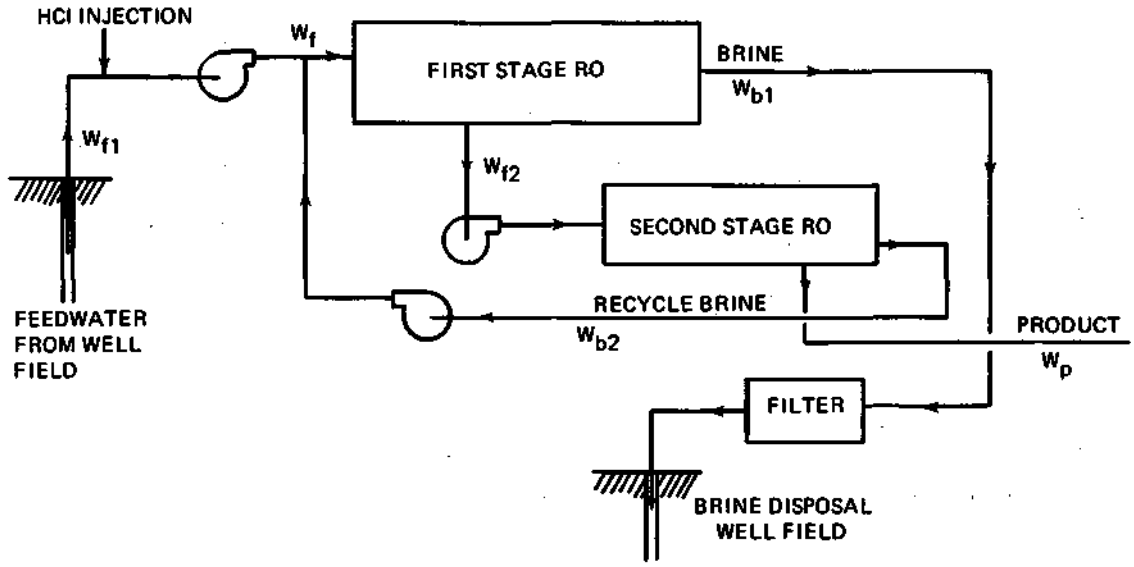

Figure 33. Schematic flow diagram of two-stage reverse osmosis process

the second stage the concentrated brine is recycled to the first stage as feedwater. The product water from the second stage is then conveyed to product storage or distribution. The calculation for the two-stage RO system is shown in Appendix D.

The salt rejection factor of the RO membranes is assumed here to be 0.9. Future improvements in membranes may increase this value to the point that a one-stage RO system can be used. At this time, a two-stage RO system is necessary for desalting the Mt. Simon aquifer water.

Brine Disposal

The RO process evaluation gives the following ranges for operation over a 30-year period:

1 mgd, 20 percent penetration

	0 year		*30 years*
Concentration ratio	8.19		2.3
Brine to feed ratio	0.09		0.44
Brine TDM	21,200	mg/l	39,100 mg/l

1 mgd, 50 percent penetration

Concentration ratio	2.52		1.79
Brine to feed ratio	0.40		0.56
Brine TDM	39,000	mg/l	49,400 mg/l

The brine is injected into deep wells (discussed in detail in a later section). Several important points are to be considered in designing this deep well injection method:

1) The system should be airtight to prevent any air in-leakage. Any oxygen leaking into the system would oxidize iron from the ferrous to the ferric state and precipitation would occur. This precipitation would tend to block the well, causing increased pumping power or, more seriously, stopping the flow of brine into the well.
2) The brine flow rate at the 30-year condition should be used in the design and sizing of the well and injection equipment.
3) A filter should be included ahead of the disposal well to remove any precipitates which may have formed during the concentration of the brine.

Economic Evaluation

The cost centers for an RO plant are grouped into two major categories: capital cost centers and operation and maintenance cost centers. Because of the developmental status of the RO process, an accuracy of about ±20 percent can be expected for plant capital costs (28). The annual fixed cost is obtained by use of carrying charge multipliers on the capital costs. Table 19 presents the cost summary for an RO plant with 1 mgd capacity. These costs apply for 20 percent and 50 percent penetrations in the Mt. Simon aquifer. The brine disposal cost is not included. This cost is considered in a later section.

Capital Cost Centers. The capital costs include the costs for equipment, construction, land, insurance, working capital, and taxes. The capital costs are estimated by use of References 29, 30, and 31. The cost of installation is estimated at 35 percent of the equipment cost.

TABLE 19

COST SUMMARY FOR REVERSE OSMOSIS DESALTING PLANT

Interest rate: 5 ⅜ %
Plant life: 30 years
Basis: . 1972 dollars;
Water plant: 1 mgd
Capacity factor: 0.9
Process: RO

	Capital cost ($)	Carrying charge multiplier	Annual cost ($)	Water cost ¢/1000gal	%
Capital cost centers					
1. Total Plant Cost	1,010,000	0.0705	70,500	22.7	29.8
2. Working Capital	31,000	0.068	2,100	0.64	0.8
Total Capital Cost	1,041,000		72,600	23.34	30.6
Operation and maintenance cost centers					
3. Labor Cost (Incl. G&A and payroll extras)			24,820	7.5	9.8
4. Membrane replacement			33,000	10.0	13.1
5. Supplies and maintenance			10,100	3.1	4.0
6. Chemical cost			33,300	10.1	13.1
7. Power cost (@ 1.27 ¢/kwh)			73,200	22.2	29.0
Total operation and maintenance cost			174,420	52.9	69.4
Total fixed plus O&M costs			247,020	76.2	100.0

Operation and Maintenance Cost Centers.

1) *Operation and maintenance labor cost.* This cost depends on the crew wage rate and crew size. An average rate of $4.00 per hour is used, and two crew members are assumed for operation of a 1 mgd plant.
2) *General and administrative overhead.* This cost is estimated as 30 percent of the operation and maintenance labor cost (18).
3) *Payroll extras.* This cost is estimated at 15 percent of the sum of the operation and maintenance labor cost and the G & A cost.
4) *Supplies and maintenance materials.* This cost includes all expendable materials other than fuel, chemicals, and membranes. It is estimated as 1 percent of capital cost.
5) *Membrane assembly replacement.* A cost of 10¢/1000 gal of product water is assumed for membrane assembly replacement (18).
6) *Chemical cost.* This is mainly the HC1 cost for acid pretreatment.
7) *Power cost.* This includes cell pumping power and power for the transport of product water and for plant auxiliary equipment.

The cost estimation in table 19 is based on water quality at the end of 30 years. It can be applied to both 20 percent and 50 percent penetrations since the water qualities are similar at the end of 30 years. The unit cost of HC1 is estimated as 1.¢/lb (32) (20° Be', corresponding to 31.45 percent of HC1). The unit power cost is estimated on the basis of the Aurora local power rate for a demand of 666 kw and a consumption of 16,000 kwh/day (33). The table shows a water cost of 76.¢/1000 gal. A reduction from this unit cost may be attainable in the future by the use of singlerstage seawater membranes which are being developed by several manufacturers.

VAPOR COMPRESSION-VERTICAL TUBE EVAPORATION-MULTISTAGE FLASH DISTILLATION

The vapor compression distillation process converts mechanical energy to heat energy by the compression of vapor produced by boiling feedwater. The high pressure and high temperature steam then passes through the tubes in the evaporator-condenser, giving up its heat to the saltwater and, thereby, condensing into fresh water. The process is a well-established desalting method that has been used extensively for small capacity marine applications. Figure 34 shows the principle of the vapor compression process. The vapor compressor takes water vapor from the evaporator-condenser and compresses it. The compression of the vapor increases the pressure and temperature. The vapor is then returned to the evaporator-condenser to serve as the heating medium for the incoming feedwater. After giving up enough heat to boil more feedwater, the vapor is condensed into fresh water. The feedwater is preheated in the heat exchanger by the brine discharge and product water streams.

The vapor compression process is particularly applicable to requirements for compact, low capacity desalting plants. Because of its relatively small cooling water requirement, which is an advantage at inland sites, the vapor compression process can be advantageously combined with other thermal processes, such as multistage flash (MSF) and vertical tube evaporator (VTE).

The chemical analysis of the Mt. Simon aquifer shows that the water has high salinity and high hardness initially and that the water quality will deteriorate as time goes on. The high salinity water makes the distillation processes applicable, but the high content of scale-forming constituents makes the scale problem serious. A detailed investigation with respect to scale control is necessary for the application of a distillation process to desalt this water.

Process Description

A schematic flow diagram of a VC-VTE-MSF distillation process is shown in figure 35. Feedwater is pumped into an MSF unit after undergoing pretreatment. In the MSF unit, the feedwater is preheated by condensing vapor flashed in the unit, and then it enters a heat-exchanger to raise its temperature to a few degrees below the operating temperature of the vertical tube evaporator. The preheated water is now introduced into the VTE unit where it is evaporated by exchanging heat with the compressed vapor. The newly formed vapor from the VTE unit is sent to the vapor compressor for recycling and the brine flows to the MSF unit for further flashing and final discharge.

The prime mover used to drive the vapor compressor may be an electric motor, a steam turbine, or a gas turbine. Communications with local power and gas companies indicated that no large amounts of gas and steam are available in the area (33); therefore, an electric motor drive must be selected as the prime mover for this application.

Pretreatment

The formation of scale and sludge deposits on heat transfer surfaces is a serious problem encountered in distillation plants. Pretreatment for removing objectionable substances from the feedwater is necessary. The scale-forming constituents are the same in a distillation

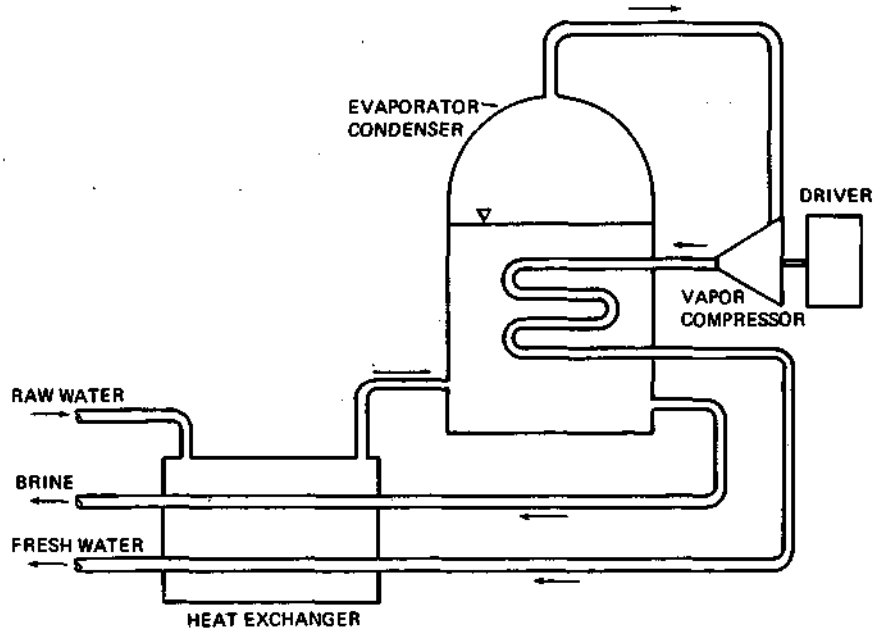

Figure 34. Principle of the vapor compression process

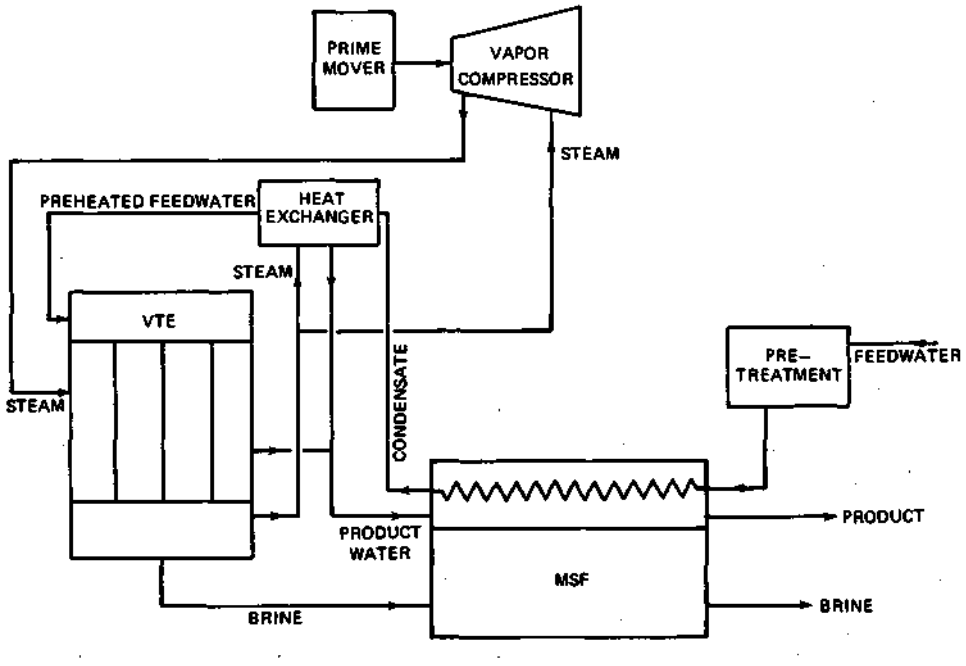

Figure 35. Schematic flow diagram of the VC-VTE-MSF process

plant as in an RO plant, but the problem is much more serious in distillation processes because of the effect of temperature on scale-forming salts. The solubilities of the scale-forming salts usually decrease with increase in temperature. Consequently, the higher the temperature of operation is, the more insoluble are the scale-forming salts. Therefore, the effect of temperature on the different constituents in the water must be taken into consideration in the selection of a pretreatment method. As mentioned before, only the required minimum treatment would be used to avoid a high pretreatment cost.

As discussed for the RO process, three different precipitates should be dealt with in the water pretreatment: 1) Iron and manganese compounds, 2) $CaCO_3$, and 3) $CaSO_4$.

Iron and Manganese Control. The discussion with respect to iron and manganese treatment in the RO system indicates that the economical way to avoid iron precipitation is iron retention, but application of this method to distillation processes requires consideration of two points. The first is the effect of temperature on iron precipitation, and the second is the fact that oxygen can leak into the system because the system is operated at pressures lower than atmospheric pressure.

The solubility line of Fe^{+2} at a temperature of 77 F was previously shown in figure 31. The solubility of iron in the ferrous state increases as the temperature increases. The reason is that the pH value of the water decreases as the temperature increases. For example, the pH value of pure water decreases from 7 to 6 as the temperature increases from 25 C to 120 C (34). Figure 31 indicates that the solubility of Fe^{+2} in water increases with decreasing pH value; therefore, Fe^{+2} becomes more soluble in water as the temperature increases.

Unlike the RO process, which is operated at high pressure, distillation processes are operated at pressures below atmospheric pressure. Oxygen can enter the system by air infiltration. Therefore, chemical deaeration is necessary, in addition to mechanical deaeration, for the removal of the last traces of dissolved oxygen in order to prevent the precipitation of iron compounds.

Sodium sulfite is the chemical agent favored for chemical deaeration because of its low cost, ease in handling, and its lack of scale formation. The chemical reaction of sodium sulfite with oxygen is illustrated by the following reaction:

$$2Na_2SO_3 + O_2 \rightarrow 2Na_2SO_4 \qquad (21)$$

The removal of 1 mg/l dissolved oxygen theoretically requires 7.88 mg/l of chemically pure sodium sulfite (35). For a reasonably tight system an oxygen infiltration of about 0.5 mg/l may be expected. A sodium sulfite dosage of 5 mg/l would be adequate for the removal of dissolved oxygen.

The introduction of sulfite ion (SO_3^{-2}) has the tendency to produce sulfur dioxide, which is a very corrosive gas, by the following chemical reactions:

$$SO_3^{-2} + H^+ \rightarrow HSO_3^- \qquad (22)$$

$$HSO_3^- + H^+ \rightarrow SO_2 + H_2O \qquad (23)$$

As shown in Appendix E, only 0.168 mg/l of SO_2 forms at the conditions of pH 5 and 25 C. This is negligibly small. If the pH value increases above 5, the formation of SO_2 decreases. Thus, the retention of iron in the water by avoiding the oxidation of the ferrous into the ferric state may be achieved by mechanical deaeration and by the addition of Na_2SO_3 for

the removal of infiltration or residual oxygen in the water.

Prevention of Scale Formation. As mentioned before, the major scale-forming constituents in the water are $CaCO_3$ and $CaSO_4$. The same method proposed for the RO system can be used here — use of HC1 treatment for the prevention of $CaCO_3$ precipitation and operation of the plant at a concentration ratio below that at which $CaSO_4$ precipitates. However, the temperature effect on $CaSO_4$ scaling must also be taken into consideration.

There are three different crystalline forms of calcium sulfate: dihydrate or gypsum ($CaSO_4 \cdot 2H_2O$), hemihydrate ($CaSO_4 \cdot l/2H_2O$), and anhydrite ($CaSO_4$). The solubilities of these three different $CaSO_4$ forms depend on temperature and also on the other ionic constituents present in the water. Their solubility curves in pure water are shown in figure 36. The higher the temperature is, the less soluble the $CaSO_4$ is. The presence of other ionic constituents increases the solubility of $CaSO_4$. For example, it is considerably more soluble in seawater than in pure water. Because its solubility is so dependent upon the other ions present in the water, the maximum temperature to which plant feedwater can be heated without exceeding the solubility limit depends upon the chemical composition. Since the constituents and their concentrations in Mt. Simon aquifer water change with time, percent penetration, and plant capacity, each water analysis must be treated as an individual case in considering scale formation.

Figures 37 and 38 present the solubility curves as functions of temperature at different penetrations and plant capacities. The equation developed by Marshall (36) is used for the calculation of solubility product in waters of different ionic strength. Appendix F gives detailed calculations applied to the Mt. Simon aquifer water. Figure 37 presents the solubility curves of $CaSO_4$ for 20 percent penetration and 1 mgd plant capacity. The solid lines are the solubility lines of anhydrite and gypsum. The anhydrite solubility is the limiting factor for attainable temperature. For example, at 0 year, the limiting temperature for HC1 treated water is 300 F as shown by the intersection point of the 0 year horizontal line and the 0 year anhydrite solubility line. At 5 years, the limiting temperature decreases to 280 F. At the end of 30 years, the limiting temperature is only 244 F. The dotted line parallel to the anhydrite solubility lines represents the allowable supersaturation line which is about 2.25 Ksp. The supersaturation line is the actual operation temperature which can be reached without precipitation. The reason for the supersaturation is that the anhydrite nucleation is very slow so that it takes a significant exposure time for precipitation to occur. Thus, without anhydrite seed crystals present, it is possible to operate above the anhydrite solubility limit for short periods of time (38).

The solid lines at the top of figure 37 represent gypsum solubility lines at 0, 5, and 30 years. The gypsum solubility is nearly constant over the temperature range of 50 to 150 F. These lines establish the limits of concentration ratios attainable in the water. For example, at 0 year the highest concentration ratio is approximately equal to $1.6xl0^{-4}/6xl0^{-6} = 26.6$, but at 30 years it is equal to $7.4\times10^{-4}/1.3\times10^{-4} = 5.7$. There are no hemihydrate solubility lines shown in figures 37 and 38. Since hemihydrate is more soluble than anhydrite and gypsum, it poses no limiting factor with respect to scale formation.

In summary, the anhydrite solubility determines the maximum temperature for a distillation process and the gypsum solubility determines the maximum concentration ratio.

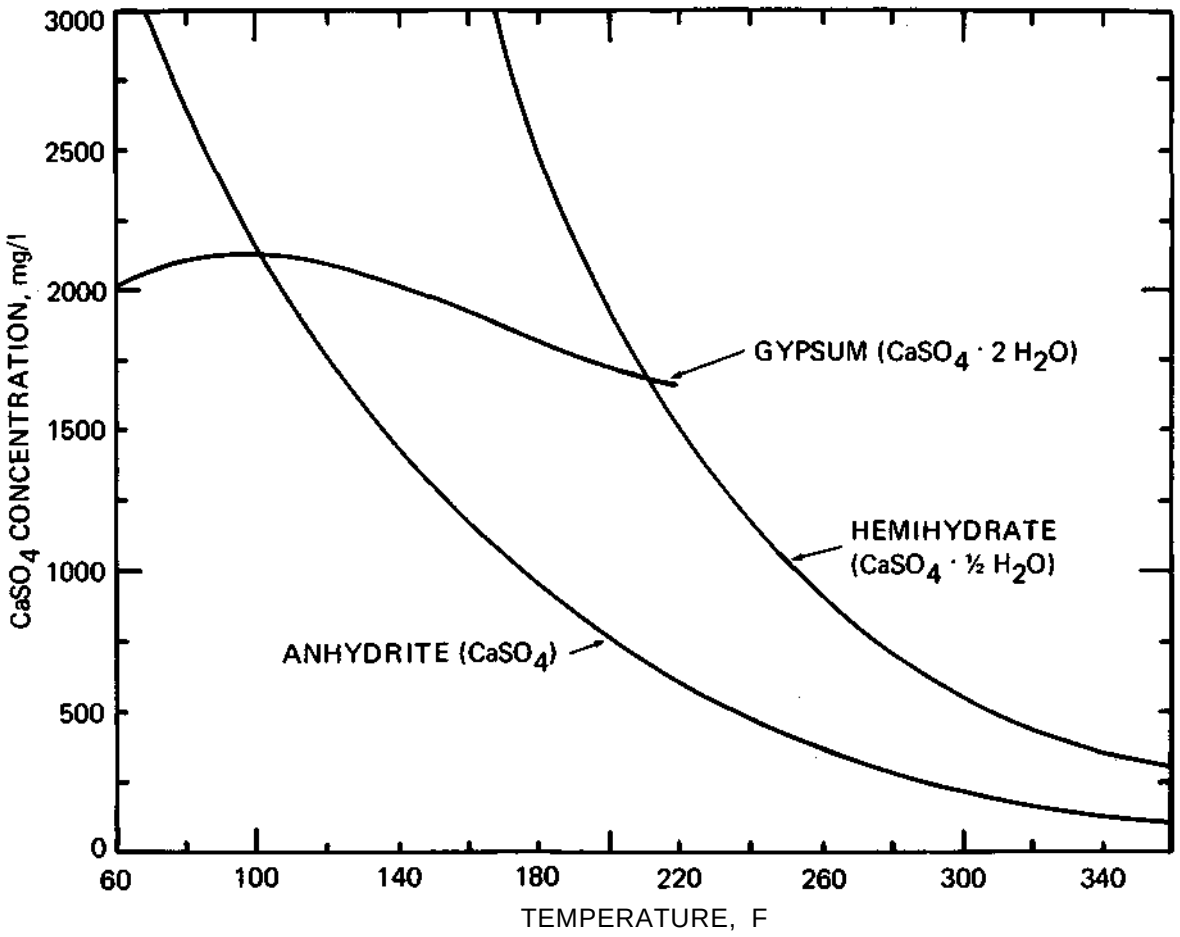

Figure 36. Calcium sulfate solubility limits in pure water

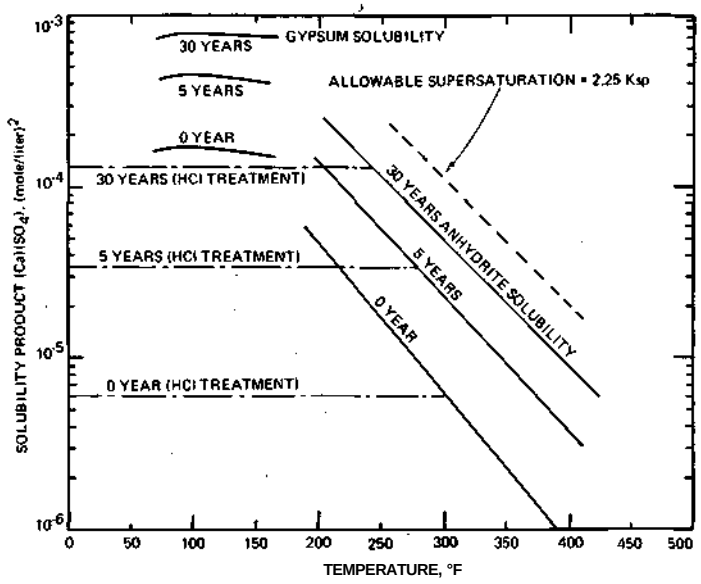

Figure 37. Solubility curves for $CaSO_4$ at 20 percent penetration and 1 mgd product

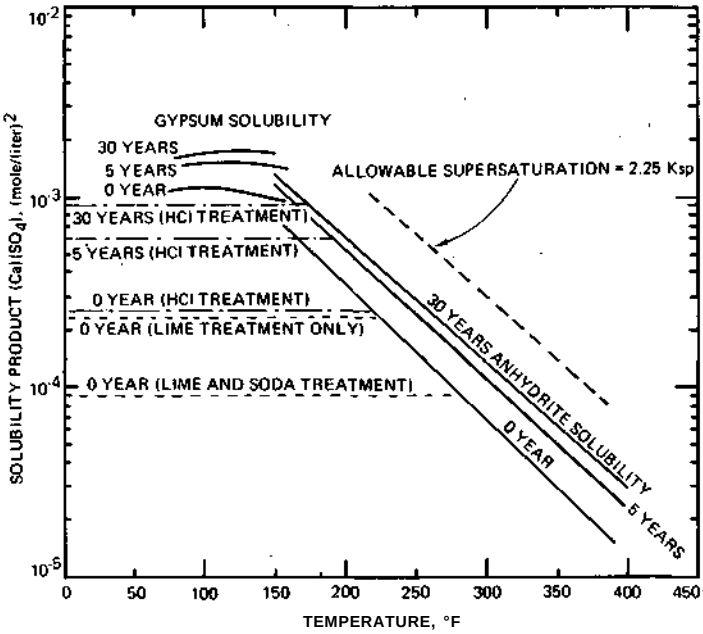

figure 38. Solubility curves for $CaSO_4$ at 50 percent penetration and 10 mgd product

Removal of Dissolved Gases. Dissolved gases must be removed from the feedwater before it enters the evaporation section of the plant. If present, dissolved gases cause lower heat transfer effectiveness and cause corrosion problems.

The removal of dissolved gases from feedwater is usually accomplished by stripping the water with live steam. The process is based on the fact that if the vapor pressure of any dissolved component in the liquid phase is higher than its partial pressure in the vapor contacting this liquid, the dissolved gas will tend to vaporize until the two partial pressures are equal. The process involves contacting the feedwater with steam under vacuum. The amount of steam must be limited so that the partial pressure of the gases mixed with the steam is below the partial pressure of the dissolved gases in the feedwater.

In summary, the pretreatment of the feedwater for the VC-VTE-MSF process would consist of the following:

1) Use of HCl injection to remove alkalinity for the prevention of $CaCO_3$ scale.
2) Retention of iron and manganese in solution by controlling the pH value and avoiding oxygen in-leakage. A small dosage of Na_2SO_3 injected into the feedwater neutralizes residual oxygen.
3) Use of a vacuum deaerator to remove dissolved gases.

Application to the Mt. Simon Aquifer

As shown in figures 37 and 38, the maximum operating temperature and the recovery ratio decrease as the penetration and plant capacity increase. In the case of 50 percent penetration and 5 mgd withdrawal rate, the operating temperature is 234 F as obtained from curves similar to those in figures 37 and 38. In distillation processes, high thermal efficiency can be obtained by operating at high temperature. Therefore, 250 F is chosen as the lower limiting operation temperature for the distillation process. Since the limiting temperature for 50 percent penetration and 5 mgd capacity is only 234 F, the use of a distillation process is impractical for these conditions. This is also the case for 10 mgd plants.

Table 20 summarizes operating temperatures and recovery ratios for different penetrations and plant capacities. The detailed method of calculating $CaSO_4$ solubility as shown in figures 37 and 38 is presented in Appendix F.

At 31 percent penetration and 5 mgd withdrawal the operating temperature is 250 F at 30 years, so it is possible to apply a distillation process for these conditions. For a 1 mgd plant, a distillation process is feasible at 20 percent and 50 percent penetrations, although the recovery ratios decrease as the penetration increases.

Brine Disposal

The distillation process evaluation gives the following data:

5 mgd, 20 percent penetration

	0 year		*30 years*
Concentration ratio	3.92		1.57
Brine to feed ratio	0.25		0.69
Brine TDM	19,200	mg/l	52,400 mg/l

5 mgd, 31 percent penetration

	0 year	30 years
Concentration ratio	3.23	1.56
Brine to feed ratio	0.31	0.64
Brine TDM	29,000 mg/l	55,200 mg/l

Brine disposal methods are discussed in a later section.

TABLE 20
OPERATION TEMPERATURES AND RECOVERY RATIOS AT DIFFERENT PENETRATIONS AND PLANT CAPACITIES FOR DISTILLATION PROCESS

Penetration	1 mgd Years	1 mgd T, RR	5 mgd Years	5 mgd T, RR	10 mgd Years	10 mgd T
20%	0	T > 250 F, RR = 0.80	0	T > 250 F, RR = 0.75	Not applicable	
	30	T = 290 F, RR = 0.60	30	T = 250 F, RR = 0.35		
31%	Not applicable		0	T > 250 F, RR = 0.68		
			30	T = 250 F, RR = 0.34	30	T < 250 F
50%	0	T > 250 F, RR = 0.60	0	T > 250 F, RR = 0.53		
	30	T = 260 F, RR = 0.44	30	T < 250 F, RR = 0.25	30	T < 250 F

T - Maximum operating temperature
RR = Recovery ratio

Economic Evaluation

The economic evaluation of the distillation plant follows that previously discussed for the RO plant. The capital cost is estimated on the basis of References 39 and 40. A unit electric power cost of 1¢/kwh, based on a demand of 10,000 kw and a consumption of 240,000 kwh/day (33), is used in the computation of the annual power cost.

Table 21 gives a cost summary for the VC-VTE-MSF plant with 5 mgd capacity. The estimated unit water cost is 100¢/1000 gal, based on the water quality at the end of 30 years and either 20 or 31 percent penetration. The cost of brine disposal is not included.

TABLE 21
COST SUMMARY FOR VAPOR COMPRESSION-VERTICAL TUBE EVAPORATION-MULTISTAGE FLASH DESALTING PLANT

Interest rate: 5 ⅜ % **Water plant: 5 mgd**
Plant life: 30 years **Capacity factor: 0.9**
Basis: 1972 dollars **Process: VC-VTE-MSF**

	Capital cost (in $)	Carrying charge multiplier	Annual cost (in $)	Water cost ¢/1000 gal	%
Capital cost centers					
1. Capital Cost	7,250,000	0.0705	511,000	31.0	30.7
2. Working capital	151,000	0.068	10,280	0.6	0.6
Total capital cost	7,401,000		521,280	31.6	31.3
Operation and maintenance cost centers					
3. Labor cost (Incl. G&A and payroll extras)			74,590	4.5	4.5
4. Supplies and maintenance			36,200	2.2	2.2
5. Chemical cost			165,000	10.0	10.0
6. Power cost (@ 1.0¢/kwh)			863,000	52.2	52.0
Total operation and maintenance cost			1,138,790	68.9	68.7
Total fixed plus O&M costs			1,660,070	100.5	100.0

FREEZING PROCESSES

The conversion of saline water to fresh water by freezing is based on the fact that ice crystals, which form when saltwater is cooled below the freezing point, are essentially salt-free. Thus, freezing processes are analogous to distillation in that both ice crystals and vapor are salt-free. Because of the low temperatures at which freezing processes operate, they have the advantage, relative to distillation processes, of minimal scale and corrosion problems.

Freezing processes are based on several well-known physical phenomena:

1) When saltwater is partially frozen, the ice crystals are essentially salt-free.
2) The specific gravity of ice is less than that of brine at the same temperature, which provides a basis for the washing of residual brine from the ice crystals.
3) The freezing point of saltwater is not affected by small pressure changes.
4) Ice crystals can be formed by evaporative freezing at or below the triple point, or by contacting the saltwater with an evaporating immiscible refrigerant.

The commercial use of freezing processes has been limited to a few small plants operated for relatively short periods of time. New processes currently under development look very promising, and it is expected that these processes will be competitive with other desalting processes, especially for feed water of high salinity.

The analysis of Mt. Simon aquifer water shows that the total TDM values at the end of 30 years will be equal to or higher than that of seawater, in the range of 34,000 to 38,000 mg/l . Also, some of the ions contributing to scale formation have higher concentrations than in seawater. For these conditions, freezing processes may prove to be more suitable than other processes.

Process Description

Two basic freezing methods may be distinguished:

1) Indirect freezing in which the heat of crystallization is removed from the saltwater through a solid barrier.
2) Direct freezing in which the heat of crystallization is removed by partial evaporation of the water at or below the triple point, or by the evaporation of an immiscible refrigerant in contact with the saltwater.

Only direct freezing processes will be considered here. Although processes using immiscible refrigerants, called secondary refrigerant processes, are currently under development, only vacuum freezing processes have thus far been in commercial service, so the discussion will be limited to these. One such process is the Vacuum Freezing Vapor-Compression (VFVC) (41,42). In this process, ice crystals are formed in a freezing chamber, or crystallizer, by reducing the vapor pressure below the triple point. The ice-brine slurry is then pumped into a counterwasher where the buoyant ice crystals rise and are washed by a stream of washwater flowing downward. The washed ice crystals are then sent to a melter where compressed water vapor is used to melt the ice into product water.

A flexible blade compressor compresses the vapor from the freezer to the melter. The vapor mass flow from the freezer is small relative to the ice mass flow. However, the low density of the vapor near the triple point results in a very large volumetric flow. A very large compressor must therefore be used to compress the water vapor from 3.4 mm Hg absolute to 4.9 mm Hg absolute. For desalting plants of 5 mgd capacity and up, there does not appear to be any practical way to scale up the compressors to the necessary size (43).

Hence, the search for an alternative to solve this problem has resulted in a new freezing process which uses a low pressure steam ejector rather than a compressor. The ejector has the advantage of no moving parts and is capable of being designed for large size plants. The process is called Vacuum Freezing-Ejector Absorption (VFEA) (43).

A schematic diagram for a VFEA process is shown in figure 39. The feedwater is pumped from an intake through a deaerator which removes any air or dissolved gases which, if allowed to remain in the system, reduce the heat transfer efficiency and may cause corrosion in the vessels.

The deaerated water is then pumped to a heat exchanger where the feedwater is cooled by outgoing product water and brine which are close to the freezing point temperature. From the heat exchanger, the cold feedwater flows into the freezer where a pressure of about 3.4 mm Hg absolute is maintained. When the entering feedwater is subjected to this reduced pressure, a portion of it is evaporated. The heat of evaporation required for formation of the vapor is given up by the feedwater and the consequent reduction of enthalpy causes ice crystals to form.

Theoretically, about seven and one-half pounds of ice are produced for each pound of vapor formed. The ice crystals and concentrated brine are continuously removed from the freezer and injected into the bottom of the counterwasher where the separation of ice and brine takes place. A density difference between ice and brine causes the ice to rise and form an ice bed. Concurrently, the top of the ice bed is washed with pure water to remove the remaining brine film from the ice. The brine-free ice at the top is continuously harvested by

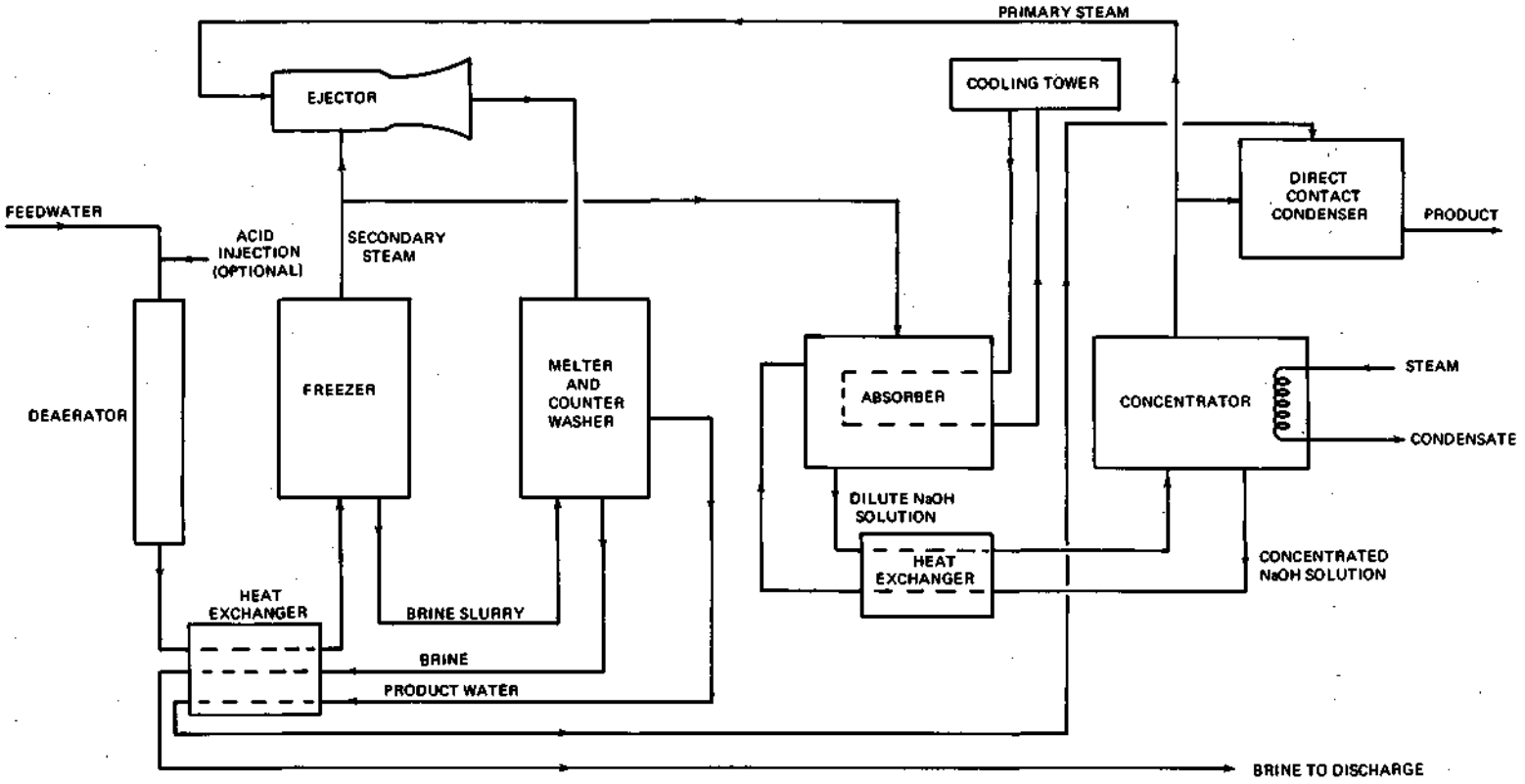

Figure 39. Schematic flow diagram of the VFEA process

means of a mechanical scraper and is then admitted to the melter. The melter is maintained at conditions slightly above the triple point of pure water to allow a transfer of heat between ice and the water vapor compressed by the ejector.

The vapor formed in the freezer is divided into two streams, one of which flows to the ejector and the other to the absorber. In the ejector, the water vapor from the freezer, called secondary steam, is entrained and compressed by the primary steam flow which is produced in the concentrator. From the ejector, the combined mixture of primary and secondary steam is passed to the melter where direct contact condensing of this vapor takes place by impingement onto the ice to produce product water. This cold product water is then passed through the heat exchanger, the absorber, and the direct contact condenser as a coolant, and finally is discharged from the process.

The absorber and concentrator use a solution of sodium hydroxide to absorb water vapor from the freezer and to produce primary steam to the steam ejector nozzle. In the absorber, the solution of sodium hydroxide is sprayed over cooling coils and absorbs water vapor introduced from the freezer. Outgoing brine and product water flow through the cooling coils to remove the heat of absorption from the absorbent. The diluted sodium hydroxide solution is pumped through an absorbent heat exchanger where it is heated by the concentrated sodium hydroxide solution and admitted into the concentrator. In the concentrator, steam is introduced to heat the diluted sodium hydroxide, and water vapor is produced and directed to the ejector as primary steam. Concentrated sodium hydroxide is then recycled back to the absorber.

The amount of vapor generated in the concentrator exceeds the ejector primary steam requirement because of mechanical and thermal process inefficiencies. The excess vapor must be removed to maintain the process in thermal equilibrium. The vapor is condensed by outflowing product water in a direct contact condenser where the vapor is recovered as additional product water. In addition, waste heat is removed in the brine stream and by the use of a cooling water stream. The ultimate heat rejection may be by either discharge to a body of water or to a cooling tower. For the Mt. Simon aquifer application, a water cooling tower would be necessary for the heat rejection.

A freezing process using a secondary refrigerant instead of water vapor is also currently under development (44). A nontoxic, nonflammable refrigerant is used in this process, which appears to be competitive in cost with the vacuum freezing process described above.
Scale **Control**

One of the advantages of the freezing processes is the elimination or reduction of scale formation. As the temperature becomes lower, the solubility of scale-forming constituents in the water becomes higher and the nucleation time becomes longer (supersaturation can be sustained). The need for pretreatment for most brackish waters and seawater can generally be avoided in the freezing processes. However, analysis of the Mt. Simon aquifer water shows a much higher Ca^{+2} concentration than exists in seawater. Scale may be formed in the brine as it is concentrated in the process and as the temperature is raised to about 80 F. Two major scale formations are analyzed in the following paragraphs.

$CaSO_4$ Scale. Since the freezing process is operated in the temperature range between 25 F and 80 F, calcium sulfate scale may be expected to take the form of gypsum ($CaSO_4$

$2H_2O$) because it has the lowest solubility of the three crystalline forms of calcium sulfate in this temperature range. The saturated solubility product of $(Ca)(SO_4)$ as presented earlier in figure 32 gives the limitation to which the $CaSO_4$ can be concentrated. In the freezing process the concentration polarization effect can be neglected. However, the dotted line for Ksp' should be used as a safety factor in freezing processes. The corresponding concentration ratios for application of a freezing process to different feedwaters are presented in table 22. These are the maximum values which can be safely used in the process.

TABLE 22
MAXIMUM CONCENTRATION RATIOS OF FREEZING PROCESSES TO AVOID PRECIPITATION OF $CaSO_4$

	1 mgd		5 mgd		10 mgd	
	0 Year	30 Years	0 Year	30 Years	0 Year	30 Years
20%	10.6	2.30	3.92	1.57		
31%			3.23	1.56	2.82	1.39
50%	2.52	1.78	2.16	1.35	1.97	1.32

$CaCO_3$ Scale. The formation of $CaCO_3$ scale depends on Ca^{+2} concentration, alkalinity, pH value, temperature, and total TDM. Figure 40 presents the stability diagram of $CaCO_3$ in seawater. This diagram was developed from Reference 45. From this diagram, a saturation pH value, pH_s, can be found and compared with the actual pH value of the water. The saturation index can then be calculated to determine whether the scale will tend to form. The following example gives a method for finding the saturation index:

> For the case of 31 percent penetration, 10 mgd, and 30 years, the concentration ratio is 1.39 as shown in table 22. The calcium and alkalinity concentrations in the brine are
>
> Ca^{+2} = 16,000 mg/l as $CaCO_3$
>
> Alk = 239 mg/l as $CaCO_3$
>
> pH = 6.5
>
> The saturation pH value is found from figure 40 to be 6.53. Then
>
> Saturation Index = 6.5 - 6.53 = -0.03
>
> The negative saturation index implies that no scale-forming tendency exists, but for the purpose of safety, a partial acid treatment may be employed.

Application to the Mt. Simon Aquifer

Technically, the freezing process can be applied to the Mt. Simon aquifer in the whole range of 1 to 10 mgd capacities and 20 percent to 50 percent penetrations, but the concentration ratio (and recovery ratio) decreases as the plant capacity and penetration increase. The concentration ratios were presented earlier in table 22.

Economic Evaluation

The economic analysis procedure follows that used for the RO process. The cost estimation is based on Reference 43. Table 23 gives the cost estimation for a freezing plant of 1 mgd capacity. Since the freezing process is still under development, it is difficult to estimate

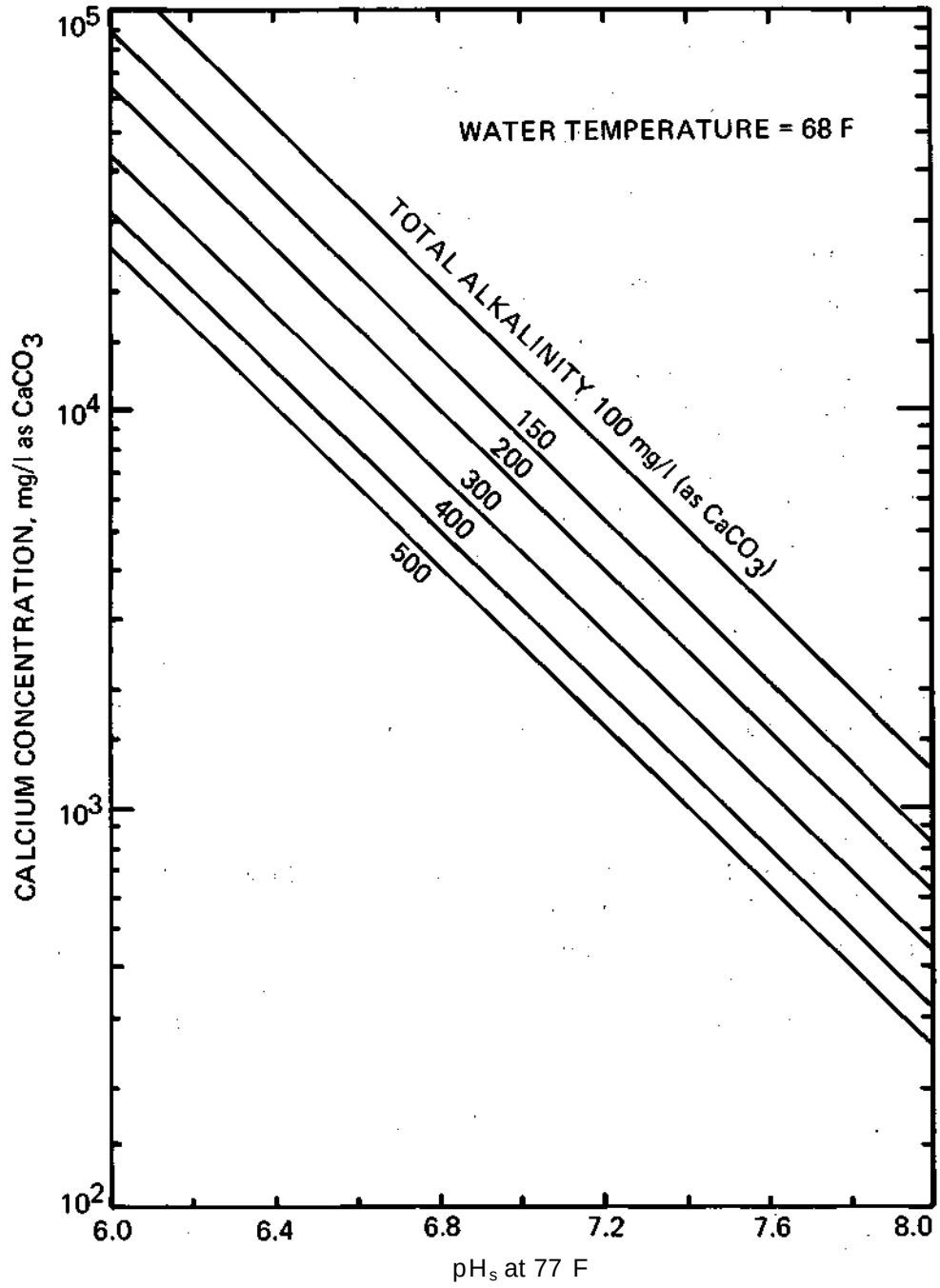

Figure 40. Calcium carbonate stability diagram in seawater

TABLE 23
COST SUMMARY FOR FREEZING PROCESS DESALTING PLANT

Interest rate: 5 ⅜ % Water plant: 1 mgd
Plant life: 30 years Capacity factor: 0.9
Basis: 1972 dollars Process: VFEA

	Capital cost ($)	Carrying charge multiplier	Annual cost ($)	Water cost ¢/1000 gal	Water cost %
Capital cost centers					
1. Capital cost	860,000	0.07	60,100	18.2	22.2
2. Working capital	41,000	0.068	2,800	0.8	1.0
Total capital cost	901,000		62,900	19.0	23.2
Operation and maintenance cost centers					
3. Labor cost (Incl. G&A and payroll extras)			60,600	18.4	22.5
4. Supplies and maintenance			4,100	1.2	1.5
5. Chemical cost			500	0.2	0.2
6. Power cost: (@ 1.34 ¢/kwh)			48,800	14.8	18.0
7. Steam cost (@ 0.50 ¢/10^6 Btu)			93,200	28.3	34.5
Total operation and maintenance cost			207,200	62.9	76.8
Total fixed plus O&M costs			270,100	81.9	100.0

cost for plants larger than 1 mgd. For the 1 mgd plant, the estimated unit water cost is 81.9 ¢/1000 gal, based on the water quality at the end of 30 years and 20 or 50 percent penetration. The cost of brine disposal is not included. A unit electric power cost of 1.34 ¢/kwh is used, based on a demand of 420 kw and a consumption of 10,100 kwh/day. A steam cost of 50 ¢/10^6 Btu is assumed.

CONCLUSIONS

Five different desalting processes have been investigated for desalting the Mt. Simon aquifer water. The results can be summarized as follows:

1) The ion exchange process is rejected because the high salinity water requires a very high chemical cost.

2) The electrodialysis process is rejected because of the prohibitively high cost for electric power.

3) The reverse osmosis process can be applied only to 1 mgd plants at 20 percent penetration. The $CaSO_4$ scale formation prevents the application of the RO process in other cases.

4) The distillation process can be applied to both the 1 and 5 mgd cases. In the cases of 5 mgd at 50 percent penetration and 10 mgd at all penetrations, the $CaSO_4$ scale formation limits the maximum working temperature to values below 250 F, which is set in this study as the minimum value for the working temperature. Therefore, the distillation process is rejected in the case of 5 mgd at 50 percent penetration and in all 10 mgd cases.

5) The freezing process is applicable to all cases, but the concentration ratio decreases to low values for large capacity plants, thereby aggravating the brine disposal

problem.

Table 24 presents the feasible desalting processes applicable to the Mt. Simon aquifer. Table 25 gives the waste brine characteristics for the different cases.

TABLE 24
FEASIBLE DESALTING PROCESSES FOR MT. SIMON AQUIFER

Penetration	Plant capacity 1 mgd	5 mgd	10 mgd
20%	RO Distillation Freezing	Distillation Freezing	Not applicable
31%	Not applicable	Distillation Freezing	Freezing
50%	Distillation Freezing	Freezing	Freezing

As shown in table 25, for plants of large capacity, the allowable concentration ratios at the end of 30 years are so small that brine flow rates reach approximately three-fourths of the feed water flow rate.

The difficulties in desalting the Mt. Simon aquifer water are:

1) The feedwater salinity will change greatly during the 30-year operation and thus the water flow rate and concentration ratio will vary accordingly. The design and operation of a desalting plant with such large variations will pose some challenging problems.
2) The high content of Ca^{+2} and SO_4^{-2} increases the scale-forming tendency and thus puts limitations on the recovery ratio.
3) The high Fe^{+2} and Mn^{*2} concentrations require special procedures to prevent the formation of precipitates.

In spite of all difficulties, a bench scale or pilot plant study for desalting the Mt. Simon aquifer water is considered desirable. Since it is an enormous water resource, and a water shortage is predicted in the near future in the rapid population growth area of northeastern Illinois, continued early planning for augmentation of the water supply is necessary. Since the water characteristics differ so greatly from those of ordinary groundwater and seawater, a pilot plant is considered to be a necessary first step. As a starting point, it is suggested that a small scale RO or freezing pilot plant be constructed and the data obtained from the pilot plant be used as a guideline for the construction of future plants.

TABLE 25
WASTE BRINE CHARACTERISTICS

Penetration	Plant capacity 1 mgd	5 mgd	10 mgd
20%	Process: RO CR = 8.19 to 2.3 W_b/W_f = 0.094 to 0.435 TDM = 21,200 to 39,100 pH = 6.0 ± 0.5	Process: Distillation CR = 3.92 to 1.57 W_b/W_f = 0.25 to 0.64 TDM = 19,200 to 52,400 pH = 6.0 ± 0.5	Not Applicable
31%	Not applicable	Process: Distillation CR = 3.23 to 1.56 W_b/W_f = 0.31 to 0.64 TDM = 29,000 to 55,200 pH = 6.0 ± 0.5	Process: Freezing CR = 2.82 to 1.39 W_b/W_f = 0.35 to 0.72 TDM = 31,000 to 53,100 pH = 6.0 ± 0.5
50%	Process: RO CR = 2.52 to 1.79 W_b/W_f = 0.4 to 0.56 TDM = 39,000 to 49,400 pH = 6.0 ± 0.5	Process: Freezing CR = 2.16 to 1.35 W_b/W_f = 0.46 to 0.74 TDM = 43,200 to 51,300 pH = 6.0 ± 0.5	Process: Freezing CR = 1.97 to 1.32 W_b/W_f = 0.51 to 0.76 TDM = 44,300 to 51,900 pH = 6.0 ± 0.5

NOTES: Where a range is given, the first value is for 0 year, and the second value is for 30 years.
W_b/W_f = Brine flow rate/feed flow rate
CR = Concentration ratio (concentration of brine/concentration of feed)
TDM = Total dissolved minerals in brine
The feedwater rate (W_f) changes with time when product rate (W_p) is kept the same. The relation is as follows:

$$W_f = \frac{W_p}{(1 - \frac{W_b}{W_f})}$$

BRINE DISPOSAL

DISPOSAL METHODS

As environmental regulations become more and more stringent, brine disposal from inland desalting plants may be considered as a critical factor in determining the economic feasibility of desalting. For many years, waste disposal has been a problem in industry, and various disposal methods have been developed and used. Some of these methods can be applied to the disposal of brine from desalting plants. In this study, three different methods of brine disposal were considered: deep well injection, evaporative ponds, and crystallizer and. evaporator. As discussed below, deep well injection was considered to be the most suitable method.

Deep Well Injection

The petroleum industry has used deep well injection as a method of oil field brine disposal for over 60 years (46). In determining the feasibility of deep well injection, the following factors are to be considered: state regulations, the geological structure, brine mineral content, and the cost of the injection system.

State Regulations At the present time, there does not appear to be any state regulation which prohibits the use of deep well injection in the state of Illinois. Several injection wells have been used for industrial waste disposal in the state. Therefore, it is assumed that there is no legal problem in using deep well injection as a brine disposal method in the state of Illinois provided that it poses no danger of polluting the natural water resources.

Geological Structure. Most deep well injection waste disposal systems use sandstone or limestone formations. These formations have sufficient porosity and permeability to act as storage reservoirs. The formation used should be deep enough to prevent communication of fluids between the injection zone and aquifers containing usable groundwater, and it should have sufficient capacity to receive and contain the brine from the desalting plant over the life of the plant. A thorough geological and hydrological investigation would be necessary to select a suitable site for deep well injection.

Water Mineral Content. The water analysis data for the Mt. Simon aquifer show high iron and calcium contents. Precautions should be taken to protect the deep well disposal formation against damage by fracturing or plugging. The injection system should be airtight to avoid the oxidation of iron in the brine. Since the desalting plant would be operated in a concentration range where no scale formation is possible, theoretically the brine would be scale free. However, a sudden change of concentration or nonuniform mixing may cause some scale formation in the brine. Careful monitoring of the system would be necessary so that corrective chemical treatment could be applied when warranted.

Evaporative Pond

Evaporative ponds may offer an effective method of brine disposal if the net evaporation rate (gross annual evaporation minus annual rainfall) exceeds approximately 40 inches per year. The net evaporation rate in the northeastern part of Illinois is estimated at only 30

inches per year, which indicates that an evaporative pond is not suitable for brine disposal in the area.

Crystallizers and Evaporators

Crystallizers and evaporators are widely used in industry for reclaiming solids from solution. Applying this method to a desalting plant would reduce the waste brine to residual solids that may more easily be stored or shipped away for dumping.

Preliminary estimates indicate disposal costs by this method to be several times as large as those for injection wells, so this method would not be economically feasible.

INJECTION WELL AND WELL FIELD DESIGN

Well Design

Design criteria were investigated for waste brine injection wells in connection with desalting processes. Well designs were based on the use of standard materials consistent with criteria of the Illinois Environmental Protection Agency.

For a maximum design injection rate of 1 mgd per well, each well would include 16 inch outer casing to a point below the depth at which Mt. Simon water quality reaches 10,000 mg/l of dissolved minerals and a 12 inch long-string to the top of the injection zone in the lower portion of the Mt. Simon (figure 41). Both casings would be run with suitable centering devices and would be cemented from the bottom up to the surface. An 8 inch injection string would run inside the 12 inch long-string, and the annulus between the two strings would be filled with oil or fresh water. A seal would be placed at the bottom of the annulus, and at the surface a monitoring device would be used to detect changes in the annulus fluid pressure.

A 10 inch borehole would continue below the long-string to the bottom of the Mt. Simon and would constitute the injection zone. The length of the injection zone must accommodate the following constraints: 1) flow into the well borehole must not exceed 2 ft/min, 2) injection pressure must not exceed 0.65 psi per foot of depth at the injection zone, and 3) the mineral concentration of the injected brine must not exceed that of the native water in the injection zone.

On the basis of the above constraints and design parameters a determination was made of the required length of open borehole for injection purposes. The average open area per lineal foot of borehole was calculated, with use of an effective porosity of 10 percent (average porosity of drill cores was 11 to 13 percent), to be 0.0547 ft^2/ft. For Q = 1 mgd (694 gpm) and V = 2 ft/min, the required length of borehole is:

$$L = Q/7.48AV = 850 \text{ feet}$$

Thus, as shown in figure 41, injection wells were designed with an 850 foot injection zone.

Injection Well Field Schemes

Schemes for deep well injection of waste brine were investigated. An example of one disposal well scheme is given in figure 42. Several computer runs were made with the same

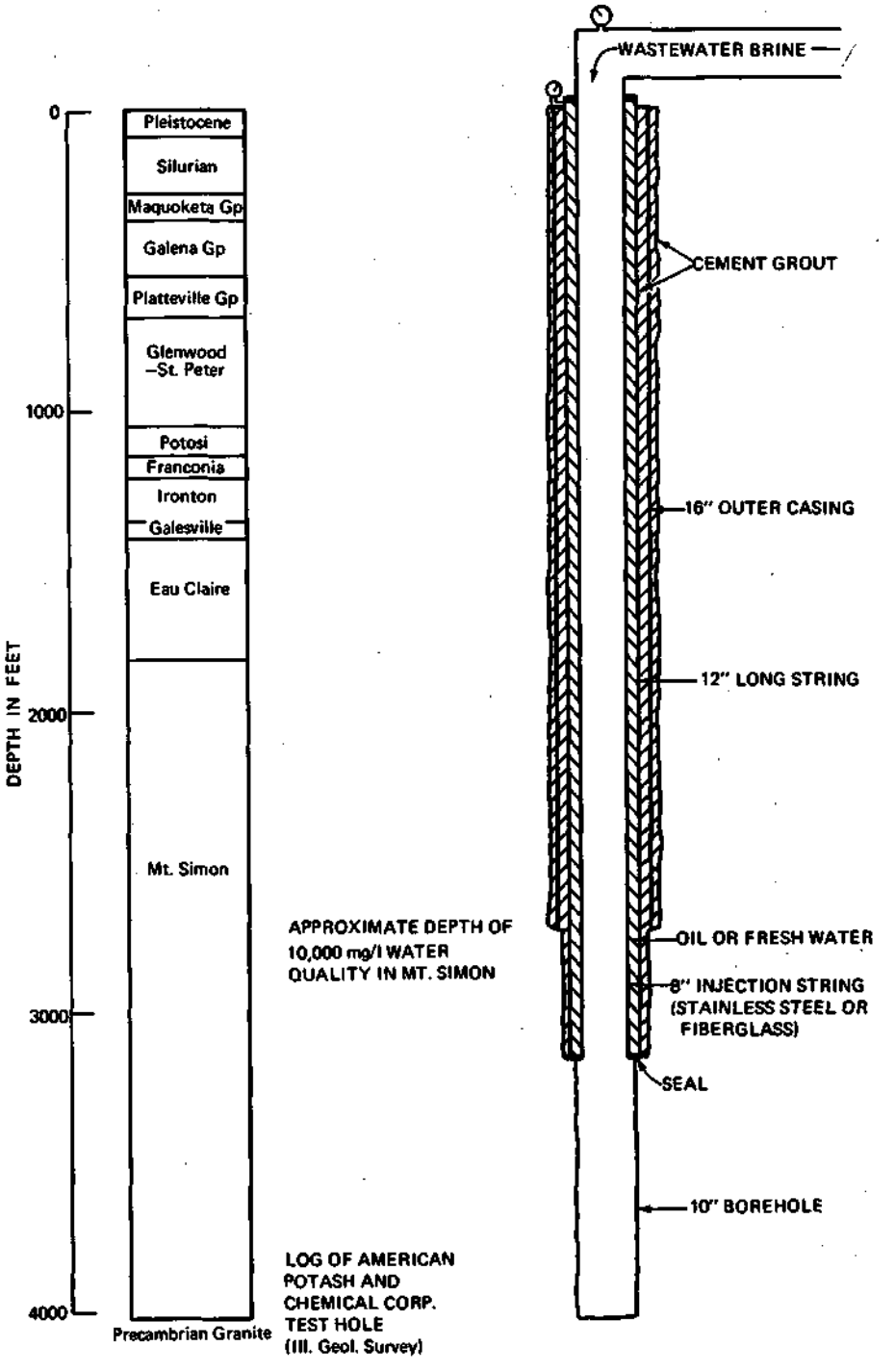

Figure 41. Injection well construction features

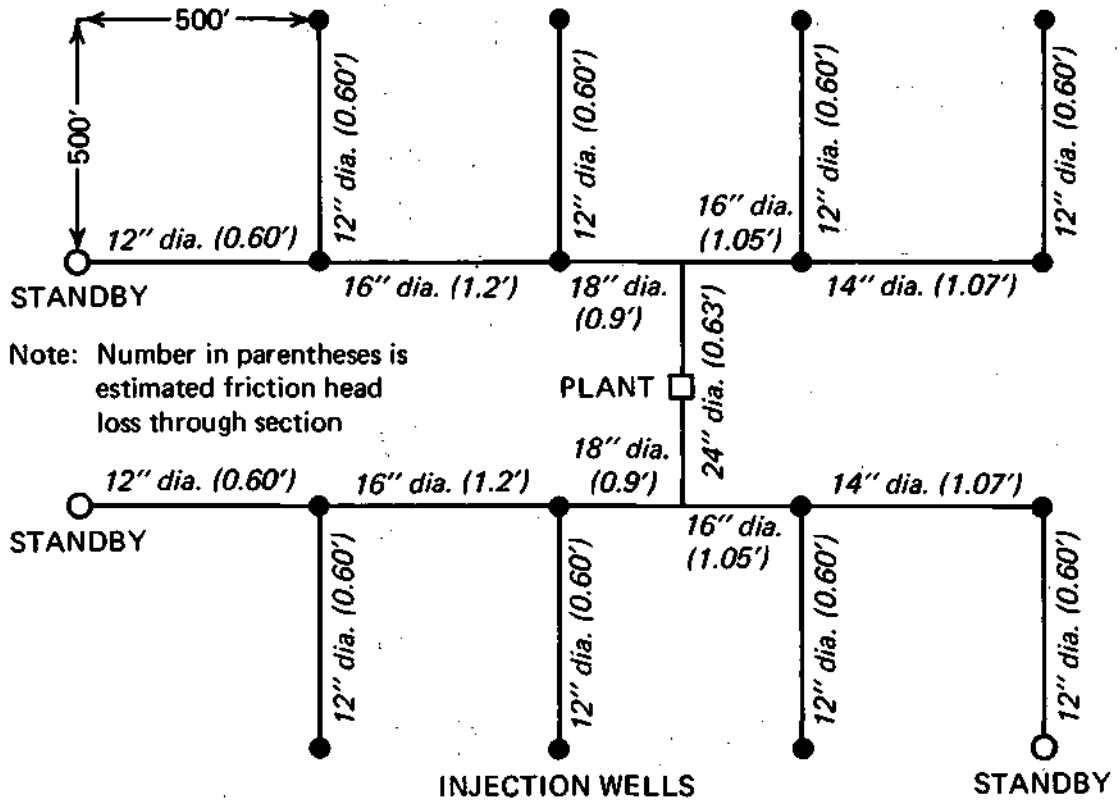

Figure 42. Injection well layout for maximum injection of 15 mgd

model as described in the sections on the *Digital Computer Model* by injecting (negative pumping) instead of pumping. The design of all 1 mgd capacity individual injection wells used was identical, as shown in figure 41. In addition, multiple injection well fields were laid out in such a way as to accommodate the variable waste brine rates, to eliminate possible contamination of pumped feed water, and to keep injection pressures within acceptable limits.

The injection well field layouts for the 1 mgd and 5 mgd product water schemes incorporated injection wells spaced 500 feet apart in a square pattern centrally located around the desalinization plant. The number of wells varies for these schemes according to the waste brine rates.

The total number of brine injection wells in any scheme is the sum of the 1 mgd wells necessary to dispose of the ultimate wastewater brine flow from the desalting plant plus standby wells (utilizing a 20 percent standby factor). Thus, the simplest scheme, which disposes of 1 mgd of brine, requires one injection well plus a standby or a total of two wells; and the largest scheme, which ultimately disposes of 35 mgd of brine, uses 35 injection wells plus 7 standbys for a total of 42 wells.

The injection well field layouts for the 10 mgd product water schemes were shown earlier in figure 21. The spacing of injection wells within these particular fields is the same as that for the pumping wells shown in figure 19.

Tables were prepared of estimated water level declines in pumped wells and pressure buildups in injection wells for the variable feedwater and brine disposal rates. This was done by measuring distances between pumping and injecting well fields, preparing time-water level decline or buildup graphs for these distances from the computer output data, and applying the principle of superposition to account for the time phasing of pumping and mutual interference effects between well fields.

Tables 26 and 27 illustrate an example of the above calculated water level declines and pressure buildups in the 50 percent penetration 5 mgd product water scheme. A comparison of tables 8 and 26 shows the large effects of reducing water level declines in the pumping fields as a result of injection. Also, note that the injection buildup reaches a peak at about 15 years and then declines slowly thereafter. This is due to time delay of interference from pumping wells at a distance and the fact that, as a total, the rate of water withdrawal is greater than the injection rate. Therefore, with time, the injection pressure declines, since water levels recede because of continuing withdrawal of water from storage in the aquifer.

It should be pointed out that heads in the immediate vicinity of the injection wells will be several feet above land surface as a result of pressure buildup. Thus, any wells drilled into the Mt. Simon aquifer, near the injection wells, should be designed against the possibility of flowing. In addition, although the injection and pumping wells have been spaced so that no contamination of the feedwater will take place, any wells drilled into the Mt. Simon aquifer near the injection wells may experience some deterioration in water quality. The degree of any deterioration of water quality under these circumstances should be the subject for further research.

TABLE 26
ESTIMATED AVERAGE WATER LEVEL DECLINE FOR 5 MGD
50 PERCENT SCHEME WITH INJECTION
(In feet below original static level)

Years of pumping	Field 1	Field 2	Field 3	Field 4
0.27	480	470	-8*	-8*
1	485	480	27*	27*
2	488	487	420	70*
3	490	490	470	160*
4	492	492	485	320
5	495	495	490	380
10	505	505	500	480
15	525	525	520	510
20	535	535	530	520
25	550	550	545	535
30	570	570	565	560

*These water level declines (- denotes a rise) are due only to interference from other pumping or injecting wells, as pumpage here has not started yet.

TABLE 27
ESTIMATED AVERAGE INJECTION PRESSURE BUILDUP
FOR 5 MGD 50 PERCENT SCHEME
(In feet of water above original static level)

Years of injecting	Pressure buildup in injection well field
0.27	460
1	530
2	590
3	640
4	710
5	800
10	1000
15	1020
20	980
25	960
30	950

ECONOMICS

WELLS

Well Designs

Feedwater production wells, designed for a maximum development of 1 mgd per well, utilize 12 inch diameter boreholes penetrating 20, 31, and 50 percent of the Mt. Simon aquifer. For an estimated aquifer thickness of 2600 feet and a depth of 1800 feet to the top of the Mt. Simon in the DuPage County area, these penetration values correspond to well depths of approximately 2300, 2600, and 3100 feet, respectively. Feedwater wells were designed to include 20 inch surface casing through the drift and the Silurian dolomite and a 13⅜ inch long-string to the top of the Mt. Simon. Both casings would be cemented by forcing grout material up from the bottom of the cased section to the surface. Construction features are shown in figure 43.

Brine injection wells were designed as discussed on page 92 and shown in figure 41.

WellCosts

Well construction costs for feedwater production wells and brine injection wells are the same. Gibb and Sanderson (47) collected cost data for deep sandstone wells in northern Illinois and by regression analysis developed the following cost-depth relationship:

$$C_W = 0.029d^{1.87} \quad (24)$$

where C_W is well construction cost in 1966 dollars and d is well depth in feet. Equation 24 was adjusted to 1972 prices for this report by applying Engineering News-Record Cost Indexes for 1966 and 1972. Construction cost for production and brine injection wells then becomes:

$$C_W = 0.0497d^{1.87} \quad (25)$$

Annual costs for wells were obtained by amortizing capital costs at 5⅜ percent interest over an assumed 30-year service life. When the capital recovery factor (CRF) for n = 30, i = 5⅜ percent is applied, the annual cost becomes:

$$C_{AW} = 0.00337d^{1.87} \quad (26)$$

To insure continuous operation during periods of well maintenance and repair, standby feedwater and injection wells are provided for under the following schedule:

Rate (mgd)	Total number of wells including standby
1	2
5	6
10	12

For pumping and injection rates in excess of 10 mgd, well fields were separated into units of 5 and 10 mgd capacity, for which the above schedule applied.

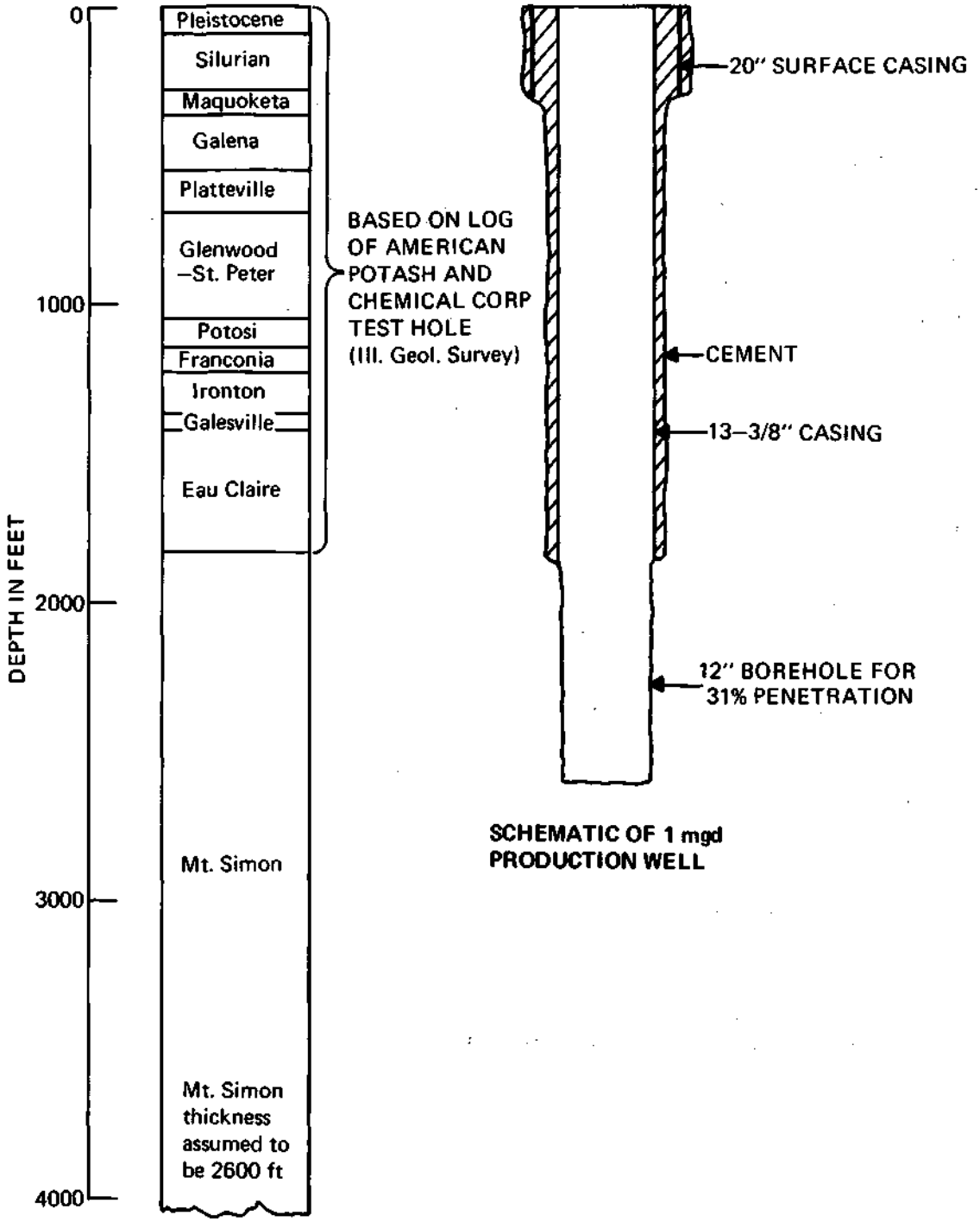

Figure 43. Construction features of 31 percent penetrating production well

PUMP COSTS

Feedwater Pumps

Gibb and Sanderson (47) determined pump costs for submersible and vertical turbine pumps in Illinois. Their cost equation for submersible pumps was modified for use in a study of cost comparisons for alternative water supplies in northeastern Illinois by Moench and Visocky (48). The latter study included the following modifications:

1) Cost of switches, wiring, and miscellaneous appurtenances increased pump costs by 50 percent.
2) The number of wells (pumps) was increased by 50 percent to allow for peaking supply.
3) For standby, the number of wells (pumps) was increased an additional 20 percent.
4) Costs were presented in 1970 dollars.

Item 2 was not considered in this report and item 4 was adjusted upward to 1972 dollars. Standby wells (pumps) were provided for as listed above. Individual pump costs, including item 1, are as follows:

$$C_P = 500\ H^{0.658} \qquad \text{for } H < 800 \text{ ft} \qquad (27)$$

$$C_P = 452 H^{0.721} \qquad \text{for } H > 800 \text{ ft} \qquad (28)$$

where H is total pumping lift (see discussion under electrical costs).

Brine Injection Pumps

On the basis of a recent study by Singh et al. (49), the cost of brine injection pumps, including equipment and housing, can be expressed as:

$$C_{BIP} = 31{,}770 \left(\frac{H}{300}\right) + 252\, P_i \qquad (29)$$

where

C_{BIP} = cost of brine injection pumps in 1972 dollars
H = total pumping head in feet
P_i = installed horsepower

P_i is defined by the relation:

$$P_i = 0.17546\ QHJ/E \qquad (30)$$

in which

Q = flow in mgd
J = firming factor or standby factor
E = efficiency at peak load (assumed as 0.5)

The value of J is dependent upon Q as:

$Q \leq 2.0$ mgd	$J = 2.08 - 0.18\,Q$
$2.0 < Q \leq 5.0$ mgd	$J = 1.9666 - 0.1233\,Q$
$5.0 < Q \leq 10.0$ mgd	$J = 1.42 - 0.014\,Q$

Annual injection pump costs were obtained by amortizing capital costs at 5⅜ percent

over an assumed service life of 15 years. Thus,

$$C_{ABIP} = 0.0988 C_{BIP} \quad (31)$$

The cost of routine operation, maintenance, and repair of pump stations, in 1972 dollars, is given as

$$C_{OMRBIP} = 1590 \left(\frac{H}{300}\right) \quad (32)$$

ELECTRICAL COSTS

Electrical cost determinations for feedwater wells and injection wells were made on the basis of an assumed unit power charge of 1.0¢/kwh and the expression for pumping energy presented by Ackermann (50):

$$kwh = 1.88 \times 10^{-4} QGht/E \quad (33)$$

where

Q = flow in gpm
G = specific gravity of fluid
h = total pumping head in feet
t = time in hours
E = wire-to-water efficiency (assumed to be 0.5)

On the basis of a plant capacity factor of 90 percent (330 days per year) and an assumed wire-to-water efficiency of 0.5, annual power costs may be expressed as:

$$C_E = 0.0297\ QGh \quad (34)$$

Total pumping head for feedwater wells is the sum of drawdown, well loss, static lift, friction head, and delivery pressure at the plant. Drawdowns were computed by the digital model for each pumping scheme. Well losses for 1 mgd pumping rates were estimated from empirical studies at the State Water Survey to be 100, 80, and 50 feet, respectively, for wells penetrating 20, 31, and 50 percent into the Mt. Simon. Static lift, the depth from land surface to nonpumping water levels, was estimated from gas storage field information to be approximately 150 feet. Friction head was computed for each well scheme by applying the Bernoulli equation to the appropriate pipe diameter and flow velocity. It was assumed that water delivered to the plant would be under a nominal pressure head of 25 feet.

Total pumping head for brine injection wells is the sum of injection pressure buildup, well loss, static lift (negative), and friction head. Pressure buildups were computed by the digital model as in the case for feedwater wells. Well losses for 1 mgd injection rates were estimated as above to be 80 feet, and static lift was taken to be minus 150 feet. Friction head was computed as described above.

TRANSMISSION COSTS

The construction cost of pipe, transportation, installation, valves, and other appurtenances that are integral parts of a transmission line is expressed (51) in 1972 dollars as

$$C_T = 4038 D^{1.2} L \quad (35)$$

where

C_T = transmission cost in dollars
D = pipe diameter in inches
L = length of pipe in miles

The annual cost of operation, maintenance, and repair for transmission lines (49) is:

$$C_{OMRT} = 10DL \quad (36)$$

The placement of transmission lines along the-right-of-way of highways or rail lines incurs an additional cost for easements. Singh et al. (49) estimated such cost to be:

$$C_{ROWT} = 1700L \quad (37)$$

The total annual cost of transmission lines is the sum of OM&R and amortized capital costs (amortized at 5^{3}-$_{8}$ percent interest over the 30 year project life):

$$C_{AT} = C_{OMRT} + CRF(n=30, i=5\tfrac{3}{8}\%)\sum(C_T + C_{ROWT}) \quad (38)$$

Pipe diameters used in equations 35 and 36 are chosen from considerations of pipe flow and unit conveyance cost. Singh (52) determined optimum diameters for pipes which resulted in minimizing unit conveyance costs.

Figure 44 illustrates the transmission lines for a 20 mgd feedwater pumping scheme which utilizes four 5 mgd well fields with 50 percent penetrating wells. The pumping scheme is designed to furnish feedwater for a 5 mgd desalting operation.

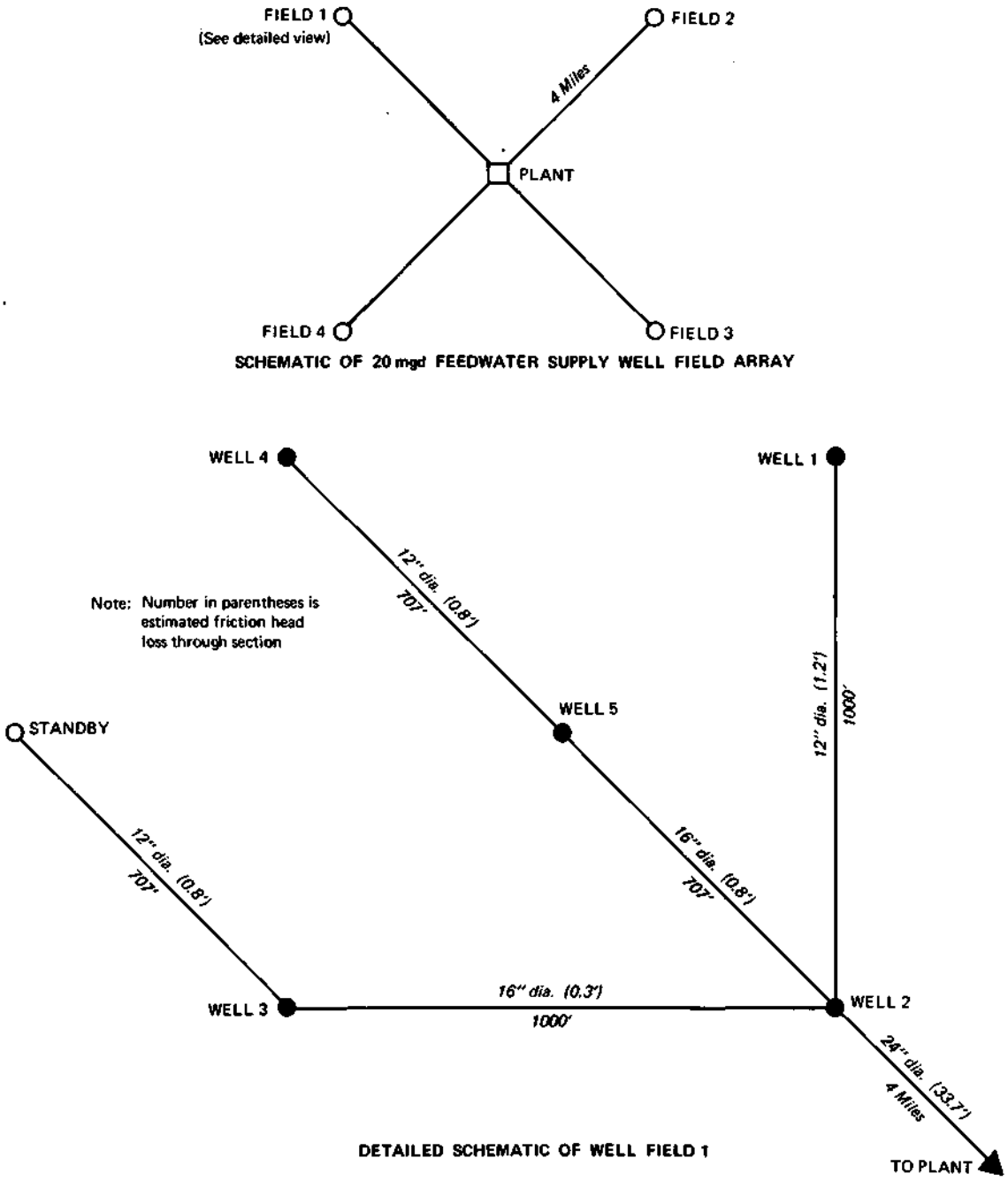

Figure 44. Schematic of 20 mgd feedwater well field array and well field detail

COST SUMMARY

The cost of producing water of 500 mg/l total dissolved minerals from the Mt. Simon is summarized in table 28. Costs are shown as unit costs (¢/1000 gal) and their totals range from 132.9¢/1000 gal for a 1 mgd RO plant to 184.9¢/1000 gal for a 5 mgd distillation plant. In this table, "not feasible" indicates the desalting process cannot be applied economically to the particular feedwater; "not determined" indicates the process is feasible but the cost was not determined for other reasons. For example, in the freezing process, plant costs are given only for 1 mgd capacity plants, since it is difficult to estimate costs for larger plants because of the continuing development of this process. In addition to these exceptions, the 31 percent well penetration 1 mgd scheme is not included because of lack of convergence of chemical analysis results, and the 20 percent 10 mgd scheme is not included because of lack of available drawdown.

TABLE 28
COST OF PRODUCING WATER (INCLUDING BRINE INJECTION)
FOR FEASIBLE DESALTING PROCESSES

	1 mgd Plant		5 mgd Plant			10 mgd Plant	
Cost element	20%	50%	20%	31%	50%	31%	" 50%
Non-plant costs							
Feedwater	43.0	38.5	50.3	48.5	62.1	73.0	86.5
Brine injection	17.2	18.2	34.1	35.4	58.2	56.2	75.3
Total non-plant cost	60.2	56.7	84.4	83.9	120.3	129.2	161.8
RO plant costs							
Capital	23.3	23.3					
OM&R	52.9	52.9		Not feasible		Not feasible	
Total, plant	76.2	76.2					
Non-plant	60.2	56.7					
Total, process	136.4	132.9					
VC-VTE-MSF plant costs							
Capital			31.6	31.6	Not		
OM&R	Not determined		68.9	68.9	feasible	Not feasible	
Total, plant			100.5	100.5			
Non-plant			84.4	83.9			
Total, process			184.9	184.4			
VFEA **plant** costs							
Capital	19.0	19.0					
OM&R	62.9	62.9		Not determined		Not determined	
Total, plant	81.9	81.9					
Non-plant	60.2	56.7					
Total, process	142.1	138.6					

Percentages are well penetrations, and costs are given in ¢/1000 gal of product water

All costs shown are based on conditions after 30 years of operation, with the use of 1972 dollars and a plant capacity factor of 0.9 (330 operating days per year). Capital costs are

TABLE 29
COST ELEMENTS OF FEEDWATER AND BRINE INJECTION

Cost element	1 mgd Plant				5 mgd Plant						10 mgd Plant			
	20% Pen.		50% Pen.		20% Pen.		31% Pen.		50% Pen.		31% Pen.		50% Pen.	
	¢/1000 gal	% of total	¢/1000 gal	% of total	¢/1000 gal	% of total	¢/1000 gal	% of total	¢/1000 gal	% of total	¢/1000 gal	% of total	¢/1000 gal	% of total
Feedwater														
Wells	5.92	13.8	10.35	26.9	7.11	14.1	8.94	18.4	16.56	26.7	14.82	20.3	18.63	21.6
Pumps	8.32	19.3	4.01	10.4	10.88	21.6	9.74	20.1	11.03	17.7	13.17	18.0	15.64	18.1
Transmission	16.54	38.5	16.54	43.0	10.20	20.3	10.20	21.0	13.60	21.9	18.21	24.9	19.75	22.8
Power	12.20	28.4	7.58	19.7	22.06	44.0	19.61	40.5	20.89	33.7	26.84	36.8	32.44	37.5
Total feed-water cost	42.98	100.0	38.48	100.0	50.25	100.0	48.49	100.0	62.08	100.0	73.04	100.0	86.46	100.0
Brine injection														
Weils	11.11	64.6	11.11	61.0	13.33	39.1	13.33	37.6	20.01	34.4	20.01	35.6	23.34	31.0
Pumps	4.73	27.5	5.35	29.4	10.66	31.2	11.26	31.8	20.42	35.1	14.79	26.3	21.45	28.5
Transmission					0.62	1.8	0.62	1.7	0.66	1.1	4.61	8.2	6.61	8.8
Power	1.36	7.9	1.75	9.6	9.52	27.9	10.24	28.9	17.12	29.4	16.77	29.9	23.87	31.7
Total brine injection cost	17.20	100.0	18.21	100.0	34.13	100.0	35.45	100.0	58.21	100.0	56.18	100.0	75.27	100.0

amortized at 5⅜ percent interest over the expected life of each cost element. Plant life is assumed to be 30 years.

Plant power costs (included in OM&R) are computed from unit electrical charges of 1.0 -1.23¢/kwh, depending on power requirements, while electrical costs for well pumps and brine injection pumps assume a uniform charge of 1.0¢/kwh.

Individual cost elements of producing feedwater and injecting brine are shown in table 29. The largest individual cost elements of producing feedwater are transmission (20.3 to 43.0 percent) and power (19.7 to 44.0 percent), while those for injecting brine are well construction (31.0 to 64.6 percent) and pumps (26.3 to 35.1 percent). Ordinarily one might expect economies of scale to affect unit costs. However, no such effect is seen in unit costs of feedwater production or brine injection. This is because worsening feedwater quality at higher pumping rates causes decreasing concentration ratios and increasing brine/feedwater flow ratios for all of the desalting processes studied so that proportionately much greater amounts of feedwater must then be procured. It cannot be concluded from the data whether or not unit costs of plants exhibit a decline with increasing plant capacity.

Plant costs range from 54.4 to 59.0 percent of the total costs (see tables 19, 21, 23). Of the individual plant cost elements, OM&R costs were the largest, ranging from 68.5 to 76.9 percent. Power costs amounted to 52 percent of the total plant cost for the distillation process (table 21) but only 18.1 percent of the freezing process cost (table 23). On the other hand, labor costs were lowest (4.5 percent) for the distillation process and highest (22.5 percent) for the freezing process.

Costs of desalted water are apparently higher than costs of other alternatives but become more competitive when used in conjunction with the fresh groundwater. Table 30 shows a comparison of costs and the total cost for the combined waters from four selected townships which will have groundwater deficits by 1980. The township numbers and the deficits are shown in figure 45.

TABLE 30
COSTS OF MEETING WATER DEFICITS WITH DESALTED WATER

Township number	Demand (mgd)	Deficit (mgd)	Treated water produced locally		Desalted water		Total combined waters	
			Quantity (mgd)	Cost (¢/1000 gal)	Quantity (mgd)	Cost (¢/1000 gal)	Quantity (mgd)	Cost (¢/1000 gal)
1	14	6	8	34*	6	185	14	99
2	10	6	4	34	6	185	10	125
3	11	6	5	34	6	185	11	116
4	15	4	11	34	4	185	15	74

*Costs from (48)

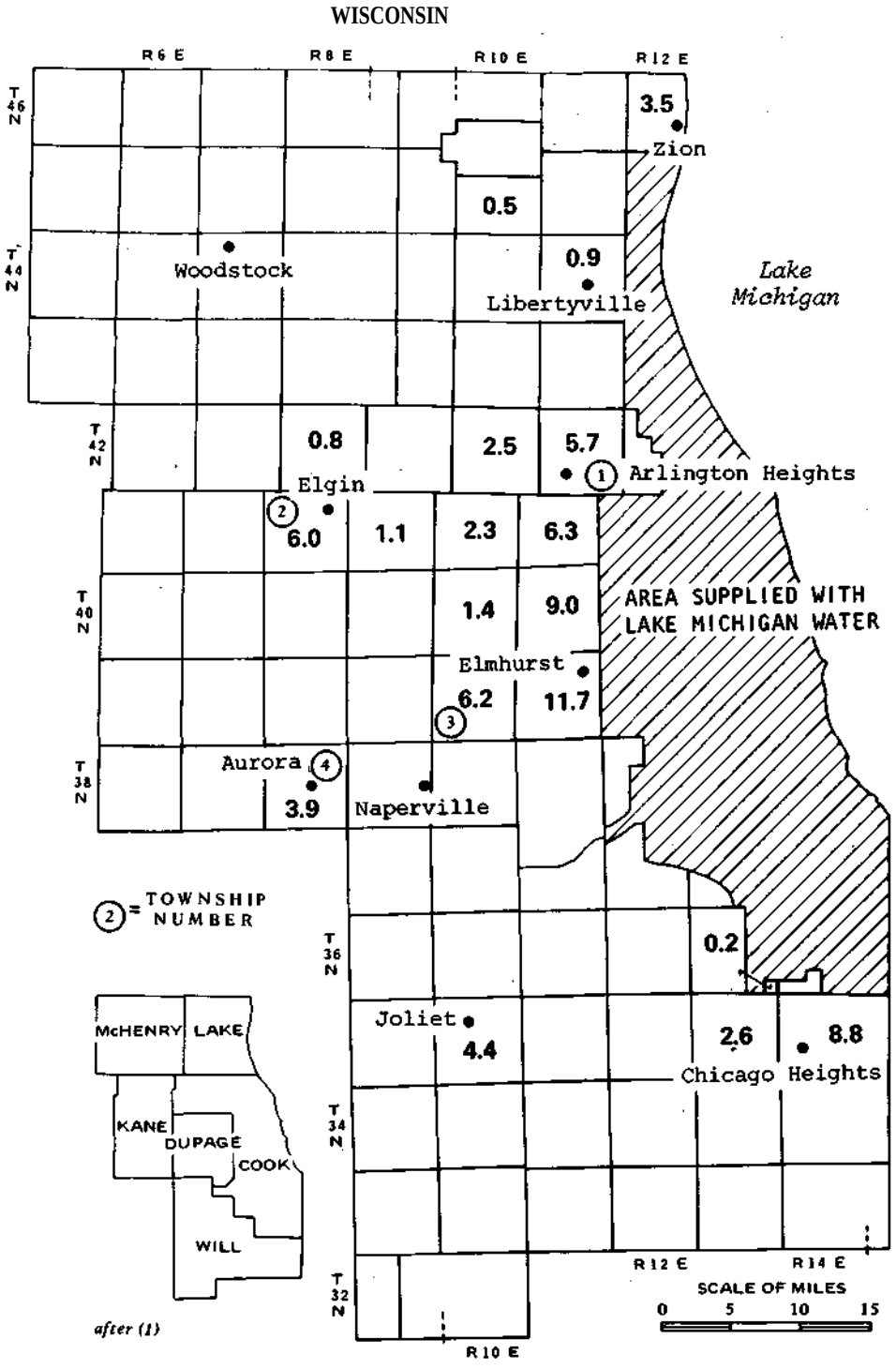

Figure 45. Water demands (mgd) in 1980 in excess of groundwater available from natural recharge

APPENDIX A

CALCULATION OF ED PLANT ELECTRIC POWER COST (20 PERCENT PENETRATION, 1 MGD, 30 YEARS)

1) To determine rating factor F_r (an index denoting the effectiveness of each individual stack based on the feedwater temperature and the chemical composition of dissolved solids):

a) Calculate the percent of Na, K, and Cl in the total dissolved solids in the feedwater (Na + K = 4220 mg/l, Cl = 9700 mg/l, TDM = 17,000 mg/l)

$$\frac{4220 + 9700}{17{,}000} = \frac{13{,}920}{17{,}000} = 0.82$$

b) Obtain F_r from figure 4, p. 11, Reference 18

$F_r = 0.9$

2) To determine stages required:

a) Assume stack throughput to be 0.216 mgd. From figure 5 in Reference 18, the decimal fraction of dissolved solids remaining (FSR) after each stage is 0.55.

b) For 17,000 TDM feedwater, the reduction will be

1st Stage	0.55× 17,000 = 9350
2nd Stage	0.55 × 9,350 = 5140
3rd Stage	0.55 × 5,140 = 2820
4th Stage	0.55 × 2,820=1550
5th Stage	0.55 × 1,550= 850
6th Stage	0.55 × 850= 467

So six stages will be needed in the ED process to obtain a product with less than 500 mg/1 TDM.

3) To determine electric power cost:

a) Pumping power

(1 kwh/1000 gal x number of stages) + 1 kwh/1000 gal
= 1 × 6 + 1 = 7 kwh/1000 gal

b) Stack power. The stack power is about 5 kwh per thousand gallons of product water and per thousand mg/1 of dissolved minerals removed.

$$\frac{\text{kwh}}{1000\ \text{gal}} = 5 \times \frac{17{,}000 - 467}{1000} = 82.7\ \text{kwh/1000 gal}$$

c) The total electric power requirement is 7+82.7 = 89.7 kwh/1000 gal. If the power cost is assumed to be 1¢/kwh, the power cost alone would be 89.7¢/1000 gal.

Because of this high electric power cost, the ED process is not economically feasible for desalting Mt. Simon aquifer water.

APPENDIX B

SAMPLE CALCULATIONS FOR ION EXCHANGE PLANT OF 1 MGD CAPACITY (20 PERCENT PENETRATION)

Water analysis at 20 percent penetration, 1 mgd feed, and 30 years:

Cations	*mg/l*	*mg/l (as* $CaCO_3$)
Ca^{+2}	1580	3950
Mg^{+2}	314	1292
Na^{+}	4220	9160
Anions		
Alk	220	220
SO_4^{-2}	320	333
Cl	9700	3670

Calculation of Operating Data:

a) Anion Column

Resin — IRA68
Effective Capacity— 14.2 Kgr/ft^3 (1 Kgr = 1000 grains)
Actual Capacity — 13.2 Kgr/ft^3
Flow Rate — O.8 gpm/ft^3

Calculation of Anion Resin Volume

Kgr into column per day

$$\frac{(SO_4^{-2} + Cl^-) \times \text{total product water *(gal/day)}}{17{,}100 \text{ mg/l /Kgr/gal}}$$

$$= \frac{(333 + 13{,}670) \times 1.1 \times 10^6}{17{,}100} = 9.0 \times 10^5 \text{ Kgr/day}$$

$$\frac{9.0 \times 10^5}{24} = 3.75 \times 10^4 \text{ Kgr/hr}$$

**Including 10 percent of product water for regeneration purposes.*

Ft^3 of Resin Exhausted Per Hour

$$3.75 \times 10^4 \frac{\text{Kgr}}{\text{hr}} \times \frac{1}{14.2 \text{ Kgr/ft}^3} = 2.64 \times 10^3 \text{ ft}^3/\text{hr}$$

The service time is 3.8 hrs. The anion resin volume per service is

2.64×10^3 ft^3/hr × 3.8 hr = 1.0×10^4 ft^3

Anion Regeneration

The actual capacity is the amount of Cl and SO_4 actually exchanged onto the resin per unit volume of the resin. The actual capacity is 13.2 Kgr/ft^3

Kgr of Cl and SO_4 on the resin = actual capacity x resin volume

13.2 Kgr/ft^3 × 1.0×10^4 ft^3 = 13.2×10^4 Kgr (as $CaCO_3$)

Lbs of Ammonia Per Regeneration

$$\text{Kgr (as } CaCO_3) \times \frac{\text{equiv. wt. } NH_3}{\text{equiv. wt. } CaCO_3} \times \frac{1}{7} \frac{\text{lb}}{\text{Kgr}} \times \text{regeneration level}$$

$$= 132{,}000 \times \frac{17}{50} \times \frac{1}{7} \times 1.43 = 9200 \text{ lbs of } NH_3\text{/regen.}$$

Lbs of NH_3 *Per Day*

$$9200 \times \frac{24}{4.6} = 48{,}000 \text{ lbs/day } NH_3$$

b) Cation Column

Resin — IRC-84
Effective Capacity — 16.7 Kgr/ft^3
Actual Capacity — 15.7 Kgr/ft^3
Flow Rate — O.8 gpm/ft^3
Exhaustion Time — 228 min.

Calculation of Cation Resin Volume

Kgr into column per day

$$\frac{(Ca + Mg + Na) \times \text{total product water (gal/day)}}{17{,}100 \text{ mg/l /Kgr/gal}}$$

$$\frac{(3950 + 1292 + 9160) \times 1.1 \times 10^6}{17{,}100} = 9.26 \times 10^5 \text{ Kgr/day}$$

$$\frac{9.26 \times 10^5}{24} = 3.85 \times 10^4 \text{ Kgr/hr}$$

Ft^3 of Resin Exhausted Per Hour

$$3.85 \times 10^4 \frac{\text{Kgr}}{\text{hr}} \times \frac{1}{16.7 \text{ Kgr/ft}} = 2.31 \times 10^3 \text{ ft}^3\text{/hr}$$

The service time is 3.8 hrs, the anion resin volume per service is

$$2.31 \times 10^3 \frac{\text{ft}^3}{\text{hr}} \times 3.8 \text{ hr} = 8.78 \times 10^3 \text{ ft}^3$$

Cation Regeneration

Kgr of cations on the resin = actual capacity x resin volume

$$8.78 \times 10^3 \text{ ft}^3 \times 15.7 \frac{\text{Kgr}}{\text{ft}^3} = 1.38 \times 10^5 \text{ Kgr (as } CaCO_3)$$

Lbs of H_2SO_4 *Per Regeneration*

$$\text{Kgr (as } CaCO_3) \times \frac{\text{equiv. wt. } H_2SO_4}{\text{equiv. wt. } CaCO_3} \times \frac{\text{lb}}{\text{Kgr}} \times \text{regen. level}$$

$$1.38 \times 10^5 \times \frac{49}{50} \times \frac{1}{7} \times 1.4 = 27{,}000 \text{ lbs of } H_2SO_4$$

$$\text{lb of } 66° \text{ Bé } H_2SO_4 = 27{,}000 \times \frac{100}{93.19} = 29{,}000 \text{ lb/regen}$$

Lbs of H_2SO_4 *Per Day*

$$29{,}000 \times \frac{24}{4.6} = 152{,}000 \text{ lb/day}$$

c) Cost of Chemicals Required in Regeneration

1) NH_3

The cost of NH_3 is \$62.55/ton,* the daily cost is

$$\frac{48{,}000}{2000} \times 62.55 = \$1501/\text{day}$$

2) H_2SO_4

The cost of H_2SO_4 (66° Be) is \$34.6/ton,** and the daily cost is

$$\frac{152{,}000}{2000} \times 34.6 = \$2630/\text{day}$$

**From Mid-West Ammonia Product Co., Chicago [including transportation to Aurora, Illinois].*
***From Arco Chemical Petrochems Department, Chicago [including \$3 freight to Aurora, Illinois].*

3) The total chemical cost is 1501 + 2630 = \$4131/day for a 1 mgd plant or

$$\frac{4131}{10^3} = \$4.13/1000 \text{ gal}$$

Because ot this high chemical cost, the ion exchange process is not economically feasible for desalting Mt. Simon aquifer water.

APPENDIX C

THE DETERMINATION OF RECOVERY RATIO FOR THE RO PROCESS AT DIFFERENT PENETRATIONS AND PLANT CAPACITIES

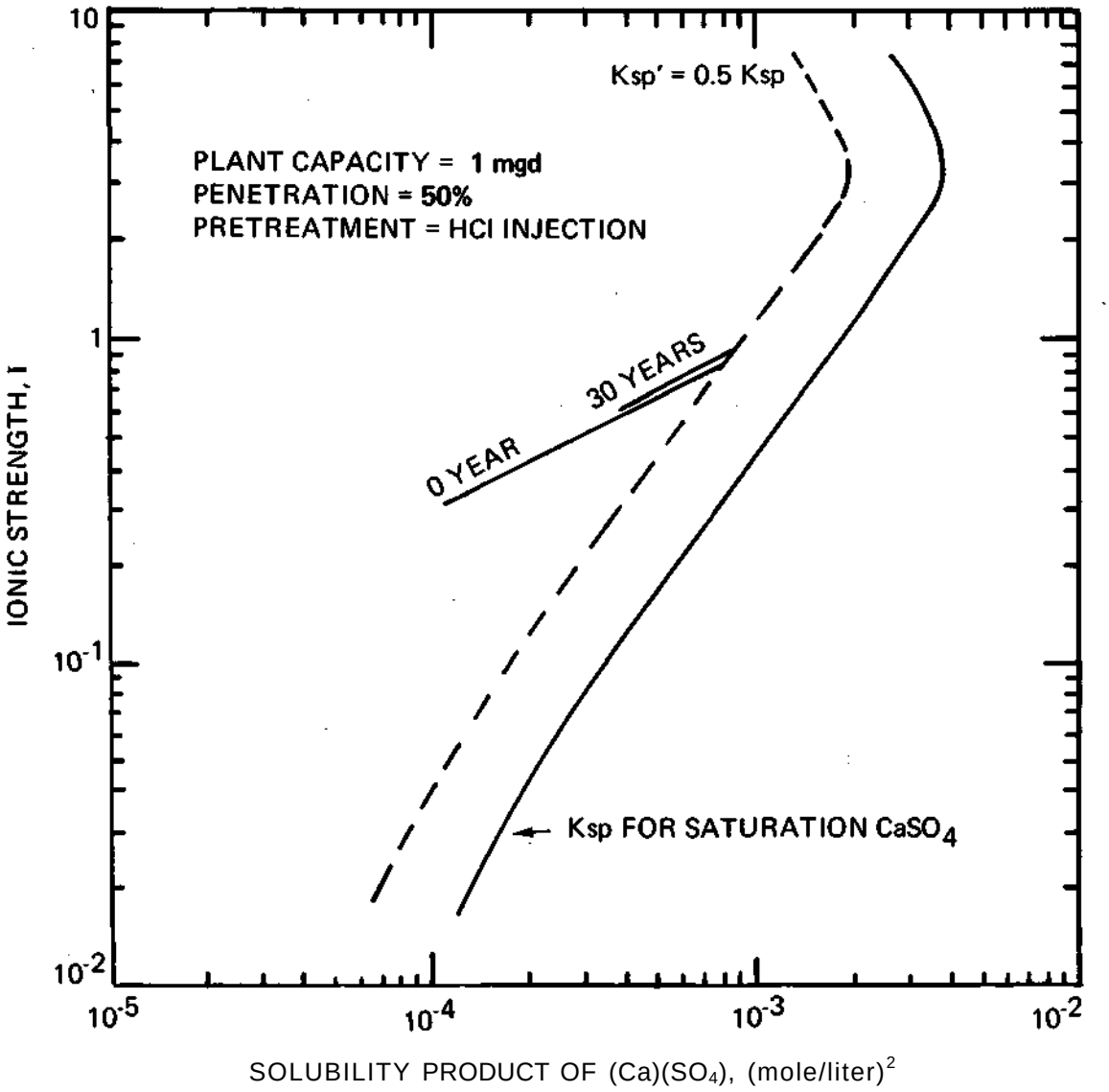

Figure C-1. Determination of concentration ratios at 0 and 30 years

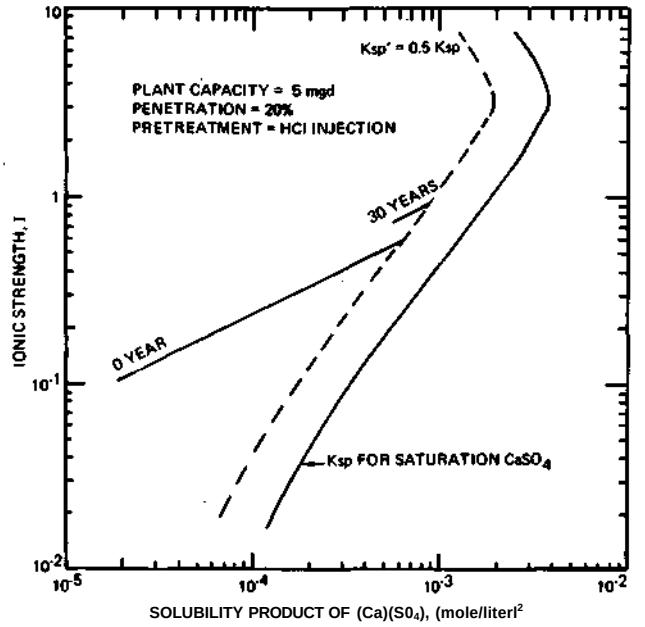

Figure C-3. Determination of concentration ratios at 0 and 30 years

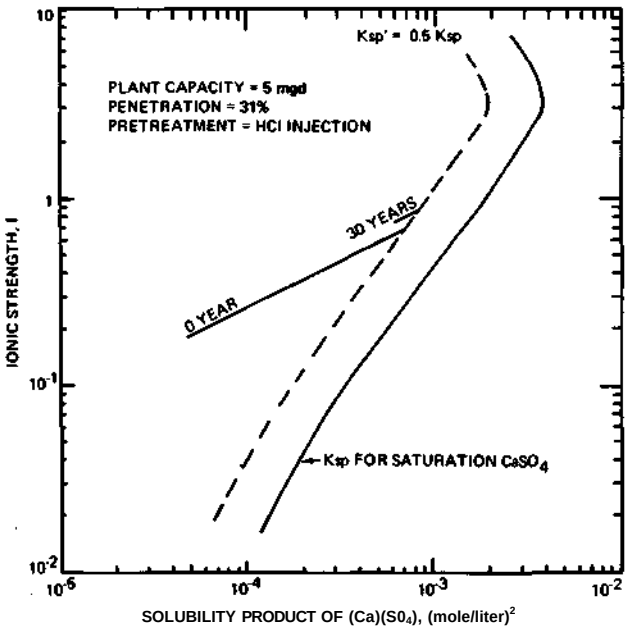

Figure C-2. Determination of concentration ratios at 0 and 30 years

APPENDIX D
THE CALCULATION OF TWO STAGE RO SYSTEM

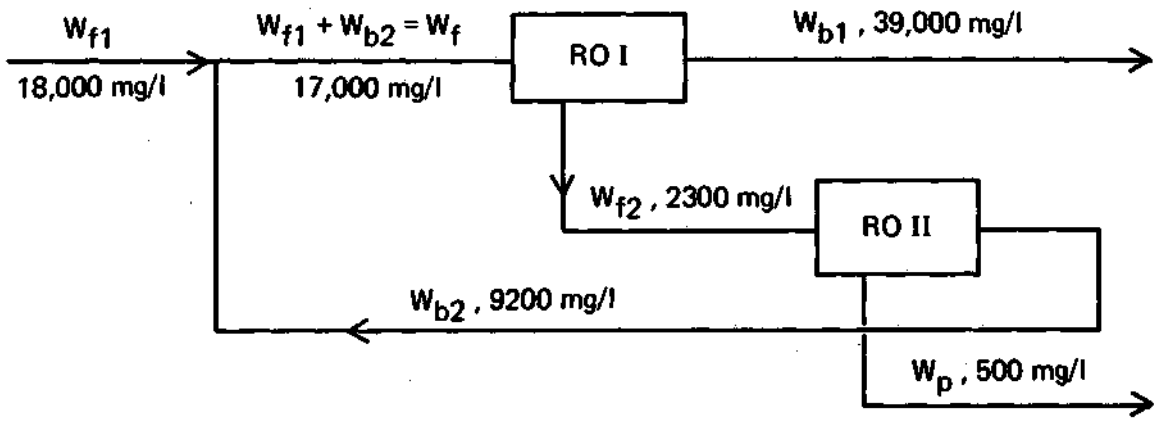

At 20 percent penetration, 1 mgd, and 30 years, the concentration ratio was found to be 2.27 for the first stage. The product to brine ratio, R, can be calculated as follows:

$$2.27 = \frac{C_b}{C_f} = \frac{1 + R + \frac{1-\eta}{2}R}{1 + \frac{1-\eta}{2}R}$$

The salt rejection, η, is assumed to be 0.9,

$$2.27 = \frac{1 + R + \frac{1-0.9}{2}R}{1 + \frac{1-0.9}{2}R} = \frac{1 + 1.05R}{1 + 0.05R}$$

Solving for R

$$R = 1.35$$

or $$\frac{W_{f2}}{W_{b1}} = 1.35$$

or $$\frac{W_f - W_{b1}}{W_{b1}} = 1.35$$

$$W_f = 2.35\, W_{b1}$$

$$\frac{W_{f2}}{W_f} = \frac{1.35}{2.35} = 0.574$$

then

$W_{f2} = 0.574\, W_f$ (for first stage)

In the second stage, the concentration ratio is assumed to be 4.0. The same procedure is followed as for the first stage

$$4 = \frac{1 + 1.05R}{1 + 0.05R}$$

Solving for R,

$$R = 3.53$$

or $$\frac{W_p}{W_{b2}} = 3.53$$

or $$\frac{W_{f2} - W_{b2}}{W_{b2}} = 3.53$$

$$W_{f2} - W_{b2} = 3.53\, W_{b2}$$

$$\frac{W_{f2}}{W_{b2}} = 4.53$$

By assuming Wp = 1 mgd and solving all of the above equations, the following results are obtained

$W_p = 1$ mgd
$W_{b2} = 0.283$ mgd
$W_{f2} = 1.283$ mgd
$W_{b1} = 0.96$ mgd
$W_f = 2.24$
$W_{f1} = 1.96$

$$\frac{W_{b1}}{W_{f1}} = 0.49$$

APPENDIX E
CALCULATION OF SO_2 FORMATION AS THE RESULT OF Na_2SO_3 INTRODUCTION

The chemical equations for SO_2 formation are

$$H^+ + SO_3^{-2} \rightarrow HSO_3^- \quad \text{(E-1)}$$

$$H^+ + HSO_3^- \rightarrow SO_2 + H_2O \quad \text{(E-2)}$$

The disassociation constants of equations (E-1) and (E-2) are $K_1 = 6.3\times10^{-8}$ and $K_2 = 1.72\times10^{-2}$ moles/1, respectively (34). Equations (E-l) and (E-2) can be combined as

$$2H^+ + SO_3^{-2} \rightarrow SO_2 + H_2O \quad \text{(E-3)}$$

and the new disassociation constant is $K_3 = K_1K_2$. The equilibrium expression for equation (E-3) is

$$K_3 = \frac{(SO_2)}{(H^+)^2\,(SO_3^{-2})} \quad \text{(E-4)}$$

Taking logarithms of both sides, the result is

$$\log K_3 = \log(SO_2) - 2\log(H^+) - \log(SO_3^{-2}). \quad \text{(E-5)}$$

It is assumed that the water is kept at pH 5 and the addition of Na_2SO_3 is 5 mg/l [corresponding to $(SO_3^{-2}) = 3.96\times10^{-5}$ mole/1]. Inserting all the values in equation (E-5), the concentration of SO_2 formed is expressed in the following equation

$$\log(SO_2) = 7.2 + 1.76 - 10 - 4.4 = -5.44$$

$$(SO_2) = 10^{-5.44} = 3.62\times10^{-6}\ \text{mole/l} = 0.168\ \text{mg/l}$$

APPENDIX F
CALCULATION OF $CaSO_4$ SOLUBILITY PRODUCT (Ksp) FOR MT. SIMON AQUIFER WATER

The equation developed by Marshall (36) is used in the form

$$\log Ksp = \log Ksp^{\circ} + 8s\frac{\sqrt{I}}{1 + A\sqrt{I}} - x \log a_{H_2O} \qquad \text{(F-1)}$$

where:

Ksp^{o} = solubility product in pure water

s = the limiting Debye-Huckel slope

A = a constant = 1.5

I = ionic strength

aH_2O = activity of H_2O

x = number of moles of H_2O in crystallized calcium sulfate
2 for dihydrate ($CaSO_4 \cdot 2H_2O$)
1/2 for hemihydrate ($CaSO_4 \cdot 1/2H_2O$)
0 for anhydrite ($CaSO_4$)

Ksp = solubility product dependent on ionic strength, I

TABLE F-1
EXPERIMENTAL VALUES OF s AND Ksp° AT DIFFERENT TEMPERATURES (Ref. 36)

T,°C	s	Anhydrite ($CaSO_4$)	Dihydrate ($CaSO_4 \cdot 2H_2O$)
25	0.5080	63×10^{-6}	42.2×10^{-6}
30	0.5128	54.4×10^{-6}	43.6×10^{-6}
40	0.5226	47.8×10^{-6}	42.5×10^{-6}
60	0.5449	28.7×10^{-6}	35.7×10^{-6}
100	0.6006	7.73×10^{-6}	
125	0.6422	2.25×10^{-6}	
150	0.6499	1.00×10^{-6}	
175	0.7451	0.336×10^{-6}	
200	0.8097	0.114×10^{-6}	

Table F-1 presents the experimental data for s and Ksp° at different temperatures. These values can be used in equation (F-1) to calculate the solubility constant.

1) In the case of anhydrite ($CaSO_4$) solubility, x = 0 in equation (F-1) which reduces to the following form

$$\log Ksp = \log Ksp^{\circ} + 8s\frac{\sqrt{I}}{1 + 1.5\sqrt{I}} \qquad \text{(F-2)}$$

For the water in 50 percent penetration and 10 mgd at 0 year, the total ionic strength can be calculated as 0.433.

Example: The limiting slope s is 0.6006 and Ksp° is 7.73×10^{-6} at 100 C (212 F). The solubility

product can be obtained as follows:

$$\log Ksp = \log 7.73\times10^{-6} + 8\times 0.6006 \times \frac{\sqrt{0.433}}{1+1.5\sqrt{0.433}}$$

$$= -6 + \log 7.73 + 4.8048 \times \frac{0.658}{1.987}$$

$$= -3.52$$

$$Ksp = 10^{-3.52} = 3.02\times 10^{-4} \text{ at } 100\ C$$

Similarly the solubility product Ksp at other temperatures can be calculated. The values are plotted in figures 37 and 38.

2) In the case of dihydrate ($CaSO_4 \cdot 2H_2O$), the correction for water activity aH_2O should be added in equation (F-l):

$$\log Ksp = \log Ksp^{\circ} + 8s\frac{\sqrt{I}}{1+1.5\sqrt{I}} - x \log a_{H_2O},$$

where x = 2 in this case. The activity of water, aH_2O, can be found in Reference 37. The values of aH_2O are 0.99 and 0.98 in 0.3 and 0.6 molal NaCl-H_2O solutions, respectively.

Example: Calculation of Ksp for $CaSO_4 \cdot 2H_2O$ in the water at 50 percent penetration, 10 mgd, 0 year and 60 C (140 F) process temperature:

$$\log Ksp = \log 35.7\times10^{-6} + 8x0.5449\frac{\sqrt{0.433}}{1+1.5\sqrt{0.433}}$$

$$- 2 \log 0.99$$

$$= -5 + 0.553 + 1.44 + 0.0087 = -2.998$$

$$Ksp = 10^{-2.998} = 1.0046\times10^{-3}$$

Figure 38 gives the solubility curves for the 50 percent penetration and 10 mgd case. Curves for both anhydrite and dihydrate (gypsum) are shown for 0, 5, and 30 years.

REFERENCES

1. Schicht, R. J., and Allen Moench. 1971. *Projected groundwater deficiencies in northeastern Illinois, 1980-2020.* Illinois State Water Survey Circular 101.
2. Buschbach, T. C. 1964. *Cambrian and Ordovician strata of northeastern Illinois.* Illinois State Geological Survey Report of Investigation 218.
3. Hughes, George M., Paul Kraatz, and Ronald A. Landon. 1966. *Bedrock aquifers of northeastern Illinois.* Illinois State Geological Survey Circular 406.
4. Hutchinson, Rickard D. 1970. *Water resources of Racine and Kenosha Counties, southeastern Wisconsin.* U.S. Geological Survey Water-Supply Paper 1878.
5. Suter, Max, Robert E. Bergstrom, H. F. Smith, Grover H. Emrich, W. C. Walton, and T. E. Larson. 1959. *Preliminary report on ground-water resources of the Chicago region, Illinois.* Illinois State Geological Survey and State Water Survey Cooperative Ground-Water Report 1.
6. Cotter, R. D., R. D. Hutchinson, E. L. Skinner, and D. A. Wentz. 1969. *Water resources of Wisconsin Rock-Fox River Basin.* U.S. Geological Survey Hydrologic Investigations Atlas HA-360.
7. Walton, W. C, and Sandor Csallany. 1962. *Yields of deep sandstone wells in northern Illinois.* Illinois State Water Survey Report of Investigation 43.
8. Sasman, R. T., C. R. Benson, G. L. Dzurisin, and N. E. Risk. 1973. *Water-level decline and pumpage in deep wells in northern Illinois, 1966-1971.* Illinois State Water Survey Circular 113.
9. Sasman, R. T., C. K. McDonald, and W. R. Randall. 1967. *Water-level decline and pumpage in deep wells in northeastern Illinois, 1962-1966.* Illinois State Water Survey Circular 94.
10. Zeizel, Arthur, William C. Walton, Robert T. Sasman, and Thomas A. Prickett. 1962. *Ground-water resources of DuPage County, Illinois.* Illinois State Geological Survey and State Water Survey Cooperative Ground-Water Report 2.
11. Hem, John D. 1959. *Study and interpretation of the chemical characteristics of natural water.* U.S. Geological Survey Water-Supply Paper 1473.
12. Hantush, M. S. 1964. *Hydraulics of wells.* In Advances in Hydroscience, Vol. 1, Academic Press.
13. Lovelock, P. E. R. 1970. *The laboratory measurement of soil and rock permeability.* Institute of Geological Sciences Technical Communication No. 2, Exhibition Road, South Kensington, London, SW7.
14. Walton, William C. 1962. *Selected analytical methods for well and aquifer evaluation.* Illinois State Water Survey Bulletin 49.
15. Prickett, T. A., and C. G. Lonnquist. 1971. *Selected digital computer methods for aquifer evaluation.* Illinois State Water Survey Bulletin 55.
16. Trussell, R. R., and J. F. Thomas. 1971. *A discussion of the chemical character of water mixtures.* Journal of the American Water Works Association, Vol. 63, No. 1, pp. 49-51.
17. *Electrodialysis desalting state-of-the-art (1969).* October 1970. OSW R&D Report No. 610. Hittman Associates, Inc., Columbia, Maryland.
18. *Desalting cost calculating procedures.* May 1970. OSW R&D Report No. 555. Southwest Research Institute, San Antonio, Texas.
19. *Electrodialysis plant nomograph booklet.* August 1970. Report No. HIT-375. Hittman Associates, Inc., Columbia, Maryland.
20. *The potential contribution of desalting to future water supply in Texas.* November 1966. OSW R&D Report No. 250. Southwest Research Institute, San Antonio, Texas.
21. *Survey of the ion exchange process for desalination application.* April 1970. OSW R&D Report No. 616. Control System Research, Inc., Arlington, Virginia.

22. *Ion exchange: field evaluation of DESAL process.* November 1970. OSW R&D Report No. 631. Permutit Research and Development Center, Princeton, New Jersey.

23. Spiegler, K. S. 1966. *Principles of desalination.* Academic Press, New York and London.

24. *Design study of a reverse osmosis plant for sea water conversion.* April 1966. OSW R&D Report No. 176. General Atomics, San Diego, California.

25. Fair, G. M., J. C. Geyer, and D. A. Okun. 1968. *Water and wastewater engineering.* John Wiley & Sons, New York, pp. 28-29.

26. Marshall, W. L., and R. Slusher. 1968. *Journal of chemical engineering data.* Vol. 13, No. 1.

27. *High recovery optimization study.* April 1969. Report to OSW, Aerojet-General Corporation, El Monte, California.

28. *Reverse osmosis desalting state-of-the-art report.* October 1970. OSW R&D Report No. 611. Hittman Associates, Inc., Columbia, Maryland.

29. *Reverse osmosis desalting plant nomograph booklet.* August 1970. Report No. HIT-427. Hittman Associates, Inc., Columbia, Maryland.

30. Private communication with Gulf Environmental Systems, Inc., San Diego, California.

31. Private communication with Mr. Ralph E. Higdon, Permutit Research and Development Center, Princeton, New Jersey.

32. *The chemical marketing newspaper.* December 1971. Schnell Publishing Co., Inc.

33. Private communications with Messrs. R. L. Bolger and W. R. Snedden, Commonwealth Edison Company,-' Chicago, Illinois.

34. Fair, G. M., and J. C. Geyer. 1965. *Water supply and wastewater disposal.* John Wiley & Sons, Inc., New York. p. 475.

35. *Betz handbook of industrial water conditioning.* Fifth edition. June 1971. Betz Laboratories, Inc., Trevose, Pennsylvania.

36. Marshall, W. L., R. Slusher, and E. V. Jones. 1964. *Solubility and thermodynamic relationships for* $CaSO_4$ *in* NaCl-H_2O *solution for 40° C to 200°C, 0 to 4 molal* NaCl. Reprinted from Journal of Chemical and Engineering Data. Vol. 9, No. 187.

37. Robinson, R. A., and R. H. Stakes. 1959. *Electrolyte solutions.* Butterworths Scientific Publications Ltd., London, p. 476.

38. Metier, V., and A. G. Ostroff. October 1967. *The proximate calculation of the solubility of gypsum in natural brines from 28° C to 70°C.* Environmental Science and Technology, Vol. 1.

39. *Design and economic study of a gas turbine powered vapor compression plant for evaporation of sea water.* 1967. OSW R&D Report No. 377. Struthers Energy Systems, Inc., Warren, Pennsylvania.

40. *Fluor Corporation feasibility report for the city of Brownsville, Texas, — 8 million gallons per day desalting plant.* 1970. Report to OSW. Fluor Corporation, Los Angeles, California.

41. *A 100,000 gpd desalination plant using a model 100A1 vacuum freezing vapor compression desalter.* 1968. COLT Industries, Beloit, Wisconsin.

42. *Vacuum freezing vapor compression desalting state-of-the-art (1968).* October 1969. OSW R&D Report No. 491. Hittman Associates, Inc., Columbia, Maryland.

43. *Bench scale study of the vacuum freezing ejector absorption process.* September 1971. OSW R&D Report No. 477. COLT Industries, Beloit, Wisconsin.

44. *Economic optimization of the AVCO crystallization process.* June 1972. Unpublished report. AVCO Systems Division, Wilmington, Massachusetts.

45. *Saline water conversion engineering data book.* July 1965. Report to OSW. M.W. Kellogg Company, New York, New York.

46. Talbot, I. S., and P. Beardon. January 1964. *The deep-well method of industrial waste disposal.* Chemical Engineering Progress. Vol. 60, No. 1, pp. 49-52.

47. Gibb, J. P., and E. W. Sanderson. 1969. *Cost of municipal and industrial wells in Illinois, 1964-1966.* Illinois State Water Survey Circular 98.

48. Moench, A. F., and A. P. Visocky. 1971. *A preliminary 'least cost' study of future groundwater development in northeastern Illinois.* Illinois State Water Survey Circular 102.

49. Singh, K. P., A. P. Visocky, and C. G. Lonnquist. 1972. *Plans for meeting water requirements in the Kaskaskia River Basin, 1970-2020.* Illinois State Water Survey Report of Investigation 70.

50. Ackermann, W. C. 1968. *Cost of pumping water.* Illinois State Water Survey Technical Letter 9.

51. Ackermann, W. C. 1969. *Water transmission costs.* Illinois State Water Survey Technical Letter 7.

52. Singh, Krishan P. 1971. *Economic design of central water supply systems for medium sized towns.* Illinois State Water Survey Reprint Series No. 170.